THE REGULATION SURROUNDING THE TRIOSE PHOSPHATE UTILIZATION LIMITATION OF PHOTOSYNTHESIS

By

Alan M. McClain

A DISSERTATION

Submitted to
Michigan State University
in partial fulfillment of the requirements
for the degree of

Biochemistry and Molecular Biology – Doctor of Philosophy

2022

ABSTRACT

THE REGULATION SURROUNDING THE TRIOSE PHOSPHATE UTILIZATION LIMITATION OF PHOTOSYNTHESIS

By

Alan M. McClain

The triose phosphate utilization (TPU) limitation of photosynthesis is a paradigm in which the rate at which stromal phosphate is incorporated into the organic phosphate pool can exceed the rate at which inorganic phosphate is released by processing fixed carbon into end products such as starch or sucrose. TPU limitation is unique among the three canon biochemical limitations of photosynthesis in that the plant must regulate photosynthetic rate to a level below what is maximally possible in its current environment.

I investigated the methods through which the photosynthetic rate is regulated in response to TPU limitation. For the first minute after imposition of TPU limitation by excess light and CO_2, the photosynthetic rate is limited by availability of inorganic phosphate for the chloroplastic ATP synthase and availability of $NADP^+$ for photosystem 1. These restrictions cause an increase in the redox state of the electron carrier Q_a which controls energy flow during photosynthesis. After a few minutes of TPU, slower energy-dependent regulatory mechanisms at photosystem 2 and the cytochrome *b6f* complex reduce energy flow, relieving excess reduction at Q_a or photosystem 1. After a day of acclimation, photoinhibition and rubisco deactivation prevent the appearance of TPU limitation at elevated CO_2 and prevented the occurrence of oscillations in photosynthetic electron carrier redox status.

Oscillations of CO_2 assimilation rate induced by TPU limitation are temporarily able to exceed the steady-state photosynthetic rate. However, the advantage is short-lived, and overall

plants assimilate less over the course of oscillations than they would during steady-state photosynthesis. The plants can temporarily exceed the limitation on photosynthesis typically imposed by TPU limitation or the RuBP regeneration limitation, but not the rubisco limitation. This is due to the availability of metabolites caused by a brief period of inactivity. Furthermore, the amplitude of the oscillations depended on how quickly the plant entered TPU limitation and how severe TPU limitation was when imposed.

ACKNOWLEDGEMENTS

Thank you to all those who helped me along the way.

Sean, who taught me how to use our instruments and design gas circuits.

Sarathi, who taught me many assays and provided important writing advice.

Madeline, who collected valuable data that unfortunately did not make it here.

Jeff, who painstakingly taught me all the basics of leaf spectroscopy.

Geoff, who did some of the same.

Dave, who taught me how to use leaf spectroscopy to do research that counts.

Robert, who taught me so much about circuit design and assembly.

Lijun and Tony, who helped me with practical mass spectroscopy.

Rob, who pushed me to embrace opportunities to better myself.

Thank you to Alex, Isaac, Nate, and Luke, who considered my additions to their projects worthy of authorship.

Thank you to Tom, who, in addition to teaching me so much, provided me with stunning freedom to design and execute my own experiments.

Thank you to my friends and family whose support I consider invaluable.

TABLE OF CONTENTS

LIST OF TABLES

LIST OF FIGURES

KEY TO ABBREVIATIONS

A	Net assimilation of carbon, or, when negative, net respiration of carbon
C_c	Partial pressure of CO_2 at the site of carboxylation
C_i	Partial pressure of CO_2 inside the leaf
DHAP	Dihydroxyacetone phosphate
DIRK	Dark-interval relaxation kinetics. A dark period used to measure relaxation of proton-motive force
E4P	Erythrose 4-phosphate
ECS	Electrochromic shift; the change in chlorophyll absorbance by the Witt effect in response to changes in electric field
ECS_t	Total electrochromic shift caused by a dark period. A measurement of total proton-motive force
ETR	Photosynthetic electron transport rate
FBP	Fructose-1,6-bisphosphate
Fv/Fm	A ratio of variable to maximum fluorescence in a dark-adapted plant
GAP	Glyceraldehyde 3-phosphate
g_{H+}	Conductivity of the thylakoid membrane to protons through the ATPase
g_m	Mesophyll conductance to CO_2
J_{max}	Maximum rate of electron transport under infinite light
h	Hour
k_{et}	Kinetic parameter for electron transport rate from the cytochrome *b6f* complex to PSI
MEP	Methylerythritol 4-phosphate
min	Minute
NPQ	Non-photochemical quenching of fluorescence, typically comprises q_I, q_E, and q_t

NPQt Theoretical *NPQ*, calculated using a fixed *Fv*/*Fm* of 0.83 (see Tietz *et al.*, 2017)

PEP Phosphoenolpyruvate

PGA Phosphoglyceric acid

P_i Inorganic phosphate (PO^4)

PMF Proton-motive force

PPT Phosphoenolpyruvate/phosphate translocator

PSI Photosystem 1

PSII Photosystem 2

q_E Energy dependent quenching

q_I Quenching of fluorescence by photoinhibition

R Rate of RuBP consumption

R_L Rate of respiration in the light, also called R_d (day respiration)

RuBP Ribulose 1,5-bisphosphate

$S_{c/o}$ Specificity of rubisco for CO_2 versus oxygen

SBP Sedoheptulose bisphosphate

TP Triose phosphate

TPT Triose phosphate/phosphate translocator

TPU Triose phosphate utilization

V_{cmax} Maximum velocity of carboxylation

W Rate of carboxylation

α The fraction of glycolate carbon which leaves the Calvin-Benson cycle as amino acids

α_G The fraction of glycolate carbon which leaves the Calvin-Benson cycle as glycine

α_S The fraction of glycolate carbon which leaves the CB cycle as serine

Γ^* The rubisco CO_2 compensation point ignoring the effect of R_L

φ The ratio of oxygenations to carboxylations

Φ_{PS2} Quantum yield of photosystem 2

CHAPTER I

Triose phosphate utilization and beyond: from photosynthesis to end product synthesis

Updated from a review published in the Journal of Experimental Botany, 2019

McClain AM, Sharkey TD (2019) Triose phosphate utilization and beyond: from photosynthesis to end product synthesis. *Journal of Experimental Botany* **70**, 1755-1766. DOI 10.1093/jxb/erz058

Abstract

During photosynthesis plants fix CO_2 from the atmosphere onto ribulose-bisphosphate producing 3-phosphoglycerate, which is reduced to triose phosphates (TPs). The TPs are then converted into the end products of photosynthesis. When a plant is photosynthesizing very quickly it may not be possible to commit photosynthate to end products as fast as it is produced, causing a decrease in available phosphate and limiting the rate of photosynthesis to the rate of triose phosphate utilization (TPU). The occurrence of an observable TPU limitation is highly variable based on species and especially growth conditions, with TPU capacity seemingly regulated to be in slight excess of typical photosynthetic rates the plant might experience. The physiological effects of TPU limitation are discussed with an emphasis on interactions between the Calvin-Benson cycle and the light reactions. Methods for detecting TPU-limited data from gas exchange data are detailed and the impact on modeling of some physiological effects are shown. Special consideration is given to common misconceptions about TPU.

Introduction

Triose phosphate utilization (TPU) is one of the three canonical biochemical limitations of photosynthesis in gas exchange analysis of C_3 plants. It reflects a steady-state condition in which assimilation of carbon is limited by the ability to regenerate phosphate through production of end products of photosynthesis. Phosphate is required by ATP synthase to produce ATP, of which three are needed to fix a single carbon. Although all three ATP are used for phosphorylation of carbon chains, two are immediately released when the 3-phosphoglyceric acid (PGA) kinase reaction is followed by glyceraldehyde-3-phosphate (GAP) dehydrogenase. Regeneration of ribulose bisphosphate (RuBP) releases two phosphates per

three fixed carbons, one from fructose bisphosphatase (FBPase) and one from sedoheptulose bisphosphatase (SBPase). One phosphate per three carbons remains on the triose phosphates (TPs) GAP and dihydroxyacetone phosphate (DHAP), which are used for synthesis of starch and sucrose. The capacity for end product synthesis relative to carbon fixation can determine the concentration of inorganic phosphate. If the capacity for TPU is high relative to carbon fixation, the concentration of phosphate will be high. A high concentration of phosphate will inhibit starch synthesis and, less so, sucrose synthesis, changing the partitioning of carbon among the end products. A high concentration of phosphate could also make ATP synthesis easier and so interfere with the acidification of the stromal lumen, which is necessary to induce energy-dependent quenching (q_E) in PSII. If triose phosphate use is too quick relative to carbon fixation, it may deplete Calvin-Benson cycle intermediates and lead to difficulty regenerating RuBP. On the other hand, if the capacity for TPU is low relative to carbon fixation, the phosphate concentration decreases, leading to reduced conductivity of protons through thylakoid ATP synthase that ultimately slows photosynthesis (Kanazawa & Kramer, 2002; Takizawa *et al.*, 2008; Kiirats *et al.*, 2009). One minute after becoming TPU-limited, the ATP/ADP ratio can fall from 2.3 to 1.2 although after 18 minutes other regulatory processes can allow it to recover to 1.6 (Sharkey *et al.*, 1986c).

The decline in ATP is a form of feedback limitation and is potentially quite dangerous to the plant. Feedback conditions are known to cause photodamage due to the inability to move energy downstream (Pammenter *et al.*, 1993; Takizawa *et al.*, 2008; Kiirats *et al.*, 2009). To avoid photodamage, instead of maintaining phosphate-restricted feedback, a series of regulatory steps are engaged to slow photosynthetic electron transport and carbon fixation by

rubisco. While the capacity is determined by phosphate balance, the steady-state rate is set by regulatory effects that serve to ameliorate feedback conditions. This includes reduction in the photosystem 2 quantum yield (Φ_{PS2}) (Sharkey *et al.*, 1988; Kiirats *et al.*, 2009) and reduced activation state of rubisco (Sharkey *et al.*, 1986a; Socias *et al.*, 1993; Viil *et al.*, 2004; Cen & Sage, 2005). In this review we discuss the effect of end product synthesis on the overall rate and regulation of photosynthesis.

How are triose phosphates used?

The maximal photosynthetic rate under TPU limitation is primarily, but not exclusively, determined by the rate of conversion of triose phosphates into starch and sucrose. The synthesis of sugar alcohols in some plant species (Escobar-Gutiérrez & Gaudillère, 1997; Loescher *et al.*, 2000) have the same effect as sucrose synthesis. The limitation on assimilation is based on the release of phosphate from Calvin-Benson cycle intermediates that leave the cycle, and the most immediate release is from the activity of fructose-1,6-bisphosphatase (FBPase) in the chloroplast for starch synthesis or in the cytosol for sucrose synthesis. Sucrose synthesis begins with the translocation of TPs through the triose phosphate/phosphate translocator (TPT) (Riesmeier *et al.*, 1993). This removes carbon from the Calvin-Benson cycle and returns phosphate from the cytosol to the chloroplast. Each sucrose molecule requires the combination of two hexose molecules, for a total of four triose phosphates. Net phosphate release from organic phosphates during sucrose synthesis occurs at FBPase (2), UDP-glucose pyrophosphorylase (1), and sucrose-phosphate phosphatase (1). Sucrose synthesis is typically measured at between 25 and 50% of total carbon assimilation (Sharkey *et al.*, 1985; Escobar-Gutiérrez & Gaudillère, 1997; Szecowka *et al.*, 2013; Abadie *et al.*, 2018), with some studies

demonstrating up to 75% (Stitt *et al.*, 1983). It is likely the species and environmental conditions have an effect on partitioning of carbon into sucrose.

In starch synthesis, phosphate release occurs at stromal FBPase and ADP-glucose pyrophosphorylase. The flux to starch varies considerably with the growth conditions of the plant, for example *Arabidopsis* growing in an 18 h photoperiod committed only 24% of fixed carbon to starch but in a 6 h photoperiod committed 51% (Sulpice *et al.*, 2014). Other studies show between 30 and 60% of fixed carbon goes to starch (Sharkey *et al.*, 1985; Escobar-Gutiérrez & Gaudillère, 1997; Szecowka *et al.*, 2013; Abadie *et al.*, 2018) but the amount of carbon partitioned to starch can vary greatly among plant species (Huber, 1981). A small amount of phosphate is added to starch in photosynthesizing leaves by glucan-water dikinase and phosphoglucan-water dikinase but the amount is very low, 0.1-0.9% of glucose moieties (McPherson & Jane, 1999; Ritte *et al.*, 2002; Kötting *et al.*, 2004), and so is not relevant for understanding gas exchange properties of photosynthesis.

There are a number of other routes by which carbon is exported from the Calvin-Benson cycle (Figure 1.1). Any carbon metabolism pathway that begins with a phosphorylated Calvin-Benson cycle intermediate and ends with a non-phosphorylated molecule will contribute to TPU. The shikimate pathway to aromatic amino acid synthesis begins with the export of GAP from the chloroplast to make phosphoenolpyruvate (PEP). PEP is reimported into the chloroplast through the phosphoenolpyruvate/phosphate translocator (PPT) and combines with erythrose 4-phosphate (E4P) and ends with chorismate, accounting for 1 to 2% of fixed carbon (Escobar-Gutiérrez & Gaudillère, 1997; Abadie *et al.*, 2018). Fatty acids and branched chain amino acids are synthesized from acetyl-CoA from pyruvate and account for 1 to 3% of fixed

carbon (Bao *et al.*, 2000). It has been shown that oil biosynthesis can be increased as a carbon sink and this would contribute to a higher capacity for TPU (Sanjaya *et al.*, 2011). The methylerythritol 4-phosphate (MEP) pathway begins with GAP and pyruvate to produce isoprenoids consuming up to 3% of fixed carbon (Rasulov *et al.*, 2014). Pyruvate is made from triose phosphate exported from the chloroplast and dephosphorylated by pyruvate kinase freeing phosphate in the cytosol or by beta elimination of phosphate during the rubisco reaction (Andrews & Kane, 1991) freeing phosphate in the stroma.

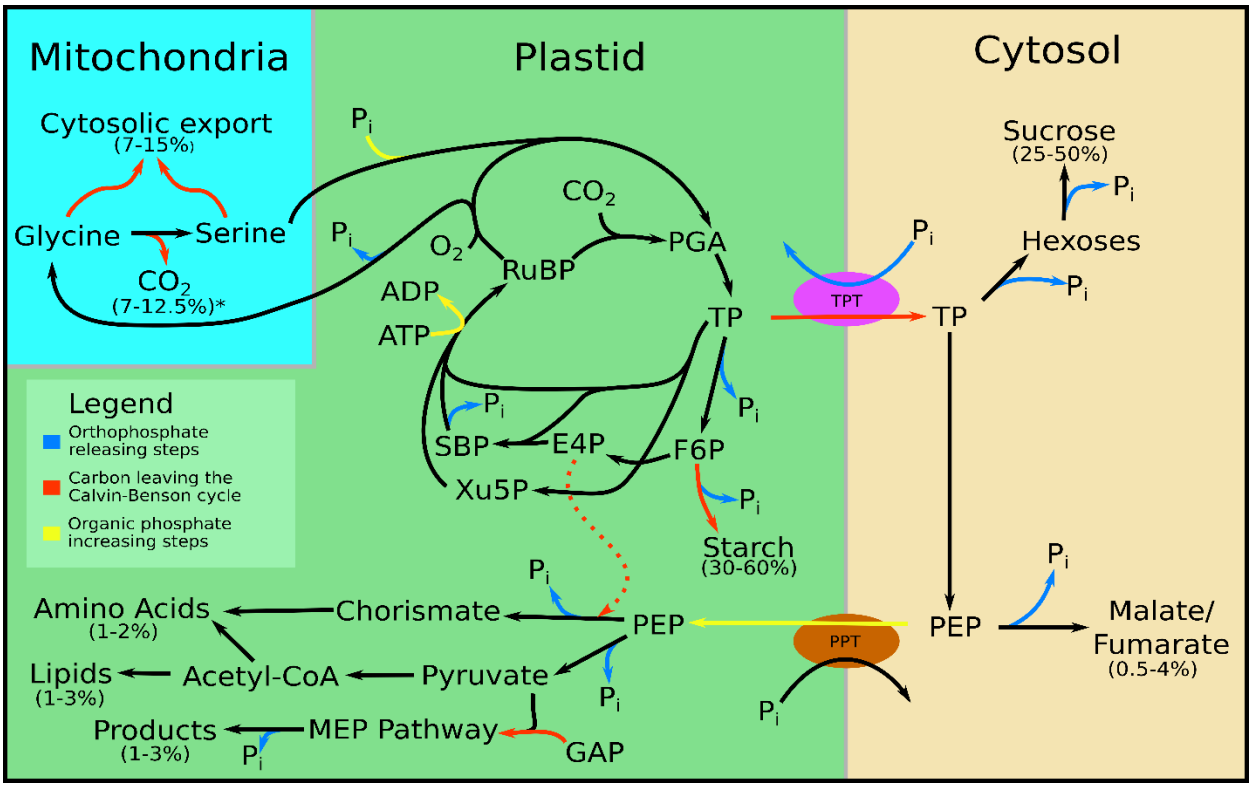

Figure 1.1 A depiction of the major phosphate and carbon exits from the Calvin-Benson cycle. Rates: Sucrose, 25-50%; Starch, 30-60%; Photorespiratory amino acids, 7-15%; Shikimate pathway, 1-2%; Lipids 1-3%; Methylerythritol pathway, 1-3%; PEP Carboxylation, 0.5-4%; CO2 release from photorespiration*, 7-12.5% of fixed carbon lost and does not contribute to TPU capacity. Abbreviations: E4P, erythrose 4-phosphate; F6P, fructose 6-phosphate; GAP, glyceraldehyde 3-phosphate; PEP, phosphoenolpyruvate; PGA, 3-phosphoglyceric acid; SBP, sedoheptulose bisphosphate; TP, triose phosphates; Xu5P, xylulose 5-phosphate.

Amino acid intermediates in the photorespiratory pathway can be exported from the leaf or used in the cytosol as carbon skeletons, for transamination, or for protein construction. It is estimated that an average of 30% to a high of 70% of photorespiratory glycolate carbon is exported from the Calvin-Benson cycle as modeled from gas exchange measurements (Busch *et al.*, 2018). If the ratio of oxygenation to carboxylation (φ) is assumed to be 0.25, this represents carbon export from the Calvin-Benson cycle equivalent to 7-15% of fixed carbon. In addition, CO_2 lost from conversion of glycine to serine will allow for increased rates of carboxylation, though it does not increase the maximum assimilation rate. If we assume φ is 0.25 and no glycine export, this represents 12.5% of fixed carbon lost, but under TPU-limited conditions excess carboxylation capacity allows fixation of the same amount of CO_2. This is part of the reason photosynthesis becomes insensitive to CO_2 even though the rate of photorespiration varies with CO_2.

Plants are capable of carboxylating PEP and releasing the phosphate on PEP. The resulting oxaloacetate can be transaminated to aspartate or reduced to malate for use in anapleurotic reactions or storage in the vacuole (sometimes as fumarate). PEP carboxylation contributes to TPU as PEP may come from triose phosphates exported from the chloroplast and the carboxylation consumes atmospheric carbon which would be measured in gas exchange. Gauthier *et al*. (2010) found that amino acids made from α-ketoglutarate are quickly labeled by ^{15}N-ammonium nitrate but not $^{13}CO_2$ fed to photosynthesizing leaves indicating that the carbon for these amino acids comes from preexisting pools and so do not contribute to TPU. Szecowka *et al.* (2013) showed that no more than 2.6% of ^{13}C-labeled carbon from CO_2 fixation goes through PEP to organic acids or amino acids, including non-carboxylation reactions. Ma *et al.*

(2014), using extensive *in silico* modeling combined with mass spectrometry measurements, found that PEP carboxylation represented 0.5 to 4% of fixed carbon, depending on how much PEP carbon is assumed to be directly from the Calvin-Benson cycle and the overall rate of photosynthesis. Another study found that the rate of PEP carboxylation varied with the rate of photosynthesis, increasing significantly in its proportion at low assimilation from 2% to 25% of fixed carbon (Abadie & Tcherkez, 2018). In Arabidopsis a significant amount of carbon is stored in the vacuole as fumarate; it is not known how much of this carbon is recent (and therefore contributes to TPU) and how much is preexisting carbon (Chia *et al.*, 2000; Pracharoenwattana *et al.*, 2010; Zell *et al.*, 2010; Ma *et al.*, 2014). This is also true of sunflower (Abadie *et al.*, 2018).

In summary, TPU is primarily starch and sucrose synthesis (approximately 80%). The next most important "use" of triose phosphates may be in removal of glycine or serine from the photorespiratory cycle, potentially reaching 15% but likely usually well below 10%. Many other metabolic pathways account for the remainder but none of these are likely to exceed 5% of the rate of carbon fixation and so usually do not have a significant impact on TPU-limitation behavior.

TPU and gas exchange

TPU is typically assessed from gas exchange data obtained using infrared gas analyzers to measure rates of CO_2 uptake. Because of the usefulness of fluorescence parameters in analyzing gas exchange data, gas exchange measurements are frequently combined with chlorophyll fluorescence analysis. Measuring the stomatal conductance to gas exchange by transpiration allows the calculation of the partial pressure of CO_2 inside the leaf (C_i) (Sharkey *et al.*, 1982). Diffusion resistance within the mesophyll will further reduce the effective partial

pressure of CO_2 resulting in the partial pressure of CO_2 at the site of carboxylation (C_c). TPU-limited photosynthesis is mostly insensitive to CO_2, so resistance to diffusion of CO_2 has little or no effect on TPU-limited photosynthesis.

Plots of carbon assimilation (A) as a function of C_i (or better C_c when mesophyll conductance can be estimated since this eliminates CO_2 diffusion effects on the results) can be interpreted using rubisco kinetics to predict what biochemical process is limiting assimilation. At low C_c, assimilation is typically limited by binding affinity of rubisco for CO_2 (and the inhibition by oxygen), known as the rubisco limitation (often abbreviated as C limitation). At intermediate C_c or when given insufficient light, assimilation is typically limited by the rate of regeneration of ribulose 1,5-bisphosphate (RuBP), frequently referred to as J limitation. TPU limitation, sometimes called P limitation, only happens when the plant has a greater capacity to fix carbon than it has to remove carbon from the Calvin-Benson cycle in end product synthesis. In many plants this can be seen at high C_c and saturating light. The requirement for high photosynthetic rate may be why TPU limitation is so hard to detect in plants with low inherent photosynthetic rates such as Arabidopsis (Yang *et al.*, 2016).

Lack of, or reverse, sensitivity of A to oxygen partial pressure changes and CO_2 partial pressure increases is the primary gas exchange behavior of TPU limitation (Sharkey, 1985a). Insensitivity had been reported for many years (Ludwig & Canvin, 1971; Jolliffe & Tregunna, 1973; von Caemmerer & Farquhar, 1981). Critically, Harris et al. (1983) found insensitivity following feeding with mannose, which sequesters phosphate. Later it was shown that oxygen insensitivity was correlated with CO_2 insensitivity (Sharkey, 1985a). Leegood and Furbank (1986) found that oxygen-insensitive photosynthesis in leaf discs was induced by a combination

of low temperature and high CO_2 partial pressure. Feeding of phosphate restored normal oxygen sensitivity and also increased CO_2 assimilation rate, showing that phosphate metabolism was involved in both oxygen sensitivity and the limitation of assimilation. From this and other considerations Sharkey (1985*a*) concluded

"(a)s the rate of CO_2 assimilation increases, starch and sucrose synthesis must increase as well. If not, triose-P and PGA will build up and phosphate will decline. These changes in pool size will stimulate starch and sucrose synthesis. However, there is a limit to how far the phosphate pool can fall before it begins to limit photophosphorylation. Once this limit is reached, CO_2 will be assimilated at the rate at which starch and sucrose synthesis can metabolize triose-P, regardless of whether oxygenation occurs or not."

When photosynthesis is limited either by rubisco or RuBP regeneration, increasing CO_2 or decreasing O_2 should increase *A*. When *A* is rubisco-limited, *A* will increase because of (1) the affinity of rubisco for CO_2 and the effects of O_2 on CO_2 affinity and (2) the reduced CO_2 release in photorespiration. When *A* is limited by RuBP regeneration, *A* will increase because of (1) the reduced CO_2 release in photorespiration (as above) and (2) the diversion of RuBP from oxygenation to carboxylation when photorespiration is suppressed. TPU limited photosynthesis does not exhibit this stimulation or exhibits a reduced stimulation when photorespiration is suppressed (Badger *et al.*, 1984; Sharkey, 1985a). The insensitivity of *A* while TPU-limited happens because the controlling factor is the ability of the leaf to make end products and this is not affected by CO_2, O_2, or the rate of photorespiration. Increasing photorespiration by increasing O_2 or decreasing CO_2 partial pressures will be compensated by increased RuBP regeneration and carboxylation but because these capacities are in excess in a TPU-limited

state, this will not affect *A*. Use of oxygen or CO_2 insensitivity to determine photosynthetic limitations in A/C_i curves is discussed in greater detail in Busch and Sage (2017).

It is not possible to determine whether C_4 plants suffer TPU limitation. The carbon pump of C_4 metabolism makes it difficult to see the gas exchange behaviors that characterize TPU limitation. C_4 plants at high photosynthetic rates are interpreted to be limited by CO_2-saturated rubisco activity, and at lower rates by PEP carboxylase activity (Collatz *et al.*, 1992). Even if rubisco is not saturated with CO_2, oxygen-dependent changes in the rate of photorespiratory CO_2 release changes the CO_2 concentration in the bundle sheaths, making C_4 photosynthesis rate independent of photorespiration rate (von Caemmerer, 2000). Thus, the CO_2 and O_2 dependence that results from the variation in the ratio of carboxylation to oxygenation is not observed in C_4 photosynthesis and because this is the gas exchange characteristic that is used to diagnose TPU limitation, it is not possible to tell if C_4 plants have a TPU-limited state.

Reverse sensitivity to CO_2 and O_2 partial pressures

While the TPU limitation offered understanding of insensitivity to increasing O_2 and CO_2 partial pressures, it did not immediately explain reverse sensitivity. It has long been known that oxygen inhibits photorespiration due to competitive binding to rubisco and photorespiratory CO_2 release (Warburg, 1919; Ludwig & Canvin, 1971; McVetty & Canvin, 1981). It was therefore unexpected to find that reducing oxygen or increasing CO_2 partial pressures could sometimes reduce the rate of CO_2 assimilation. As photorespiration releases CO_2, it is counterintuitive that altering the gas composition to favor carboxylation would result in decreased carbon assimilation. Yet data dating back decades shows that once at high CO_2, increasing CO_2 can

cause a decrease in net assimilation (Jolliffe & Tregunna, 1973; Canvin, 1978; von Caemmerer & Farquhar, 1981), and increasing O_2 can cause an increase in net assimilation (Viil *et al.*, 1977).

Photorespiration was one key to understanding the reverse oxygen sensitivity under TPU-limiting conditions. Phosphoglycolate is dephosphorylated by phosphoglycolate phosphatase before export through PLGG1 or BASS6 (South *et al.*, 2017). Photorespiratory metabolism of two glycolate molecules leads to re-import of carbon as glycerate, which is phosphorylated to phosphoglyceric acid. The extra phosphate released can be used to make ATP that phosphorylates ribulose 5-phosphate to produce RuBP that will be used to accept a CO_2, balancing the photorespiratory loss of one carbon. However, the two amino acid intermediates in the photorespiratory pathway can be used in the cytosol, resulting in net carbon export from the Calvin-Benson cycle. This carbon is effectively lost from RuBP and not directly from CO_2 fixed from the atmosphere. Photorespiratory carbon that never returns to the chloroplast was parameterized as α, the fraction of glycolate carbon that leaves the photorespiratory cycle as amino acids (Harley & Sharkey, 1991). The α parameter was later refined to α_G and α_S, the fraction of glycolate carbon that leaves as glycine and serine respectively (Busch *et al.*, 2018). When glycine is exported instead of serine, no CO_2 is released. As these amino acids come from phosphorylated plastidic metabolites, and permanently leave the Calvin-Benson cycle, they contribute to TPU capacity. Adjusting the gas composition to decrease φ reduces the export of glycine and serine and therefore reduces TPU capacity, reducing the maximum photosynthetic rate. This can explain the reverse sensitivity of A to CO_2 and O_2.

Starch synthesis is also affected by oxygen partial pressure and can contribute to severe reverse sensitivity. Beans photosynthesizing quickly then transferred to low oxygen were found to have reduced rates of starch synthesis but a minimal change in the rate of sucrose synthesis. A concurrent reduction in the ratio of glucose-6-phosphate to fructose-6-phosphate indicates inhibition of phosphoglucose isomerase (Dietz, 1985; Vassey & Sharkey, 1989). The precise mechanism of this inhibition is unclear.

Modeling

TPU models have seen some recent changes to account for our enhanced understanding of the possible role of photorespiration in nitrogen metabolism. Original models that account for triose phosphate usage relied on simple stoichiometry (Sharkey, 1985b):

$$W_p = \frac{3 \times TPU}{1 - 0.5\varphi} \qquad \text{Eq. 1.1}$$

where W_p is the rate of carboxylation when limited by phosphate metabolism and ϕ is the ration of oxygenation to carboxylation by rubisco. Under this model photosynthetic carboxylation would equal the rate of carbon export from the Calvin-Benson cycle for starch and sucrose synthesis (numerator) adjusted by the amount of carbon released during photorespiration (denominator). Under TPU limitation A is given by

$$A = W_p \cdot (1 - 0.5\varphi) - R_L \qquad \text{Eq. 1.2}$$

where R_L is respiration in the light.

When Equation 1 is plugged into Equation 2 the (1-0.5φ) term cancels out and so *A* is independent of the rate of photorespiration. This is because rubisco is not limiting so the amount of CO_2 released during photorespiration can be compensated by increased rubisco activity.

However, this model did not account for reverse sensitivity of assimilation to oxygen or CO_2 frequently observed. The model also describes all carbon export as triose phosphate usage, which is not directly true. Any carbon that leaves the Calvin-Benson cycle and is dephosphorylated will contribute to the maximum TPU capacity. While all carbon in the Calvin-Benson cycle derives from TP, some of the end products are made from Calvin-Benson cycle intermediates other than TPs. Despite this, the simple model has some advantages. It requires no estimation of R_L, mesophyll conductance (g_m) or ϕ. These three parameters are currently impossible to directly measure, and there is some debate about our ability to accurately fit them and the constancy of these parameters.

A recent model for TPU incorporates parameters for glycine or serine exit from the photorespiratory cycle. The glycine and serine need not accumulate and could have a range of metabolic fates, as long as the carbon does not reenter the Calvin-Benson cycle. From Busch *et al*. (2018):

$$W_p = \frac{3 \times TPU}{1 - 0.5(1 + 3\alpha_G + 4\alpha_S)\varphi} \qquad \text{Eq. 1.3}$$

The denominator in equation has three terms to account for carbon that exits photorespiration as glycine (α_g) or serine (α_s). As one carbon out of four is lost as CO_2 in the formation of serine, α_S cannot be greater than 0.75. If α_G and α_S are zero, equations 1 and 3 are identical. Unlike the simple model of equation 1, equation 3 requires knowledge of the relative rate of photorespiration, and therefore relies on fitting for Γ*. There is little signal to differentiate α_S and α_G by gas exchange, which can make fitting these two parameters challenging. For conversion of equation 3 to assimilation as would be measured by gas exchange, W_p must be adjusted for respiratory carbon loss:

$$A = W_p \cdot \left(1 - \frac{\Gamma^*_{\alpha G}}{C_c}\right) - R_L \qquad \text{Eq. 1.4}$$

where $\Gamma^*_{\alpha G}$ is the rubisco-C_c compensation point given the reduced rate of photorespiratory CO_2 release due to export of glycine. $\Gamma^*_{\alpha G}/C_c$ is equivalent to 0.5φ if $\alpha_G = 0$.

Current modeling software is available with varying numbers of parameters to fit. Sharkey (2016) presented an excel tool which allows picking of points from A/C_i curves, with options to fit R_L, g_m, and α_G and α_S. Bellasio, *et al*. (2016) provide a highly detailed Excel tool that uses combined gas exchange and fluorescence to fit R_L, g_m, J_{max}, V_{cmax}, Γ^* and rubisco specificity for CO_2 versus oxygen ($S_{c/o}$), but not α; much of the basis of this fitting are also discussed by Yin *et al.* (2009). Dubois *et al.* (2007) provide a SAS program which allows fitting of R_L, g_m, J_{max}, V_{cmax}, Γ^* and $S_{c/o}$, and α. Moualeu-Ngangue *et al.* (2017) propose to improve the Dubois fitting by reducing the number of assumptions made, though they do not fit α. Gu *et al.* (2010) provide a website for fully automated leaf data analysis called LeafWeb which does not

require selecting limitations point-wise or specific software. It should be noted that no current model attempts to incorporate other carbon sinks, and TPU is treated as a single variable.

Temperature sensitivity

Photosynthesis under TPU limitation is highly temperature sensitive. Though the other photosynthetic limitations demonstrate temperature sensitivity, (Cen & Sage, 2005; Sage & Kubien, 2007; Sharkey & Bernacchi, 2012; Busch & Sage, 2017), TPU-limiting conditions are the most temperature sensitive (Sharkey & Bernacchi, 2012; Yang *et al.*, 2016) perhaps because of the strong temperature sensitivity of sucrose-phosphate synthase (Stitt & Grosse, 1988; Leegood & Edwards, 1996) or altered sensitivity of cytosolic FBPase to 2,6-fructose bisphosphate (Stitt & Grosse, 1988). Other enzymes implicated in TPU limitation are also temperature sensitive, such as nitrate reductase (Leegood & Edwards, 1996; Busch *et al.*, 2018). Because of the different ways by which temperature affects the three limitations, the conditions in which they appear changes with temperature. At temperatures lower than growth conditions the plant is significantly more likely to become TPU limited (Stitt, 1986; Sage & Sharkey, 1987; Labate & Leegood, 1988). Labate and Leegood (1988) demonstrated a temperature-sensitive increase in photosynthesis from phosphate feeding. Leaf discs floated on a solution containing phosphate at 25°C saw a marginal reduction in assimilation. However, discs fed phosphate at 10°C experienced significant photosynthetic gains, indicating that reduced temperatures result in greater limitation of photosynthesis by TPU (Figure 1.2).

Acclimation of TPU

The capacity for triose phosphate utilization is not immutable. Plants grown under low temperature tend to have greatly elevated TPU capacity (Guy *et al.*, 1992; Holaday *et al.*, 1992;

Sage & Kubien, 2007). This acclimation largely comes from increased expression of sucrose biosynthesis enzymes (Guy *et al.*, 1992; Holaday *et al.*, 1992; Strand *et al.*, 1999; Hurry *et al.*, 2000), and it has been proposed that this acclimation is signaled by low phosphate levels (Hurry *et al.*, 2000). This increased capacity offsets the decreased activity of starch synthase and sucrose-phosphate synthase at low temperature and makes it less likely that the plant will be TPU-limited (Cornic & Louason, 1980; Sage & Sharkey, 1987). Plants transferred to an elevated CO_2 environment developed increased phosphate regeneration capacity, demonstrating acclimation (Sharkey *et al.*, 1988; Sage *et al.*, 1989).

Plants experiencing water stress reduce their TPU capacity, possibly reflecting the reduced internal CO_2 partial pressure that results from stomatal closure (von Caemmerer & Farquhar, 1984; Vassey & Sharkey, 1989; Cornic *et al.*, 1992). Transgenic plants overexpressing alternative oxidase cope better with water stress (Dahal *et al.*, 2014, 2015) and experience reduced negative effects on assimilation from TPU capacity. The reduced occurrence of TPU limitation in plants overexpressing the alternative oxidase was correlated with higher amounts of chloroplast ATP synthase, which might allow ATP synthesis at lower phosphate concentration. This adaptability shows that TPU will influence the metabolic investments of the plant; it will enhance the ability to handle high TP production, but only when it is required for the current output of photosynthesis.

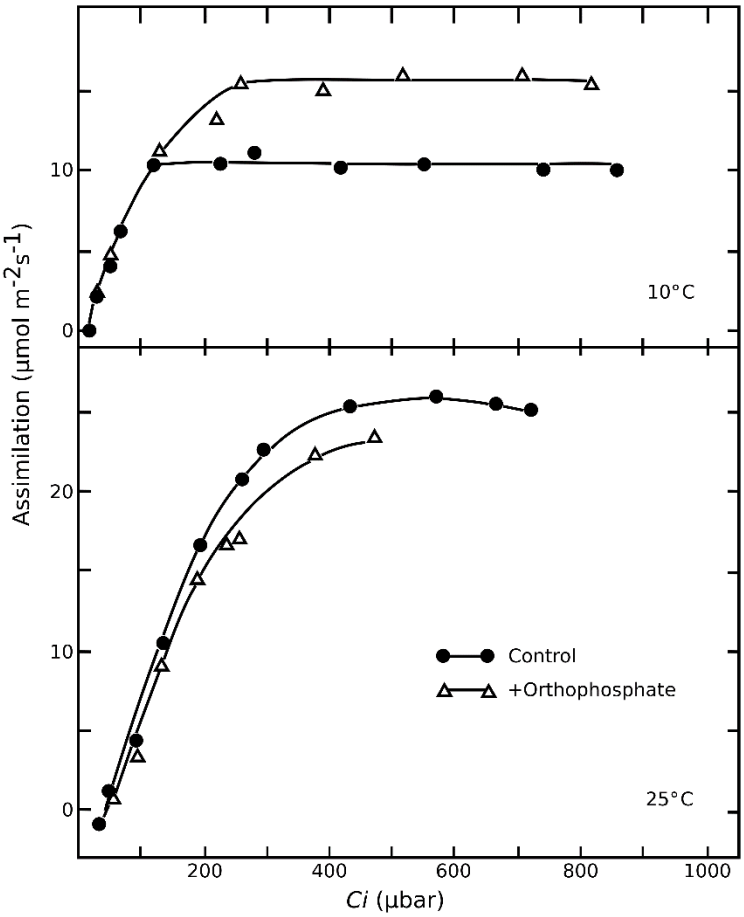

Figure 1.2 Rate of CO_2 assimilation of barley versus C_i in 10°C (top) and 25°C (bottom) with and without the addition of phosphate. A temperature-dependent increase in photosynthetic assimilation is observed upon addition of phosphate. Re-drawn from Labate & Leegood 1988.

The adaptability of TPU is important for fulfilling the role of stromal phosphate in balancing starch synthesis and ATP synthesis (Figure 1.3). Starch synthesis is highly sensitive to phosphate due to inhibition of ADP-glucose pyrophosphorylase (Preiss, 1982), and ATP synthase is kinetically (Takizawa *et al.*, 2007) and thermodynamically sensitive to phosphate. This relationship can help explain the very low partitioning of carbon into starch at low photosynthetic rate (Escobar-Gutiérrez & Gaudillère, 1997), which is exacerbated by reduced

levels of PGA which would otherwise stimulate starch production (Heldt *et al.*, 1977). If sucrose synthesis is in excess, the balance of starch versus sucrose synthesis during the day could become unfavorable for growth and the extra phosphate could even collapse the Calvin-Benson cycle by driving export of too much triose phosphate out of the chloroplast. This has been reported in isolated chloroplasts (Leegood & Walker, 1983) but not in intact leaves. High phosphate outside of chloroplasts has also been shown to result in starch breakdown in the light (Stitt & Heldt, 1981). The highest rate of photosynthesis will be achieved with a fine balance of phosphate usage and phosphate release. In an environment where expected photosynthetic rates are lower, the plant will benefit from reduced TPU capacity. This allows

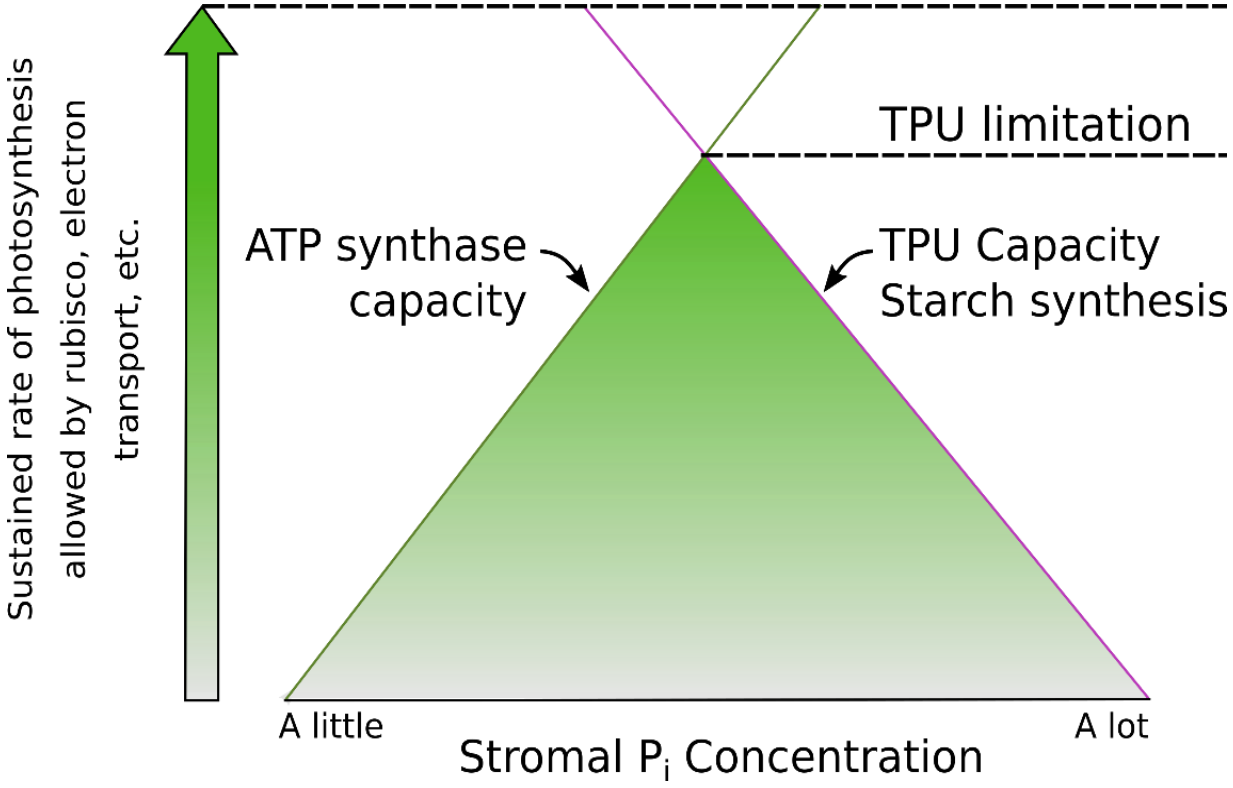

Figure 1.3 As photosynthetic rate increases, the gap between the phosphate concentration required by the ATP synthase and the phosphate concentration to inhibit starch synthesis narrows. The shapes of the responses are represented by straight lines only for simplicity. When TPU limits photosynthetic rate any increase in phosphate required for higher ATP synthase activity would inhibit starch synthesis restricting phosphate release.

phosphate to fall, correcting several issues with starch and sucrose metabolism and reducing the risk of over-consumption of triose phosphates. When expected photosynthetic rates are higher, the plant will benefit from increased TPU capacity allowing better recycling of phosphate and improved ATP synthase throughput and alleviating the potential for photodamage due to feedback conditions.

Effects on the light reactions

Elevating CO_2 partial pressure when photosynthesis is limited by TPU will cause a decrease in Φ_{PS2}. Rubisco binds CO_2 and O_2 competitively, meaning that an increase in CO_2 partial pressure reduces the rate of the light reactions needed for photorespiration. This does not lead to an increase in assimilation when TPU is controlling. Rather, it reduces the rate of carboxylation as assimilation is maximized and less carbon is lost through photorespiration, resulting in reduced total rubisco activity. Both carboxylation and oxygenation require ATP and NADPH, which come from electron transport. Therefore, increasing CO_2 partial pressures over TPU limited leaves results in an overall reduction in electron transport requirements (Stitt, 1986; Sharkey *et al.*, 1988; Stitt & Grosse, 1988). Regulatory processes lead to reduced Φ_{PS2}, a phenomenon which can be useful in discriminating TPU limitation using combined gas exchange and fluorescence data (Figure 1.4).

There are effects on the kinetics of the light reactions that happen concurrently with reduction of electron transport rate. Proton conductivity across the thylakoid membrane goes down under TPU limitation (Takizawa *et al.*, 2008; Kiirats *et al.*, 2009; Yang *et al.*, 2016). It is proposed that this kinetic change occurs because of a reduced pool of available phosphate in the stroma, which reduces the rate of ATP synthase. The K_m of chloroplast ATP synthase for

phosphate has been measured at 0.2-1 mM (Selman-Reimer *et al.*, 1981; Grotjohann & Gräber, 2002). Stromal phosphate concentration during feedback conditions is estimated to be between 0-1.7 mM depending on how much phosphate is assumed to be free (Sharkey & Vanderveer, 1989), so it is reasonable to suggest that the phosphate concentration may drop below the K_m of ATP synthase. Joint with a decrease in ATP synthase conductivity is an increase

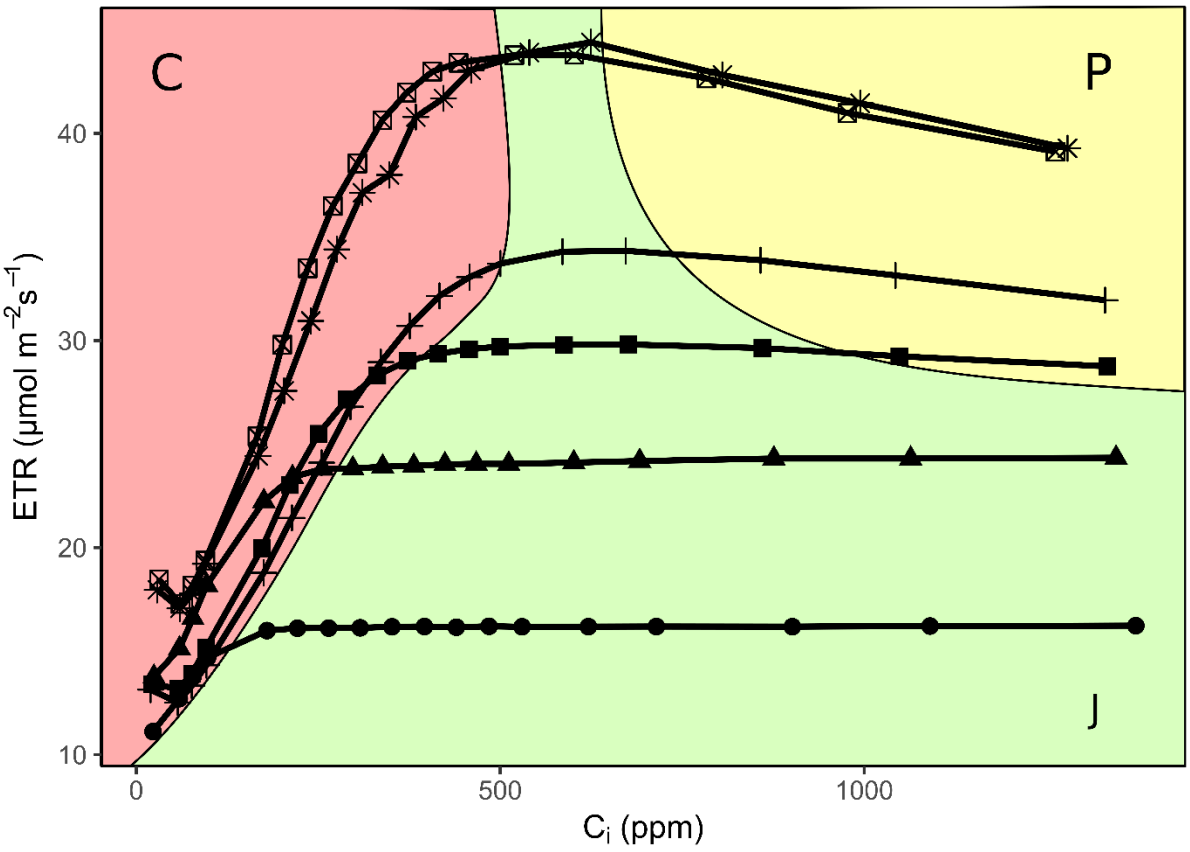

Figure 1.4 The decline in electron transport rate is diagnostic of TPU limitation. From combined gas exchange and fluorescence data in A/C_i curves of *Nicotiana benthamiana* at varying light intensity and 35°C. At low CO_2, plants are limited by rubisco activity (C limitation, red), characterized by a sharp upwards slope of both A and ETR with increasing CO_2. When light is insufficient, plants will be limited by the rate of RuBP regeneration (J limitation, green), characterized by a flat slope of ETR with increasing CO_2. Only when the plant has ample CO_2 and electron transport will TPU limitation (P, yellow) be seen, characterized by a decline in ETR with increasing CO_2. ETR is calculated from fluorescence-derived Φ_{PS2}. Light intensity (µmol m^{-2} s^{-1}): ● - 250, ▲ - 400, ■ - 550, + - 750, ⊠ - 1000, ✳ - 1500.

in proton-motive force (*PMF*). The energy needed to make ATP will depend on the concentration of phosphate.

$$\Delta G_{ATP} = \Delta G'^{0}_{ATP} + R \cdot T \cdot ln \frac{[ATP]}{[ADP] \cdot [P_i]} \quad \text{Eq. 1.5}$$

As the effective [P_i] declines, ΔG_{ATP} will increase, requiring a greater *PMF* for ATP synthesis. Increased *PMF* leads to controls on electron transport through q_E, reducing energy arrival at P680 or reduction in the rate of electron flow at the cytochrome b_6f complex, leading to reduced rates of electron transport (Kramer & Crofts, 1996; Owens, 1996). While phosphate seems to play a role in linking the light reactions and the Calvin-Benson cycle, it is less clear what other molecular mechanisms may be important. It is likely that we do not yet know some important regulatory components that control *ETR* when TPU limits the rate of photosynthesis.

TPU and sink strength

TPU limitation is a form of very short-term sink/source disequilibrium, separate from long-term sinks such as fruit or root growth, though the two could be related. TPU is concerned with the ability to quickly dephosphorylate and remove carbon from the Calvin-Benson cycle. The half-life of Calvin-Benson cycle intermediates tends to be very short, with many under one second, and some larger pools such as glucose 6-phosphate and UDP-glucose have a half-life of under one minute (Stitt *et al.*, 1980; Arrivault *et al.*, 2009). Pool lifetimes this short mean that TPU limitation can build up and diminish very rapidly. Over a longer timeframe, a greater sink can be important in freeing up short-term sinks. It has been reported that defruited wheat experiences significant downregulation of photosynthesis (King *et al.*, 1967), though not all

plants experience this effect (Farquhar & von Caemmerer, 1982). Buildup of sucrose in source leaves could result in reduced TPU capacity due to reduced sucrose-phosphate synthase activity as shown in some experiments (Huber, 1981; Paul & Foyer, 2001), or increased invertase activity (Mengin *et al.*, 2017). In some experiments using conditions consistent with TPU limitation, starch builds up and causes a decline in photosynthetic rate (Sasek *et al.*, 1985; Peet *et al.*, 1986; Ramonell *et al.*, 2001). The source of this decline is still to be conclusively determined. A long-term sink which can absorb carbon will allow the plant to recover (Sasek *et al.*, 1985; Arp, 1991).

TPU and plant nutrition

TPU limitation is often incorrectly interpreted as a nutritional deficiency. It is true that plants transferred to media without any phosphate experience significant reduction in photosynthetic capacity (Brooks, 1986; Foyer & Spencer, 1986). However, less dramatic differences in phosphate nutrition result in relatively small changes in photosynthetic rate. This is due to the vacuole buffering phosphate concentration in the rest of the cell on an hours timescale (Rebeille *et al.*, 1983; Woodrow *et al.*, 1984). Under increased or decreased phosphate nutrition, large changes in vacuolar phosphate concentration are seen, but only relatively small changes are seen in plastidic phosphate concentration (Rebeille *et al.*, 1983; Foyer & Spencer, 1986). Plants grown with different phosphate nutrition are therefore not significantly more or less likely to experience TPU limitation. Most phosphate in photosynthesizing cells will be used by nucleic acids and phospholipids (Dissanayaka *et al.*, 2018) and growth is more sensitive to phosphate nutrition than is photosynthetic rate (Mo *et al.*, 2018). Ellsworth *et al*. (2015) showed a survey of Australian plants growing in the wild with

varying phosphate availability were adapted to their environment, and TPU limitation was more likely at ***high*** phosphate nutrition. Furthermore, TPU limitation can only be seen when the plant is photosynthesizing very quickly, which usually cannot be seen if the plant is nutritionally deprived. Plants with reduced nitrogen were not capable of photosynthesizing quickly enough to reach TPU limitation (Sage *et al.*, 1990).

Oscillations

Oscillations in carbon assimilation rate are a common side-effect of TPU limitation (Ogawa, 1982; Sivak & Walker, 1986, 1987). They are typically seen after a perturbation in the environment of a plant that results in high photosynthetic rates, such as sharp increases in illumination or CO_2. Oscillations then continue without further input for a variable amount of time. Oscillations include tandem changes in carbon assimilation and fluorescence parameters, indicating simultaneous changes in both the light reactions and the Calvin-Benson cycle (Ogawa, 1982; Walker *et al.*, 1983; Peterson *et al.*, 1988; Stitt & Grosse, 1988). The amplitude of oscillations can increase with conditions that further exacerbate TPU limitation, such as low temperature or low O_2 (Peterson *et al.*, 1988; Stitt & Grosse, 1988). Oscillations showed a significant impact on organic phosphates and their relevant ratios, notably large initial spikes in PGA, reduction in RuBP and ATP pools (Sharkey *et al.*, 1986c; Sage *et al.*, 1988; Stitt & Grosse, 1988; Laisk *et al.*, 1991).

A few models have been produced to explain oscillations. The most significant theory is that there is a delay in activation of sucrose synthesis after a photosynthetic increase that causes oscillations (Laisk & Walker, 1986). The delay may also originate from cytosolic fructose-1,6-bisphosphatase inhibition by fructose-2,6-bisphosphate (Stitt *et al.*, 1984; Laisk &

Eichelmann, 1989; Laisk *et al.*, 1989) or post-translational regulation (Huber & Huber, 1996). An additional interpretation of these oscillations has been proposed originating from the light reactions, with damping caused by a slow leak of protons across the thylakoid membrane (Kocks & Ross, 1995).

Environmental impact

The changing climate, resulting, in large measure, from increasing CO_2 in the atmosphere, has the potential to affect the frequency and severity of TPU limitations to photosynthesis. Since this syndrome occurs when carbon fixation and light capture have a greater capacity than end product synthesis, increasing CO_2 should increase the occurrence of TPU limitation. However, because TPU is stimulated by increasing temperature, there could be a reduction in the occurrence of TPU limitation in the future. It is hard to predict which effect will dominate, and whether TPU limitation will be observed more or less frequently based on climate change predictions. However, beyond the short-term effects of temperature and CO_2 it is important to consider how the plant responds when it is TPU-limited. Generally, plants growing in elevated CO_2 show less propensity for TPU limitation because they have reduced capacity for other processes in photosynthesis (Sage *et al.*, 1989). This suggests that plants cannot or do not make full use of the greater potential for photosynthesis. We hypothesize that understanding TPU will help in predicting acclimation responses of plants to increasing atmospheric CO_2. How plants might acclimate could depend on such things as stochasticity of their environment and the typical day/night change in temperature. If night (and dawn) temperature rises more than day temperature this could affect optimal TPU capacity.

It is often found that TPU-limitation occurs whenever photosynthesis is stimulated to be about 20% higher than was occurring in the plant under natural conditions (Yang *et al.*, 2016). Increasing CO_2, decreasing oxygen, or lowering the temperature usually allows TPU-limitation to be observed. In a large study of published A/C_i curves Wullschleger (1993) found 23 cases (out of 109) where investigators reported TPU limitations. It is likely that the phenomenon is observed but not recognized much more often. For example, a curve presented in Wullschleger *et al*. (Figure 1B, taken from Ireland *et al.*, 1988) shows evidence of TPU-limitation but this was not one of the 26 instances of TPU limitation cited. It is common for the TPU limitation to be ignored even when it is evident in data.

Since the components of photosynthesis must all work in concert and in strict stoichiometry, it is not surprising that there might be a relationship between V_{cmax} and TPU capacity. This has been invoked in global models of photosynthesis although many models do not include TPU. Lombardozzi *et al*. (2018) used several estimates of the ratio of V_{cmax} and TPU capacity and concluded that current global models may overestimate how much CO_2 will be fixed by plants in the future because TPU-limitations, or adjustments to avoid TPU limitation, will reduce photosynthetic capacity. It is important to realize that even though plants growing in elevated CO_2 do not show TPU-limitation, TPU still may be setting an upper bound and that plants adjust other capacities to keep below the upper bound of TPU because TPU can cause damage.

Conclusions

TPU is a metabolic condition that incorporates numerous signals to reflect the state of photosynthesis across the whole cell. Most metabolites in the chloroplast are phosphorylated,

and so phosphate can reflect the metabolic state of the chloroplast. Phosphate is linked through the cytosol, where sucrose synthesis takes place, and thus phosphate represents photosynthetic state across all chloroplasts. Phosphate concentrations are carefully regulated, and TPU limitation is very unlikely to be found at ambient conditions. A low phosphate level naturally signals to the other processes that photosynthesis is very fast, kinetically controls the ATP synthase, and leads to downstream effects on photosynthesis by accumulation of PMF and engaging *qE*. The reduction in phosphate signals the plant to build up starch by relieving phosphate inhibition of ADP-glucose pyrophosphorylase (Preiss, 1982). Plants which are photosynthesizing slowly can reduce their TPU capacity, which will lower their phosphate regeneration, helping to produce starch and prevent cycle collapse from over-export of triose phosphates; conversely, increasing TPU capacity in plants which are photosynthesizing quickly will raise their phosphate regeneration and help produce ATP. In this way, TPU sets the span on expected photosynthesis. We believe that the gas exchange behavior in TPU conditions reflects several important regulatory features. Yet, the role of TPU as regulation is relatively unexplored. Experimental determination of the molecular mechanisms that underpin this system, and ecological studies to examine the broader effects of TPU are exciting future directions in this field.

A number of misconceptions cloud the field in regards to TPU. Even the term "TPU" can now be seen not to be wholly accurate. It largely describes phosphate metabolism, but not all effects on carbon metabolism related to phosphate can be accurately described as triose phosphate usage. At steady state, there are other sources of phosphate release that contribute to the assimilation cap. Amino acid release from photorespiration, MEP and shikimate

pathways, and other carbon sinks for Calvin-Benson cycle intermediates will all contribute to the maximal assimilation rate when photosynthesis is TPU limited. An alternative view is that all Calvin-Benson cycle exports are downstream of TP, and thus constitute a form of TPU. The specific terminology and nuance are less important than the total understanding, which is that TPU limitation is the result of insufficient capacity for carbon export from the Calvin-Benson cycle. Other carbon metabolism pathways in the chloroplast that do not immediately originate in the Calvin-Benson cycle, while important for the overall physiology of the plant, will not be discernible in gas exchange measurements.

Maintaining TPU limitation is unhealthy for the plant due to risk of oxidative stress from photosystem oxidation (Pammenter et al., 1993). Electron transport regulation as assessed by chlorophyll fluorescence quenching analysis and deactivation of rubisco lead to an overall slowing of photosynthesis lower than TPU, eventually reaching a steady state with assimilation rate based on the rate of TPU (Sharkey *et al.*, 1988). Excess assimilation when already low on phosphate would further deprive ATP synthase of phosphate it needs. Contrary to what one might expect given the term "TPU limitation," triose phosphates do not necessarily need to build up, though phosphate levels should be low (Sharkey & Vanderveer, 1989). This is why plants can be drained of phosphate via mannose or deoxyglucose feeding and be TPU limited (Herold & Lewis, 1977; Herold, 1980; Sivak & Walker, 1986). It is the relationship between the need for phosphate for ATP synthase and the phosphate sensitivity of starch and sucrose synthesis that results in TPU (Herold, 1980).

CHAPTER II

The time course of acclimation to the stress of triose phosphate use limitation

In revision for publication in Plant Cell and Environment, 2022

Abstract

Triose-phosphate utilization (TPU) limits the maximum rate at which plants can photosynthesize. However, TPU is almost never found to be limiting photosynthesis under ambient conditions for plants. This, along with previous results showing adaptability of TPU at low temperature, suggests that TPU capacity is regulated to be just above the photosynthetic rate achievable under the prevailing conditions. A set of experiments were performed to study the adaptability of TPU capacity when plants are acclimated to elevated CO_2 concentrations. Plants held at 1500 ppm CO_2 were initially TPU limited. After 30 hours they no longer exhibited TPU limitation, but they did not elevate their TPU capacity. Instead, the maximum rates of carboxylation and electron transport declined. A time course of regulatory responses was established. A step increase of CO_2 first caused PSI to be oxidized but after 40 s both PSI and PSII had excess electrons because of acceptor-side limitations. Electron flow to PSI slowed and the proton motive force increased. After 30 hours, non-photochemical quenching reduced electron flow sufficiently to balance the TPU limitation. Over several minutes rubisco deactivated contributing to regulation of metabolism to overcome the TPU limitation.

Introduction

Photosynthesis, as measured by gas exchange, is typically assessed by the three canonical biochemical limitations of photosynthesis: the rubisco limitation, where carbon dioxide uptake is modeled assuming ribulose 1,5-bisphosphate (RuBP)-saturated rubisco kinetics; the RuBP regeneration limitation, where carbon dioxide uptake is modeled assuming a fixed rate of RuBP use as allowed by the production of electron transport products, ATP and NADPH; and the triose phosphate utilization (TPU) limitation, where carbon dioxide uptake is

modeled as the rate of production of end products, freeing inorganic phosphate from organic phosphates (McClain & Sharkey, 2019). The TPU limitation is not always observed and whether it should be included in models of global photosynthesis has been debated (Lombardozzi *et al.*, 2018; McClain & Sharkey, 2019; Rogers *et al.*, 2020).

The TPU limitation is unique among the three biochemical limitations in that it is limited by processes downstream of the Calvin-Benson cycle. Rather than running carbon fixation and electron transport as efficiently as possible, regulatory mechanisms are engaged to slow down the rate of carbon assimilation (*A*) so as not to outpace the rate of end-product synthesis. Energy-dependent quenching (q_E) is activated (Sharkey *et al.*, 1988) by elevated ΔpH across the thylakoid membrane, one component of proton-motive force (PMF) (Kramer & Crofts, 1996). The elevated ΔpH results from kinetic and thermodynamic restrictions on the ATPase due to lowered levels of available inorganic phosphate (Sharkey & Vanderveer, 1989). In addition, rubisco activation state decreases (Sharkey *et al.*, 1986a; Socias *et al.*, 1993), which may alleviate pressure on phosphate pools by limiting the maximum rate that carbon can be added to the organic phosphate pool. Because TPU limitation restricts the rate of photosynthesis rather than the availability of light, there is a potential for photodamage unless regulatory mechanisms are engaged (Powles, 1984; Pammenter *et al.*, 1993; Li *et al.*, 2002).

These regulatory mechanisms are the only aspects of TPU limitation typically observed in steady-state gas exchange. While TPU limitation results in and can be assessed through gas exchange as O_2- and CO_2-insensitive photosynthesis (Sharkey, 1985a) or reverse sensitivity to O_2 (Viil *et al.*, 1977) or CO_2 (Jolliffe & Tregunna, 1973), it is easier to assess by the decline in electron transport rate associated with q_E when CO_2 is increased or O_2 is decreased. The

appearance of transient effects on photosynthesis associated with TPU limitation (Ogawa, 1982; Walker *et al.*, 1983) lead us to believe that, in the steady state, the rate of photosynthesis is not set by TPU, but instead, the rate is set by regulatory mechanisms that match the rates of carbon input to and carbon output from the organic phosphate pool.

TPU capacity does not require many resources. The nitrogen required for rubisco and photosynthetic electron transport far exceed those required for TPU and subsequent end product synthesis (Evans & Clarke, 2019). When TPU occurs, rubisco is deactivated and q_E is increased reducing the efficiency of nitrogen use in both carbon metabolism and electron transport. Entering TPU limitation forces deactivation of systems which use much more nitrogen, an ideal plant would never experience TPU limitation under physiological conditions. However, TPU limitation is commonly seen when the photosynthetic rate is only a few percent higher than what the plant experiences in ambient conditions (Yang *et al.*, 2016). There are a few possible reasons why excess TPU capacity would be detrimental. A precise balance of phosphate flux could control stromal inorganic phosphate concentration, affecting the partitioning of carbon into starch (Preiss, 1982; Escobar-Gutiérrez & Gaudillère, 1997). If TPU capacity were in excess, it could also limit the ability to build up a PMF across the thylakoid membrane because there would be plentiful phosphate available to the ATPase, preventing any kinetic or thermodynamic restriction to proton flow. The elevated ΔpH and consequent low luminal pH can activate energy-dependent quenching mechanisms that dissipate light energy to safeguard the photosystems.

If TPU capacity is inexpensive in terms of nitrogen cost, but is typically just above ambient photosynthetic rates, we would expect that TPU capacity is plastic. It has been found

that TPU capacity is flexible, and in many cases changes in response to environmental conditions. Plants grown at low temperature can develop additional sucrose synthesis enzymes (Cornic & Louason, 1980; Guy *et al.*, 1992; Holaday *et al.*, 1992) which alleviates cold-induced TPU limitation (Sage & Sharkey, 1987). Plants with reduced access to CO_2 have reduced TPU capacity to match their lowered photosynthetic rate (von Caemmerer & Farquhar, 1984; Sharkey & Vassey, 1989). It has therefore been shown that TPU capacity can both increase and decrease in response to environmental conditions. This is reflected in environmental surveys, and plants have rarely been found to be TPU limited under ambient conditions in the field (Sage & Sharkey, 1987; Ellsworth *et al.*, 2015). For this reason, TPU limitation is often not included in global models of photosynthesis (Lombardozzi *et al.*, 2018; Rogers *et al.*, 2020).

Ideally, if a plant is TPU limited, it will increase its TPU capacity to maximize the overall rate of photosynthesis, but it is also possible that rubisco capacity and electron transport capacity will be decreased to match TPU capacity. In practice the TPU behavior is induced by reducing the temperature, lowering the oxygen partial pressure, or increasing the partial pressure of CO_2. Because low temperature has been shown to cause adaptation of TPU capacity, we used high CO_2 to induce TPU limitation to make a comparison of the adaptation. We tested the acclimation of plants to TPU limitation by exposure to elevated CO_2 to determine whether plants eventually stop being TPU limited, and if they achieve this by increasing their TPU capacity. In addition, we established a timeline of the regulatory features surrounding TPU limitation, from how the plant handles the initial influx of energy until the plant engages slower regulatory features, such as rubisco deactivation and energy-dependent quenching.

Methods

Growth of plant materials

Nicotiana benthamiana was found to exhibit very reproducible TPU behavior and so was the species used here. Seeds were germinated in 2 l pots of potting media consisting of 70% peat moss, 21% perlite, and 9% vermiculite (Suremix; Michigan Grower Products Inc., Galesburg, MI, USA) in a greenhouse from June-August. This greenhouse is located at 42°43'N, 84°28'W, East Lansing, Michigan, USA. Typical daylight PAR levels inside the greenhouse were between 300-700 µmol m^{-2} s^{-1}, and the temperature was controlled to 27°C during the day and allowed to fall to as low as 18°C at night, though nighttime temperatures typically did not reach this low. Plants were watered with half-strength Hoagland's solution (Hoagland & Arnon, 1938) as needed as juveniles and then daily as adults. Plants were used for experiments from 6-7 weeks of age.

Combined gas exchange, fluorescence, and electrochromic shift measurements

A LI-COR 6800-12A clear-top chamber (LI-COR Inc., Lincoln, NE, USA) was modified to incorporate an optical bench for making measurements. The bottom plate of the clear top chamber was removed and replaced with a 3D-printed backplate with an infrared and an optical detector. These detectors were connected to an Idea Spec (Hall *et al.*, 2013). A front plate was also 3D printed to secure a scattering optic to the top of the 6800-12A. Behind the scattering optic was an array of LEDs containing eight actinic blue and red LEDs, capable of producing up to 2,500 µmol m^{-2} s^{-1} constantly or a saturating flash up to 15,000 µmol m^{-2} s^{-1}, at an approximately 90% red/10% blue ratio. Measuring LEDs for electrochromic shift (ECS) were 520 nm, with 505 nm and 535 nm as correction wavelengths for zeaxanthin and q_E effects on

the 520 nm signal. Measuring lights for PSI measurements were at 820 nm with 910 nm as a correction wavelength. Measurements of chlorophyll fluorescence used the 520 nm LEDs as an excitation light. Measurements of PSI were performed according to Kanazawa *et al.* (2017) and measurements of ECS were performed according to Takizawa *et al*. (2007). These modifications to the chamber allowed high precision optical measurements simultaneous with high precision gas exchange measurements, especially *A* and intercellular CO_2 partial pressure (C_i) allowing construction of A/C_i curves.

Protocol for repeated A/Ci measurements

Repeated A/C_i responses were determined on the same leaves to test the acclimation of the major A/C_i curve parameters to TPU-limiting conditions. Plants were exposed to the high CO_2 partial pressure to induce TPU. The A/C_i measurements were performed by a visual basic script controlling a set of flow controllers attached to the inlet of a LI-COR 6800. Oxygen was held constant at 210 kPa (21%), CO_2 was varied to achieve ranges of CO_2 mole fractions from 50 to 1500 ppm, and humidified nitrogen made up the balance. (It is generally preferred to express gas levels as partial pressure but since we mixed gases by volume we use mole fractions generally μmol mol^{-1}, ppm.) Plants were acclimated to ambient CO_2 (about 400 ppm) for an hour after dawn before the first curve. During the first 15 min of this acclimation period, light levels were gradually raised until 1000 μmol m^{-2} s^{-1}. After that point, A/C_i curves were measured every 2.5 h until an hour before dusk, and the plants were given 8 h of darkness, then an hour of acclimation to the light the next day before resuming curves every 2.5 h. From the end of the first curve until the end of the experiment, plants were subjected to an experimental level of

CO_2, either 150 ppm (low), 400 ppm (ambient), or 1500 ppm CO_2 (elevated). Curves were analyzed according to Gregory *et al.* (2021).

High density optical measurements

To create the timeline of optical measurements after the imposition of TPU limitation, plants were first acclimated at 400 ppm CO_2 and 1000 µmol m^{-2} s^{-1} light in the chamber of the modified 6800-12A clear-top chamber. A list of times from 10-200 s was randomized by script, and for each time interval a second script was run. This script controlled a flow controller to rapidly switch the plant from 400 ppm CO_2 to 1500 ppm CO_2. A measurement of electrochromic shift was made by dark interval relaxation kinetics (DIRK) (Takizawa *et al.*, 2007) after the chosen time period. Ten s later, a measurement of PSI oxidation state decay and reoxidation by saturation flash was made. Leaves were then incubated at 400 ppm CO_2 for 10 min. The process was then repeated, but instead of a DIRK to measure ECS, a saturation flash was given to assess PSII characteristics, including the quantum efficiency of photosystem II (φ_{II}) (Baker, 2008) and oxidation status of the quinone Q_a, measured as q_L (Kramer *et al.*, 2004). Leaves were again incubated at 400 ppm CO_2 for 10 min. This process was repeated for every time interval in the list. This protocol was used so that the disruptive saturating flash did not affect subsequent measurements in the time course.

Rubisco activation state assay

N. benthamiana leaves were incubated at 400 ppm CO_2 until they reached steady state photosynthesis, then the CO_2 was switched to 1500 ppm for a specified time. The plants were then sampled by freeze-clamp (Schrader *et al.*, 2004). Rubisco activation state was assayed according to Li *et al.* (2019).

Results

Intermittent A/Ci curves show adaptation of photosynthetic processes over time

Plants were exposed to each CO_2 condition for 30 h, and A/C_i responses were determined before the start and then every 2.5 h after imposing the CO_2 treatment to assess any changes in photosynthetic parameters (Figure 2.1). After a 16-h day, plants were given an 8-h night and then an hour to acclimate to the light before resuming photosynthetic experiments. For all three conditions, V_{cmax} and J, as determined by the fitting routine of Gregory *et al.* (2021), declined over the first day. The decline in V_{cmax} and J was comparable for the low CO_2 and ambient CO_2 conditions, and the difference between the two treatments was not significant at $P \leq 0.05$ by two-sided t-test at any time in the first day except for in V_{cmax} at 12.5 hours. There was a significant difference ($P \leq 0.05$ by two-sided t-test) between the decline in V_{cmax} and J_{max} in elevated CO_2 condition compared to either of the other treatments at every sampled treatment time during the first day, excluding the 0-time point before treatment began. V_{cmax} for the elevated CO_2 plants declined by 25% before the first treated A/C_i and did not recover even overnight. J for the elevated CO_2 condition did not fully recover overnight, indicative of persistent photoinhibition. TPU capacity decreased relative to the pre-treatment A/Ci at all timepoints during treatment in the first day for elevated CO_2 treated plants, $P<0.05$ by one-sided t test.

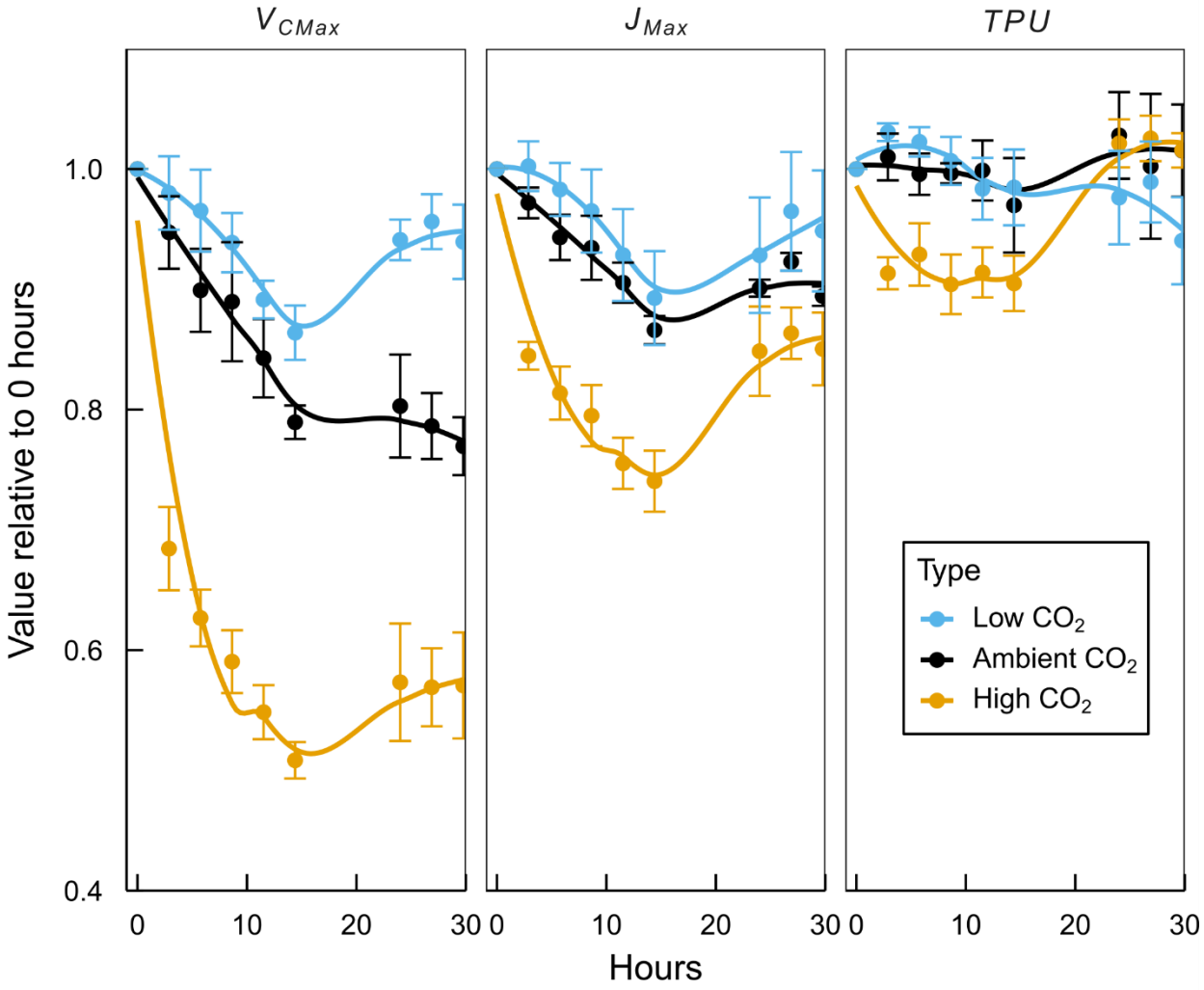

Figure 2.1 Plants were exposed to high (1500 ppm) ambient (400 ppm) or low (150 ppm) CO_2 for 30 h, including an 8-h dark period during the typical night hours, with *A/Ci* curves performed every 2.5 h. The *A/Ci* curves were fit according to Gregory *et al.*, (2021) and the three primary fit parameters, V_{cmax}, *J*, and *TPU* are plotted relative to an *A/Ci* curve run before treatment began (0 time point). Five separate plants were used for each treatment, and the error bars represent mean and standard error.

After acclimation to elevated CO_2, plants no longer appear to be TPU-limited

After the 30-h acclimation period, plants no longer showed the responses to elevated CO_2 that indicate TPU limitation. The reduced or inverse response of A to CO_2 was gone (Fig 2.2). The expected CO_2-dependent decline of φ_{II} was absent after acclimation. Elevated nonphotochemical quenching (NPQ_t) at high CO_2, one of the effects that causes the decline in φ_{II}, was gone after acclimation. TPU limitation is expected to decrease proton conductivity across the thylakoid membrane (g_{H+}), causing an increase in PMF (measured as total electrochromic shift, ECS_t). These effects were still evident after adaptation, but adapted plants showed a reduced response of ECS_t to increasing CO_2 relative to the pre-adaptation plants (Fig 2d,e). The increase in ECS_t is lower at all [CO_2] greater than 400ppm for adapted plants. Based on the absence or decline of these physiological effects, we argue that the plants no longer experienced TPU limitation after acclimation, though not as a result of increased TPU capacity.

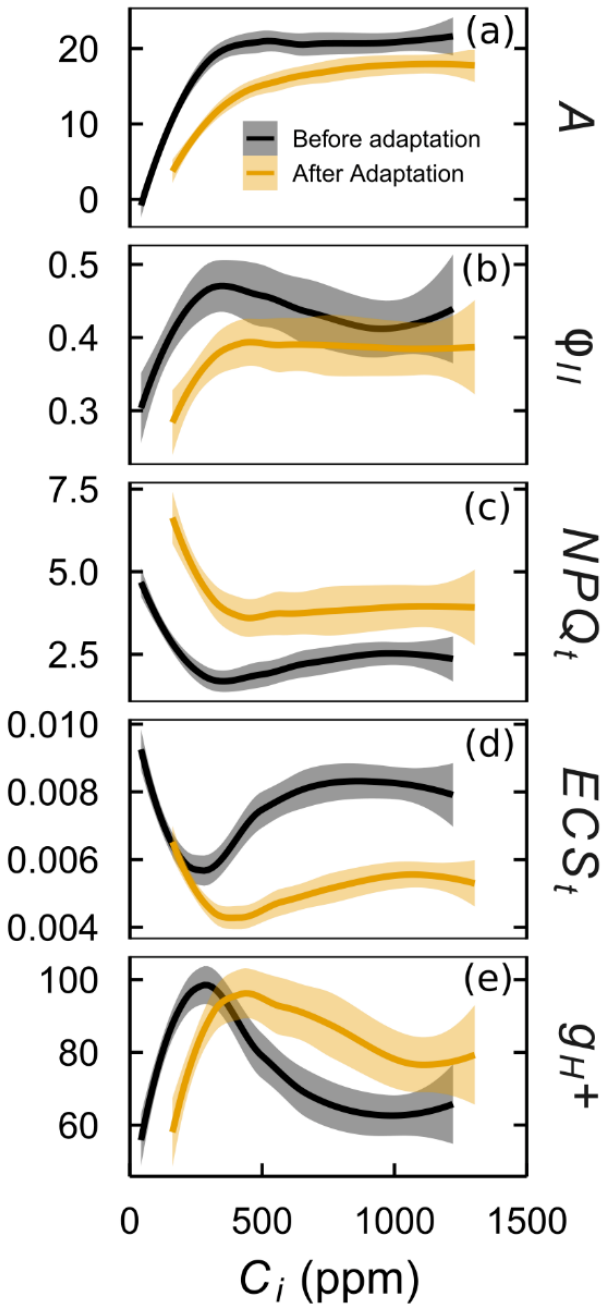

Figure 2.2 CO_2 assimilation and optical measurements from an A/C_i curve before and after a 30 h 1500 ppm CO_2 treatment. After 30 h in elevated CO_2, parameters show acclimation to TPU-limiting conditions, including reduced response of assimilation (a), φ_{II} (b), NPQ_t (c), and ECS_t (d) to increasing CO_2. The clouds are LOESS fitting (LOcal Estimation of Scatterplot Smoothing) 95% CI n=5.

Lowered rubisco activation state was a persistent effect in adaptation to TPU stress

Rubisco activation state was measured over the course of adaptation to elevated CO_2. Rubisco activation state declined over a few min (Figure 2.3c) and remained low over the course of adaptation (Figure 2.3a). The prominent decline in V_{cmax} is also an indicator of reduced rubisco activation state (Figure 2.1). In addition, the total activatable rubisco activity decreased over the course of adaptation to elevated CO_2 (Figure 2.3b). The decline in rubisco activation state caused by 2.5 h elevated CO_2 is recoverable within 10 min (Fig 3d).

Detailed kinetics of photosynthetic processes in response to CO_2 pulses

A step change in CO_2 to levels that cause TPU limitation induced kinetics in the electron transport chain (Figure 2.4). There were several kinetic stages. At first, the elevated CO_2 allowed a faster use of electrons, and PSI became oxidized (Figure 2.4b). The plant had not yet entered TPU limitation, as indicated by the high proton conductivity of the ATP synthase (g_{H+}) (Figure 2.4e). The second phase (Figure 2.4, blue), beginning 40 s after the step change in CO_2 flow and persisting until 80 s after the beginning of CO_2 flow, was characterized by the reduction of Q_a (Figure 2.4c) [q_L is a fluorescence-based measure that increases with increased oxidation of Q_a (Kramer *et al.*, 2004)]. The reduction of Q_a caused an increase in φ_{NPQ} (Figure 2.4g) and a decrease in φ_{II} (Figure 2.4f) even though NPQ (Figure 2.4i) [measured using the NPQ_t parameter (Tietz *et al.*, 2017)] did not respond within this timeframe.

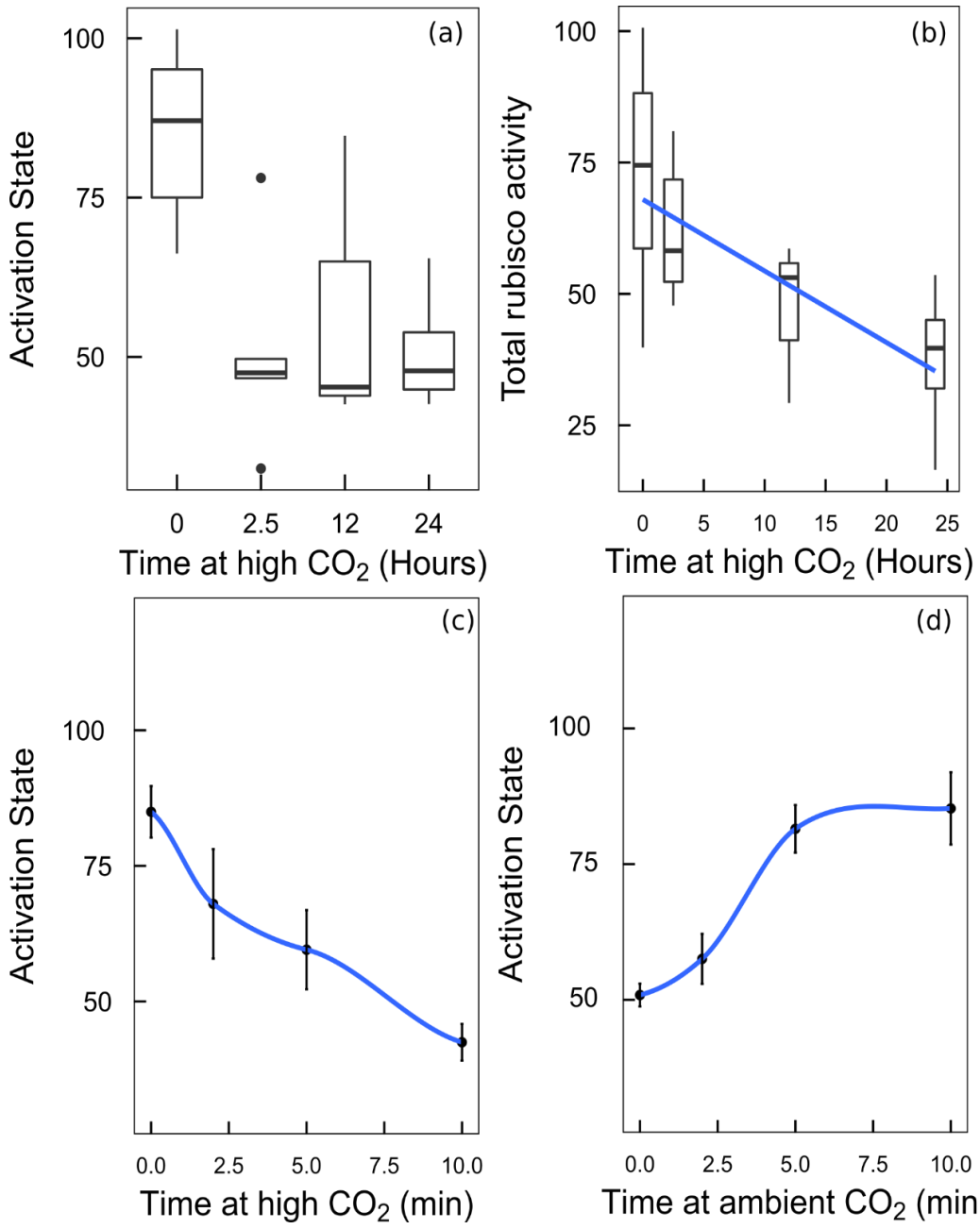

Figure 2.3 TPU limitation causes reduced rubisco activation state percentage that persists for an extended period. Rubisco activation state (a) and total activity (b) are measured at 0, 2.5, 12, and 24 h to show changes in activity over the course of a day's acclimation. Slope of the decline in total rubisco activity is significant at $P<0.05$. Rubisco activation state decreases to its minimum within 10 minutes (c), and activation state is not significantly different after 10 m and 2.5 h (d, 0 time). After 2.5 h at elevated CO_2, activation state recovers completely after 5 m (d), with activation state 5 m into recovery not significantly different from the 0 m unadapted activation state (c, 0 time) by two-sided t test.

The reduction of Q_a was correlated with the reduction of PSI. The kinetic constant for reduction of PSI by cytochrome b_6f (k_{et}, Figure 2.4d), decreased, so we conclude that the reduction of PSI was not due to excess electrons being transported downstream. Therefore, the reduction of PSI must be due to an acceptor-side limitation of PSI, indicating a lack of availability of $NADP^+$. In the same stage, a decline in g_{H+} can be seen, decreasing by over 50% (Figure 2.4e). The low g_{H+} that was observed has been shown to be associated with TPU limitation (Kiirats *et al.*, 2009; Yang *et al.*, 2016). The third kinetic stage (Figure 2.4, green) began 80 s after the beginning of the CO_2 step change and exhibited slower regulatory mechanisms. Proton-motive force (Figure 2.4h) increased up to this point, and continued to increase during this phase, which caused an increase in energy-dependent NPQ_t (Figure 2.4i), and a decrease in k_{et} (Figure 2.4d). These mechanisms prevent electrons from reaching PSI, alleviating the over-reduction of PSI. After the PMF increased sufficiently, photosynthesis entered a new steady-state (Figure 2.4, red).

The interpretation of PSI acceptor-side limitations is supported by the observed response of PSI oxidation state to flashes of saturating light (Figure 2.5). Leaves were given a brief dark interval to allow reduction of PSI and then PSI was oxidized by a saturating flash. When tested in the middle of TPU-induced transients (Figure 2.5a), PSI did not remain oxidized by the saturating flash, and instead began re-reducing due to inability to pass electrons to $NADP^+$. Tests made some time after the onset of TPU-limiting conditions showed less re-reduction (Figure 2.5b), and with more time, re-reduction was much less prominent (Figure 2.5c).

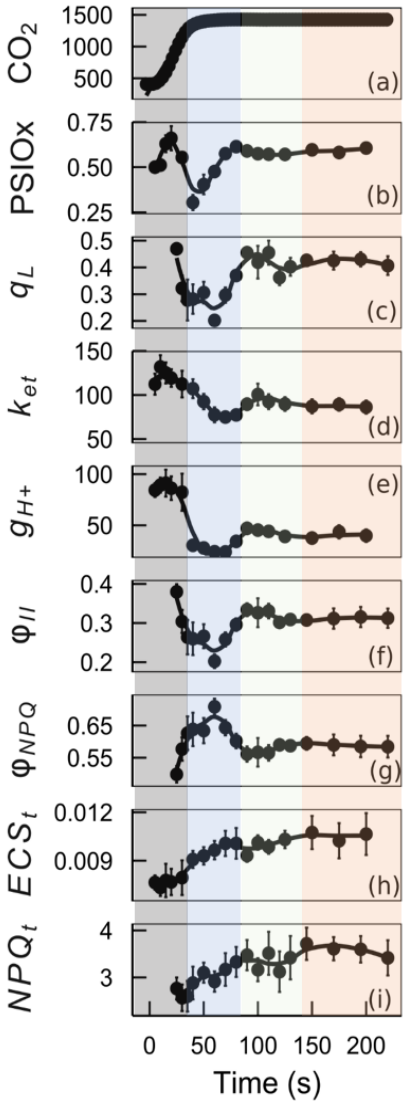

Figure 2.4 Plants are given a step change in [CO_2] from 400 to 1500 ppm, which induces oscillations in electron transport. Plants are held at 1500 ppm CO_2 for a randomized length of time (x-axis) then measurements of their PSI and PSII activity are taken, along with electrochromic shift. The data is divided into four putative kinetic periods. In the first phase (grey region), photosynthesis is unlimited by TPU and PSI becomes more oxidized (b). The second phase (blue) is the onset of TPU limitation and notably affects proton flow across the thylakoid membrane (g_{H+}, e), PSI oxidation state (b) and Q_a oxidation state (measured as q_L, c). Reduction of Q_a causes energy diversion from photochemistry (φ_{II}, f) to nonphotochemical quenching (φ_{NPQ}, g). The third phase (green) begins when proton-motive force (measured as ECS_t, h) increases along with energy dependent quenching (NPQ_t, i) and photoprotection at cytochrome *b6f* complex (d). Finally, electron transport enters a new steady-state (red). Dots represent mean value and error bars are standard error, n=5.

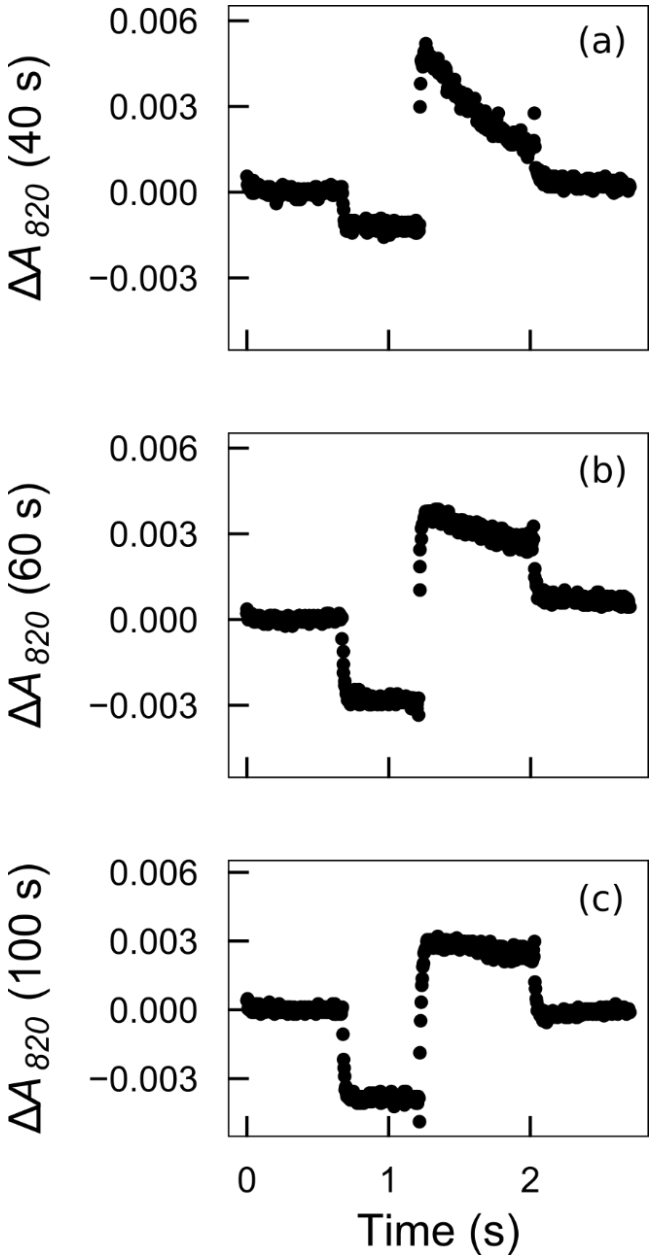

Figure 2.5 Three example traces of PSI measurements from oscillations in PSI reduction induced by step change in CO_2 from 400 to 1500 ppm, which demonstrate varying levels of re-reduction during saturating flashes. Plants at steady state are subjected to a 0.5 s dark period, causing reduction of PSI (ΔA_{820} decreases). Then, a saturating flash is applied to oxidize PSI (ΔA_{820} increases), before returning to steady state. Typically, a saturating flash should fully oxidize PSI, but kinetics in electron transport can change this. (a) Extreme re-reduction of PSI can be seen during a saturation flash when PSI is most reduced, 40 s after beginning an elevated CO_2 pulse. (b) Less re-reduction of PSI during a saturation flash is seen when PSI is less reduced, 60 s after a CO_2 step change. (c) 100 s after the CO_2 step change, PSI re-reduction is much reduced.

Transient response to TPU limitation is lost after acclimation

Five plants were tested for transient responses to TPU-limiting conditions before and after a 24-h acclimation to elevated CO_2 (Figure 2.6). A list of time points from 10-200 seconds was randomized by R script; for each plant the randomization was different. For each time-point, plants were given 10 min at ambient CO_2 (400 ppm) before pulsing with high CO_2 (1500 ppm) at the end of which chlorophyll fluorescence parameters were measured. Non-adapted plants exhibited a transient reduction of Q_a to a minimum of 21% following the introduction of TPU-limiting conditions, resulting in partitioning of energy into *NPQ* rather than photochemistry. After adaptation, plants did not exhibit reduction of Q_a significantly below the steady-state value in the elevated CO_2 environment.

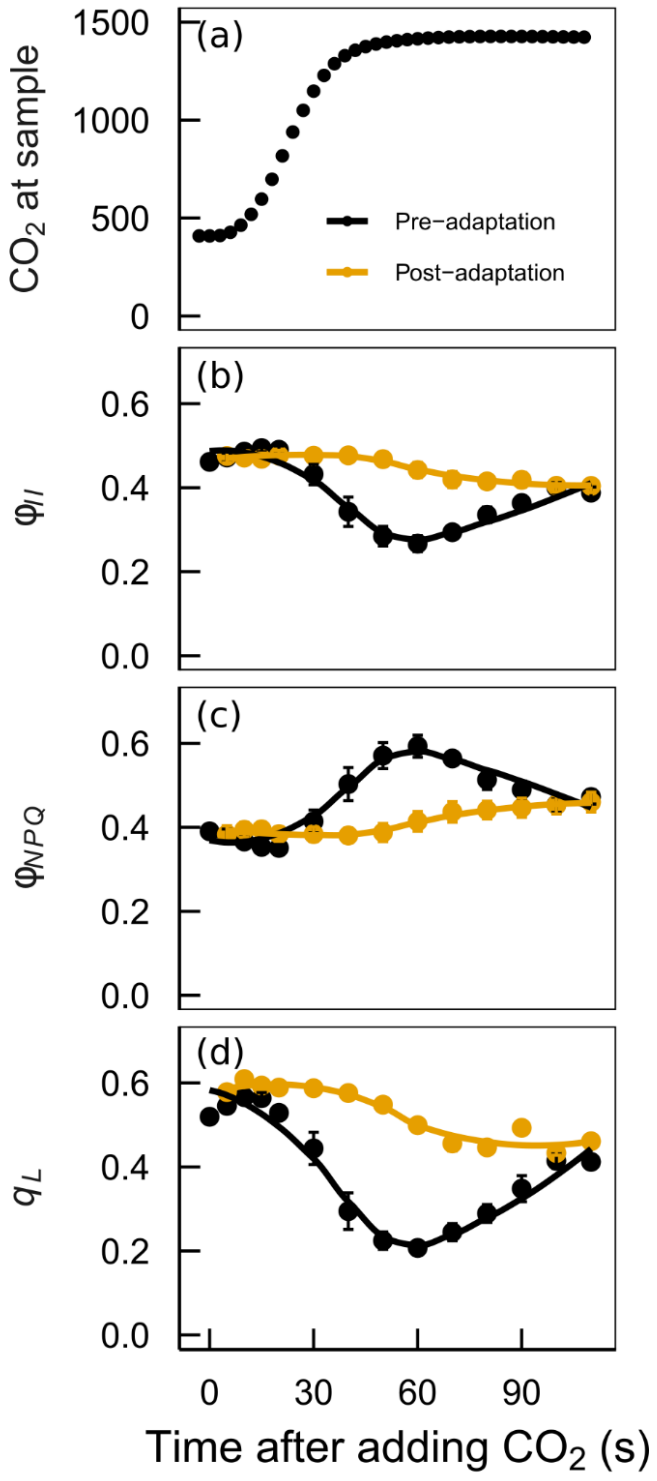

Figure 2.6 Oscillations are not seen following a step change in CO_2 in plants that have acclimated to elevated CO_2 for 30 h. The hallmark reduction of Q_a, measured here as q_L, is not seen, and so more energy is not diverted into non-photochemical quenching (φ_{NPQ}). Dots and bars represent mean ± standard error, n=5

Discussion

Fast onset kinetics in responses to TPU limitation are directed by electron build-up on Q_a

When plants were subjected to TPU-limiting conditions, the most immediate effects were transient changes in the redox states of electron transport components. It is known that while TPU-limited, increasing CO_2 levels cause a reduction in φ_{II} because, while *A* cannot increase, the rate of photorespiration will go down (Stitt, 1986; Sharkey *et al.*, 1988; Stitt & Grosse, 1988). This, combined with the common observations of elevated *PMF* and non-photochemical quenching during TPU limitation, indicates the importance of q_E in dissipating absorbed light energy when electron transport capacity exceeds TPU capacity. However, q_E does not activate instantaneously, with the xanthophyll cycle and PSBS recruitment to the reaction center operating on the minutes timescale (Li *et al.*, 2002). Therefore, we could reasonably predict excess accumulation of electrons on electron transport intermediates and PSI electron acceptors. Reduction of Q_a decreases the quantum efficiency of photochemistry because PSII cannot accept any more energy. The energy that would be going towards photochemistry is instead shunted to nonphotochemical quenching, resulting in an increased yield of nonphotochemical quenching. This means that φ_{NPQ} increases even though NPQ_t changes on a slower timescale. Immediately after entering TPU limitation, electrons build up on the electron transport chain due to decreased electron sink strength, and the bulk of the excess energy is most immediately handled by controls within the electron transport chain.

Though the reduction of Q_a reduces the yield of photochemistry, the reduction of PSI following the imposition of TPU limitation is more concerning. Acceptor-side limitation of PSI is highly stressful due to the accumulation of ROS (Li *et al.*, 2009) and the inability of PSI to repair

itself (Sonoike, 1996, 2011). Electron transfer to PSI from the cytochrome *b6f* complex is slowed by elevated PMF due to the requirement to oxidize plastoquinol (Kramer & Crofts, 1993, 1996). We found, however, that PMF does not build up fast enough to adjust to the limiting demand from the Calvin-Benson cycle and regulate electron flow to PSI, and electrons do indeed accumulate on PSI. This is not due to an accelerated rate of PSI reduction through the cytochrome *b6f* complex (k_{et}, Figure 2.4), so it must instead be due to an acceptor side limitation of PSI because of a lack of $NADP^+$. Increasing $[CO_2]$ under TPU limitation reduces the rate of photorespiration, and if *A* cannot increase due to TPU limitation the overall rate of consumption of both ATP and NADPH decreases. The NADPH pool turnover (half-time 0.01 s^{-1}) is faster than that of ATP (half-time 0.28 s^{-1}, Arrivault *et al.*, 2009), so the reduced consumption of electron transport products will affect $NADP^+$ availability first. Restriction of NADPH oxidation has been suggested previously as the cause of oscillations in TPU limitation (Furbank *et al.*, 1987). The restriction of $NADP^+$ flux can be seen in the re-reduction of PSI during a saturation flash at the point of greatest PSI reduction (Figure 2.5). During this saturation flash, light is in excess of what is required to oxidize PSI, and the only limitation would be the electron carriers removing the electrons from PSI.

The accumulation of electrons on electron carriers of the electron transport chain is resolved by slower regulation. PMF increases, causing a decrease in k_{et} and an increase in NPQ_t. As these slower control mechanisms take hold, the transients in the other parameters slow and then stop. This is one example of damped oscillations, commonly found associated with TPU limitation (Ogawa, 1982; Sivak & Walker, 1986, 1987). The oscillations are caused by perturbations in the electron requirements of the Calvin-Benson cycle forcing Q_a^- based control

of electron transport; they are damped by the onset of PMF-based controls of electron transport. Some, but not all measurements of oscillations are consistent with the period and convergence rates in our measurements of oscillations. We therefore propose that electron carrier reduction as described here is responsible for some, but not all, observations of oscillations in TPU limitation.

Slow-onset regulatory processes control TPU limitation after a period of acclimation

On the minutes timescale, TPU-limited photosynthesis is regulated by rubisco deactivation, photosynthetic control at the cytochrome b_6f complex, and q_E. Rubisco deactivation begins within minutes and persists for at least a day (Figure 2.3). It is known that photosynthetic control and q_E, are induced by acidification of the thylakoid lumen. the mechanism of rubisco deactivation less clear. Study has been made on the deactivation of rubisco under elevated temperature (Salvucci & Crafts-Brandner, 2004) but no clear mechanistic understanding of deactivation under elevated CO2 has been elucidated. Under TPU-limiting conditions, ATP synthase is constricted (Kanazawa & Kramer, 2002; Takizawa *et al.*, 2008; Kiirats *et al.*, 2009) probably due to low phosphate concentration, which leads to a lower ATP/ADP ratio (Sharkey *et al.*, 1986c; Stitt, 1986; Furbank *et al.*, 1987) and therefore reduced rubisco activase activity. We measured a reduction in total rubisco activity after activation with 6-phosphogluconate (Figure 2.3b), which could be caused by tight binding inhibitors (Keys *et al.*, 1995; Paul *et al.*, 1996; Parry *et al.*, 1997). This can contribute to reduced rubisco activity. Reversible deactivation of rubisco is the primary contributor to the reduction in V_{cmax} measured over the course of acclimation (Figure 2.1).

Over time, photoinhibition becomes responsible for dissipating more excess energy, supplanting q_E. Measured J at 1000 µmol m^{-2} s^{-1} began decreasing quickly and did not recover fully overnight (Figure 2.1). In addition, after acclimation, total NPQ_t was higher at all levels of CO_2, and NPQ_t did not increase at elevated CO_2. PMF (ECS_t) is overall lower and has a reduced response to increasing CO_2. This indicates that q_E is becoming less important in energy flux compared to q_i, especially in response to TPU limitation. The NPQ must come from other sources, such as quenching from photoinhibition or state transitions. State transitions are somewhat limited in higher plants, with only 15-20% of the light harvesting complex capable of relocation (Rochaix, 2011), so photoinhibition is the most likely cause. The energy dissipation due to photoinhibition is enough to protect the photosystems, which makes q_E unnecessary.

Acclimation to TPU limitation requires balancing of both carbon and energy flux. At the end of acclimation, we found that energy flux is balanced by photoinhibition, and that carbon flux is balanced by rubisco deactivation. These two systems work synergistically. Rubisco deactivation reduces the potential demand for ATP and NADPH when CO_2 fixation could exceed the potential for end-product production. Control of electron transport by photoinhibition decreases the potential to overload the electron transport chain from the beginning. In this way, even though photoinhibition is rightly considered a negative effect on the plant, it is effective in protecting PSI; PSII is damaged, but there are effective repair mechanisms for PSII (Ohad *et al.*, 1984; Vass *et al.*, 1992; Sonoike, 1996). These two effects combine to reduce pressure on inorganic phosphate pools by reducing the potential use of phosphate from both sides.

After a long enough period of adaptation, plants no longer appear to be TPU-limited

TPU limitation is characterized by the responses of photosynthesis to increasing CO_2 (McClain & Sharkey, 2019). Once the plant becomes TPU-limited, elevating CO_2 results in elevated PMF and NPQ, while reducing φ_{II} and g_{H+} through the thylakoid membrane. In addition, the shape of the A/C_i curve is distinct: with increasing CO_2, A remains constant or marginally decreases due to reduced export of photorespiratory intermediates (Busch *et al.*, 2018). After 30 h of acclimation to elevated CO_2, evidence of TPU is gone (Figure 2.2). *NPQ* is overall higher but doesn't show the characteristic response to increasing CO_2 typical of TPU limitation. φ_{II} is lower at some CO2 levels and not significantly different at others, but the characteristic shape of the curve is lost after acclimation. Because TPU limitation is characterized by these responses, we argue that the plants do not become TPU limited by elevated CO2 after acclimation. TPU limitation happens in three phases: first, an acute condition, where phosphate incorporation and release are most imbalanced, resulting in dynamic fluctuations in electron carrier redox state and ATP availability. Second, a position of regulatory control, where rubisco deactivation and energy-dependent quenching dominate the observable phenomena associated with TPU limitation. Third, the plant will adapt to the conditions it is embroiled in, and the middle timescale regulation is phased out by greater adaptive responses that prevent TPU limitation from occurring.

It is generally thought that extended periods of time in high light and low CO_2 will cause damage to the photosynthetic apparatus, but data reported here show that extended periods of high CO_2 are deleterious while low CO_2 are not as bad. This is interpreted as TPU being a

stressful condition that causes regulatory responses that result in a loss of TPU behavior. The acclimation shown here prevents plants from experiencing TPU stress.

Debate has recently surfaced about the relevancy of TPU limitation to global models (Lombardozzi *et al.*, 2018; Rogers *et al.*, 2020). TPU limitation is rarely diagnosed as the limiting factor of steady-state photosynthesis in the wild (Sage & Sharkey, 1987). We believe that this is due to the relatively fast adaptation to TPU limiting conditions. Within a day of acclimation to very high CO_2, TPU limitation would not be diagnosable from gas exchange or fluorescence analysis. TPU limitation would only happen transiently. For this reason, we agree that TPU limitation as an explicit parameter of photosynthesis need not factor into global models of photosynthesis. However, it is important as a component of the regulatory network of photosynthesis.

It is currently unclear as to why TPU capacity did not increase in response to elevated CO_2 (Figure 2.1). If maximizing photosynthesis were the only concern, the plant would produce extra enzymes for processing end products to relieve TPU limitation instead of reducing other photosynthetic capacities. Some experiments have been done previously connecting TPU capacity with low temperature, another primary cause of TPU limitation (Sharkey & Bernacchi, 2012) due mostly to the high temperature sensitivity of sucrose-phosphate synthase (Stitt & Grosse, 1988). Plants grown in low temperature produced significantly more sucrose synthesis enzymes (Guy *et al.*, 1992; Holaday *et al.*, 1992; Hurry *et al.*, 2000). We know therefore that plants which have been TPU limited can produce more end-product-synthesis enzymes, so it seems like an obvious inefficiency for plants to lose photosynthetic capabilities. This conundrum may reflect the interaction between plant growth and photosynthesis. Some

analyses indicated that photosynthetic rate is not the best predictor of plant growth (Körner, 2015). Factors controlling growth rate and photosynthetic rate may not always work in concert. Growth is more temperature sensitive than is photosynthesis and so it may be that at low temperature growth limits photosynthesis while at high temperature photosynthesis limits growth. In this case, while the plant may look like it is performing inefficiently, it may simply be growing as fast as possible, and any additional photosynthesis would not be useful. Thus far it has been difficult to establish explicit causality connecting sink regulation to TPU limitation (Paul & Foyer, 2001) but efforts have been reported (Fabre *et al.*, 2019; Dingkuhn *et al.*, 2020). Recent work on SnRK1, the Target of Rapamycin complex, and interactions with trehalose 6-phosphate signaling may eventually help explain the interaction between plant growth and photosynthetic rate (Sulpice *et al.*, 2009; Smeekens *et al.*, 2010; Lastdrager *et al.*, 2014; Shi *et al.*, 2018; Brunkard, 2020; Peixoto *et al.*, 2021).

Conclusions

Photosynthesis is highly adaptive to the environment, and in TPU-limiting conditions experiences a series of regulatory steps to alleviate the stress along the electron transport chain. These steps can be organized into a timeline. At first, electrons build up along the electron transport chain, and reduction of Q_a causes extra energy to be funneled into nonphotochemical quenching. This causes transients in photosynthesis, which are damped after a few minutes by accumulation of *PMF*, causing elevated energy-dependent quenching and photoprotection at the cytochrome b_6f complex, accompanied by reduction in rubisco activation state. Over a longer period of time, energy-dependent quenching decreases and is supplanted by photoinhibition. The accumulation of these regulatory mechanisms causes the

plant to no longer be TPU limited. Counterintuitively, the plant did not increase its TPU capacity, but instead limited the photosynthetic rate by rubisco deactivation and electron transport regulation.

The disappearance of TPU limitation over 30 h of adaptation justifies the removal of TPU limitation from global models. Plants that are TPU-limited will eventually not be TPU limited, through a combination of regulatory means. However, TPU limitation is still an important part of photosynthetic regulation and cannot be disregarded in experimental design or data analysis. The occurrence of TPU limitation in the field is probably very low due to the swift adaptation demonstrated here, but in artificial experiments is easy to provoke. In FACE experiments (Allen *et al.*, 2020), or experiments that involve low temperature many of the effects studied may be caused by TPU limitation or the acclimation to TPU limitation. In other cases, sugar signaling may match photosynthesis to growth without explicit TPU limitations.

CHAPTER III

Short-term kinetics associated with triose phosphate utilization stress during photosynthesis addressed with dynamic assimilation measurements

Intended for submission to Plant Cell and Environment, 2022

Abstract

Oscillations in CO_2 assimilation rate and associated fluorescence parameters have been observed alongside the triose phosphate utilization (TPU) limitation of photosynthesis for nearly 50 years. However, the mechanics of these oscillations are poorly understood. Here we utilize the recently developed Dynamic Assimilation Techniques (DAT) for measuring the rate of CO_2 assimilation to increase our understanding of what physiological condition is required to cause oscillations. We found that TPU limiting conditions alone were insufficient, and that plants must enter TPU limitation quickly to cause oscillations. We found that ramps of CO_2 caused oscillations proportional in strength to the speed of the ramp, and that ramps induce oscillations with worse outcomes than oscillations induced by spikes of CO_2. Just as oscillations begin, an initial overshoot is caused due to a temporary excess of available phosphate. During the overshoot, the plant out-performs steady state TPU and ribulose 1,5-bisphosphate regeneration limitations of photosynthesis but cannot exceed the rubisco limitation. We performed additional optical measurements which support the role of PSI reduction and oscillations in availability of $NADP^+$ and ATP in supporting oscillations.

Introduction

The triose phosphate utilization (TPU) limit on photosynthetic rate can appear when plants are capable of producing phosphorylated Calvin-Benson cycle intermediates faster than these intermediates can be dephosphorylated and converted into end-products (Sharkey, 1985a). When TPU-limited, inorganic phosphate is not released from the organic phosphate pool fast enough to sustain maximum throughput of both the ATP synthase and the Calvin-Benson cycle, so photosynthesis must be downregulated to balance the two. This regulation

imposes a cap on the rate of CO_2 fixation at the rate of end-product synthesis. Plants are not typically TPU limited under ambient conditions (Sage & Sharkey, 1987; Ellsworth *et al.*, 2015), and TPU limitation is easiest seen by elevating the rate of photosynthesis through increased light level and CO_2 partial pressure or decreased O_2 partial pressure (Sharkey *et al.*, 1986c) such that the photosynthetic rate is increased by 10 or 20% relative to ambient conditions (Yang *et al.*, 2016). It is more likely to be observed when photosynthesis is measured at a lower temperature than growth conditions (Stitt, 1986; Sage & Sharkey, 1987; Labate & Leegood, 1988), due to the high temperature sensitivity of end product synthesis (Stitt & Grosse, 1988; Leegood & Edwards, 1996), which exceeds the temperature sensitivity of the other biochemical processes in photosynthesis (Cen & Sage, 2005; Sage & Kubien, 2007). The occurrence of TPU limitation depends greatly on the species and the acclimation of the plant. For example, plants grown at low temperature are often resistant to TPU limitation because they develop additional sucrose-phosphate synthase (Cornic & Louason, 1980; Guy *et al.*, 1992; Holaday *et al.*, 1992). Expressing *Zea mays* sucrose-phosphate synthase in tomato significantly reduced the temperature at which TPU was evident (Laporte *et al.*, 2001).

TPU limitation is associated with a variety of regulatory processes. TPU-limited plants exhibit reduced rubisco activation state in as little as one min after imposing TPU conditions (Sharkey *et al.*, 1986a). Rubisco deactivation can restore the balance between the capacities to fix carbon and convert the fixed carbon to end-products. TPU-limited plants also develop an elevated transthylakoid proton-motive force (*PMF*) and an associated increase in energy-dependent quenching (Takizawa *et al.*, 2008; Kiirats *et al.*, 2009). This increase is probably associated with declining phosphate concentration in the stroma (Sharkey & Vanderveer, 1989)

driving up the ΔG_{ATP} of the stromal ATPase reaction. One consequence of this regulatory arrangement is the reduction of φ_{PSII} as [CO_2] increases (Sharkey *et al.*, 1988; Stitt & Grosse, 1988). The requirement for electron transport is set by the rate of photosynthesis and photorespiration. Increasing [CO_2] reduces the rate of photorespiration. The decline in φ_{PSII} will then balance the rate of electron transport with the reduced requirements for electrons because of the reduced rate of photorespiration.

In TPU-limited photosynthesis, photosynthetic rate is defined by regulatory features. To detect TPU limitation in gas exchange data, it is easiest to determine the presence of regulatory mechanisms, such as the increase in non-photochemical quenching or the decline in φ_{PSII} upon increasing CO_2 (McClain & Sharkey, 2019), or the CO_2- or O_2-insensitivity of the CO_2 assimilation rate (*A*), which demonstrates that *A* is not defined by rubisco properties and which is characteristic of TPU limitation (Sharkey, 1985b). These regulatory mechanisms can have different time constants. For example, Sharkey et al. (1986) observed depletions of ATP and RuBP and reductions in ATP/ADP ratio and rubisco activation state 1 min after imposing TPU. However, after 18 min, RuBP was higher than before imposing TPU conditions and the ATP/ADP ratio, and rubisco activation recovered partially. Thus, as different regulatory mechanisms are induced upon imposition of TPU limitation, there can be transients in the specific process setting the rate of photosynthesis, for example the availability of RuBP at one time versus the activation of rubisco at another time.

One consequence of these transients is oscillations in *A*, which have been frequently observed under TPU limitation (Ogawa, 1982; Walker *et al.*, 1983; Sivak & Walker, 1986, 1987). Oscillations are commonly seen when the environmental conditions are rapidly changed to

elevate the photosynthetic rate, such as a step change in CO_2 partial pressure or light availability or a reduction in O_2 partial pressure (Harris *et al.*, 1983) to increase carbon fixation by reducing photorespiration. Oscillations are visible in both carbon assimilation and fluorescence parameters, demonstrating parallel changes in the Calvin-Benson cycle and electron transport (Walker *et al.*, 1983; Peterson *et al.*, 1988; Stitt & Grosse, 1988). There have been a few models proposed to explain oscillations in photosynthetic rate. In general, biological oscillatory models, oscillations are typically caused by a delay in a feedback component of a multiple component system, leading to overshooting of steady-state before inhibition can be achieved. One theory is that there is a delay in activation of sucrose synthesis after a photosynthetic increase (Laisk & Walker, 1986). Another theory is that the delay originates from fructose-2,6-bisphosphate inhibiting fructose-1,6-bisphosphatase (Stitt *et al.*, 1984; Laisk & Eichelmann, 1989; Laisk *et al.*, 1989).

The use of ramps of CO_2 to induce oscillations should allow us to study the phenomenology of oscillations with high-speed measurements of A and C_i (Stinziano *et al.*, 2017). However, the 100 ppm/min limit on ramp speed with the Rapid A/C_i Response (RACiR, Stinziano *et al.*, 2019) technique combined with inaccurate C_i measurements, especially at the beginning and end of curves, limited this approach. Dynamic assimilation techniques (DAT, Saathoff & Welles, 2021) represent a natural evolution of RACiR that features a greater range of ramp rates and better accuracy, especially at the start and end of the ramp. Dynamic calculations of assimilation, which include an accumulation term to account for changes in the concentration of CO_2 entering the chamber that is disregarded in steady-state equations, also make measurements of assimilation possible following sharp changes in $[CO_2]$. With DAT, we

can now use advanced ramps and spikes in [CO_2] to clarify the mechanism by which TPU limitation causes oscillations, and how exactly the assimilation rate can surpass the steady-state limit.

Materials and methods

Plant materials and growth

Nicotiana benthamiana seeds were germinated in 2 l pots of potting media consisting of 70% peat moss, 21% perlite, and 9% vermiculite (Suremix; Michigan Grower Products Inc., Galesburg, MI, USA) in a greenhouse from June-August. This greenhouse was located at 42°43'N, 84°28'W, East Lansing, Michigan. Typical daylight light levels were between 300-700 µmol m^{-2} s^{-1}, and the daytime temperature was controlled to 27°C during the day. Plants were watered with half-strength Hoagland's solution (Hoagland & Arnon, 1938) as needed as seedlings and then daily as adults. Plants were used for experiments from 6-7 weeks of age, and the uppermost fully expanded leaves were used for gas exchange.

Dynamic Assimilation Techniques

Dynamic measurements of gas exchange were made in a LI-COR 6800 with a LI-COR 6800 12A 3 cm x 3 cm clear top chamber (LI-COR Biosciences Inc., Lincoln, NE, USA). Plants were acclimated at experimental conditions until steady state with 1000 µmol m^{-2} s^{-1} photosynthetically active radiation and an air flow rate of 800 µmol s^{-1}. Dynamic calibrations and range match were performed as recommended in the LI-COR 6800 version 2.0 manual (https://licor.app.boxenterprise.net/s/kt6wwzmnvnlu4vc004pzp9u7cv9bvzj8 pp. 9-66 – 9-109). For experiments presented here, CO_2 was ramped at rates of 100 to 500 ppm/min (approx. 10-50 Pa CO_2/min. Typical atmospheric pressure was 98 kPa).

Combined optical measurements with gas exchange

A LI-COR 6800 12A 3 cm x 3 cm clear top chamber (LI-COR Biosciences Inc., Lincoln, NE, USA) was connected to a scattering optic with an array of LEDs behind it (Hall *et al.*, 2013; Lantz *et al.*, 2019), while the backplate was replaced with a 3D-printed plate containing an optical and an infrared detector, described in chapter 2. The LED array contained actinic red and blue lights producing up to 2500 µmol m^{-2} s^{-1} with a ratio of 90% red (630 nm) and 10% blue (480 nm) light at 1000 µmol m^{-2} s^{-1}. The saturation flash provided approx 15,000 µmol m^{-2} s^{-1}. Electrochromic shift measurements were made with a 520 nm LED, with 505 nm used to correct for changes in zeaxanthin. Activity of PSII was assessed by chlorophyll fluorescence using 520 nm as the excitation light. Measurements of PSI absorbance were made at 820 nm. While the absorbance at 820 nm may include other signals, such as reduced pheophytin or ferredoxin, these species are in low proportion and change more slowly than $P700^+$ and should not significantly affect the kinetics (Christof & Ulrich, 1994). Measurements of PSI were taken according to Kanazawa *et al.* (2017) and measurements of ECS were taken according to Takizawa *et al.* (2007).

To take optical measurements along with the dynamic ramp of CO_2, plants were first acclimated at 400 ppm CO_2 and 1000 µmol m^{-2} s^{-1} light until steady state was achieved. CO_2 was then abruptly lowered to 50 ppm CO_2 at the reference IRGA, and the plant acclimated at this CO_2 level for 60 s. Afterwards, CO_2 was ramped at a rate of 400 ppm/min (approx. 40 Pa/min) (or other rates as indicated) until 1500 ppm CO_2 in the reference IRGA was recorded. (Because CO_2 assimilation is a function of partial pressure, assimilation rates are reported as a function of partial pressure. However, the LI-COR 6800 mixes gases in terms of mole fraction, so in explaining experimental design CO_2 levels are given in ppm). Typical atmospheric pressure at

the site of experimentation was 98 kPa and was measured at the time of experimentation for exact calculations. A list of times from 20 to 140 s in 10 s intervals was randomized, and individual ramps were performed sequentially for each interval, allowing assimilation to return to steady state at ambient CO_2 before beginning the next ramp. At the chosen time, PSI and PSII activity, as well as the dark interval relaxation kinetics (DIRK) of the electrochromic shift (ECS), were measured.

Results

Oscillations are intensified when induced through ramps rather than CO_2 spikes

The photosynthetic rate oscillated when the CO_2 partial pressure was increased sufficiently to cause TPU limitation. When CO_2 was ramped at rates of 100 to 500 ppm min^{-1}, oscillations were more pronounced than when CO_2 was increased abruptly (Figure 3.1). The higher amplitude/lower damping oscillations caused by a ramp up of CO_2 resulted in a lower integral of *A* compared to an abrupt increase (Table 3.1). Oscillations induced by ramping CO_2 resulted in on average a 20% loss of total assimilation compared to the steady-state over the course of the ramp, significantly less at p=0.95. Oscillations induced by a spike of elevated CO_2 performed comparably to the steady state assimilation value at the same CO_2 level, no

Type	Mean difference (%)	Difference s.d.	95% CI
Ramp	-20.0	2.6	-25.1 to -15.0
Spike	-2.2	3.9	-9.9 to 5.5

Table 3.1 A comparison of the total integrated assimilation during oscillations relative to the steady-state assimilation.

significant difference at p=0.95. We fitted a line through the middle of the oscillations. This midline trended down when oscillations were induced by a ramp of CO_2 but trended up when CO_2 was changed abruptly.

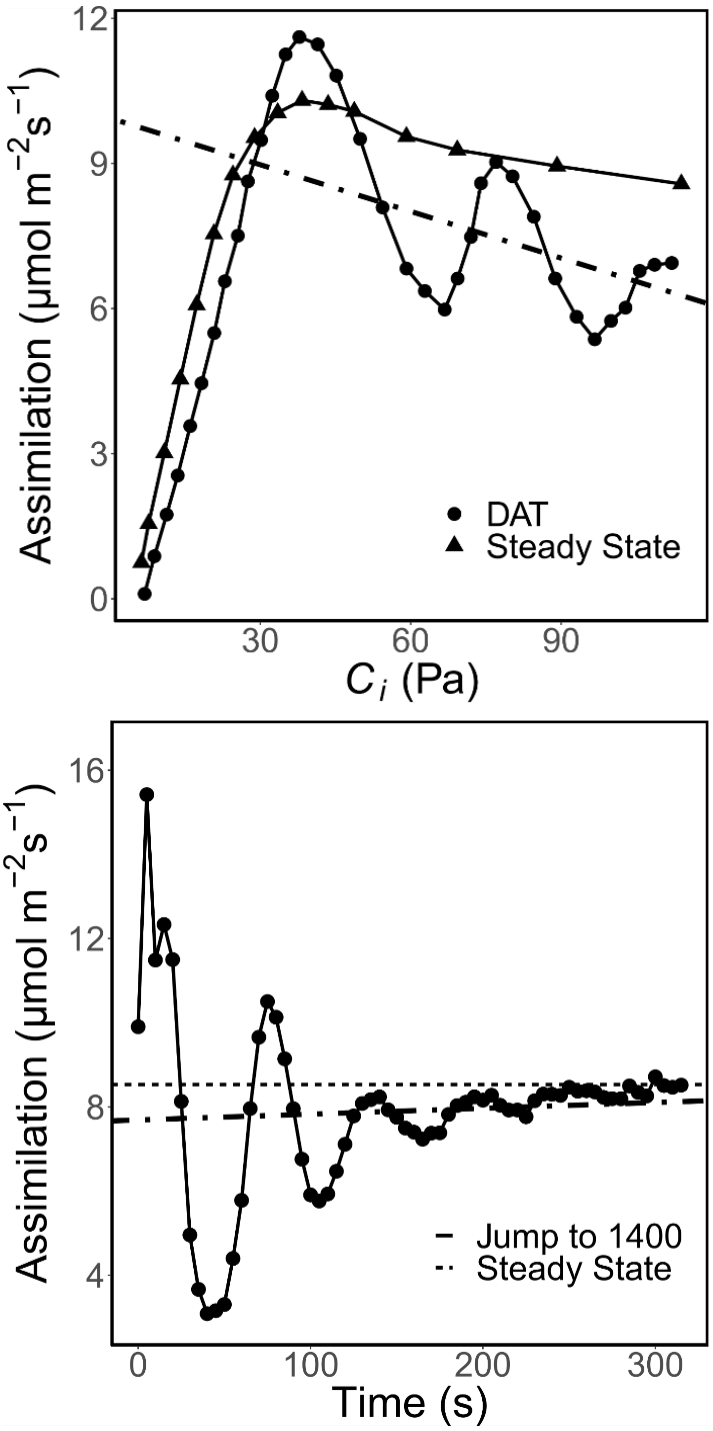

Figure 3.1 Oscillations induced by elevated CO_2 compared to the steady state. Top: Full ramp of CO_2 from 50 ppm to 1500 ppm at a rate of 400 ppm/min compared to a steady-state A/C_i curve. Bottom: Oscillations induced by step-change of CO_2 from 50 ppm to 1400 ppm compared to steady-state assimilation rate at 1400 ppm CO_2. For both, a linear model is fit to the oscillating data to show the midline of oscillations.

Oscillations are induced specifically by entering TPU limitation

Oscillations were observed only when plants entered TPU limitation (Figure 3.2). Plants were acclimated at 400 ppm CO_2 and either 25°C (Figure 3.2 top and middle) or to prevent the occurrence of TPU limitation, 35°C (Figure 3.2, bottom). Plants were then prepared to ramp through a range of CO_2 values, starting at either 50 ppm (low to high, Figure 3.2 middle and bottom) or 1500 ppm (high to low, Figure 3.2, top). Once the assimilation rates were steady the CO_2 was ramped through a range of CO_2 values, either from 50 to 1500 ppm (Figure 3.2 middle and bottom) or from 1500 to 50 ppm (Figure 3.2, top) at a rate of 400 ppm min^{-1}. When measured at growth temperature and a ramp from low to high CO_2, oscillations were observed beginning at a C_i of approx. 30 Pa. When ramped high to low, the plant did not exhibit oscillations at all. When ramped at a higher temperature to prevent TPU limitation, the plant did not exhibit oscillations. Therefore, the oscillations are caused specifically by entering TPU limitation, rather than any of the individual environmental conditions the plant experiences. Leaving TPU conditions does not result in oscillations.

Oscillations are intensified when the ramp rate is increased

Plants were acclimated at ambient conditions, then after a 1-min delay at 50 ppm CO_2, were ramped at a variable rate to 1500 ppm CO_2 (Figure 3.3). Sustained oscillations are not observed at a ramp rate of only 100 ppm CO_2/min but an initial overshoot was seen. The height of the peak of the first oscillation increased with ramp rate. The initial peak value of *A* was greater than the steady state rate except at 100 ppm/min. The initial peak value increased with ramp speed, however, there was a corresponding increase in the depth of the following trough in assimilation.

In Figure 3.3 the assimilation rates are plotted versus C_i but there is also a time element given the variation in the rate of CO_2 ramp. Figure 3.4 shows the same assimilation rates as in Figure 3.3 but as a function of time (we put time on a log scale for convenience). Figure 3.4 shows that the peak assimilation rate decreases with time to reach said peak.

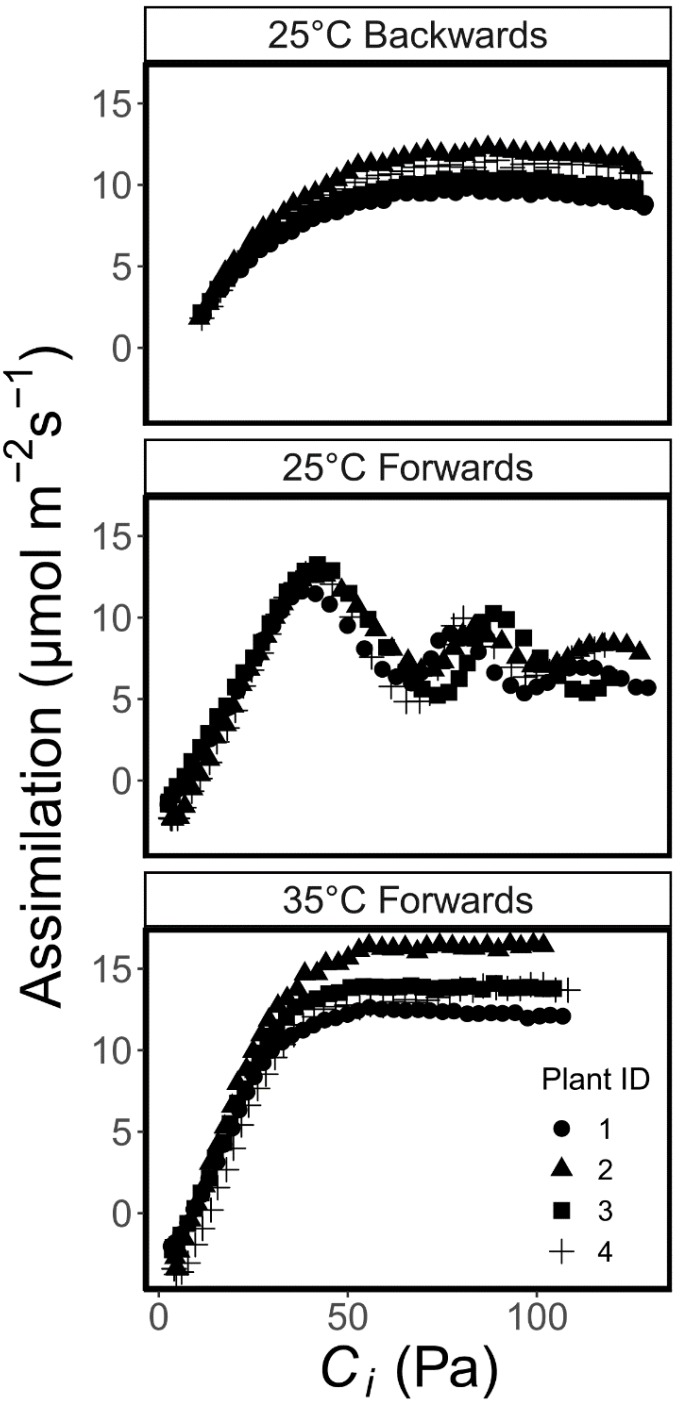

Figure 3.2 Assimilation measured using dynamic assimilation technique ramps of CO_2 in three styles. Top: Reference CO_2 is ramped from 1500 ppm to 50 ppm at 25°C. Middle: Reference CO_2 is ramped from 50 ppm to 1500 ppm at 25°C. Bottom: Reference CO_2 is ramped from 50 ppm to 1500 ppm at 35°C. For all curves, CO_2 is ramped at a rate of 400 ppm/min. Assimilation and C_i are logged every 5 seconds. Different symbols indicate replicate leaves.

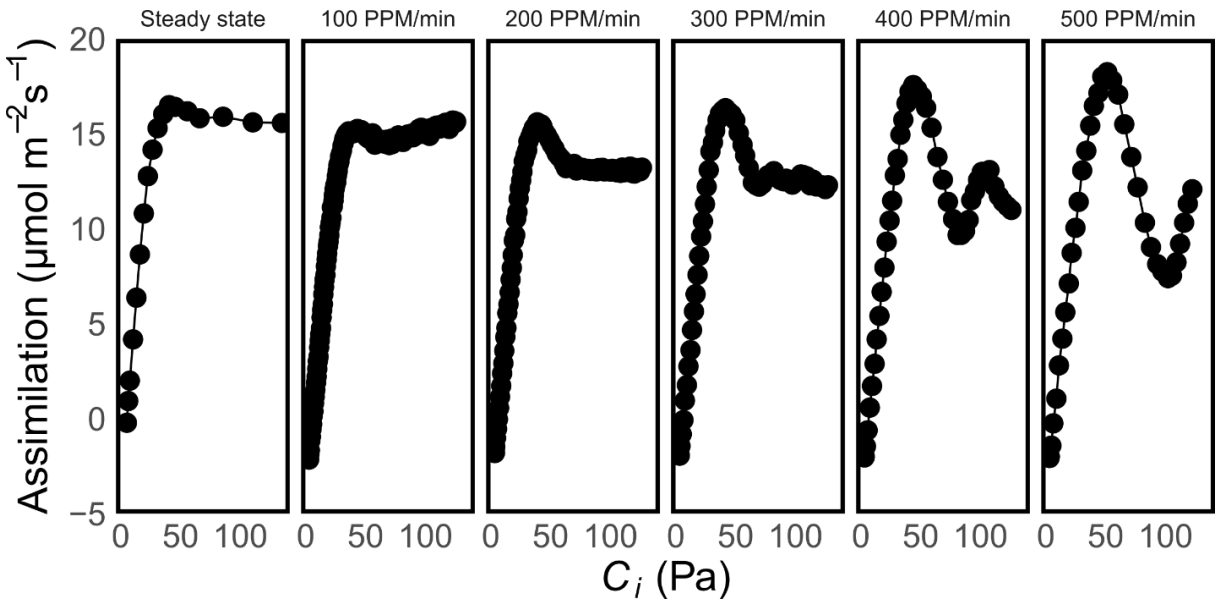

Figure 3.3 An example set of DAT ramps at various ramp rates, compared against the steady-state A/C_i curve. Reference CO_2 is ramped from 50 to 1500 ppm at rates of 100 to 500 ppm/min at 25°C. For the steady-state A/C_i, 18 points were collected over a range of reference CO_2 values from 50 to 1500 ppm over a period of 2.9 – 14.5 min. The amplitude of the oscillations increases in proportion to the ramp rate.

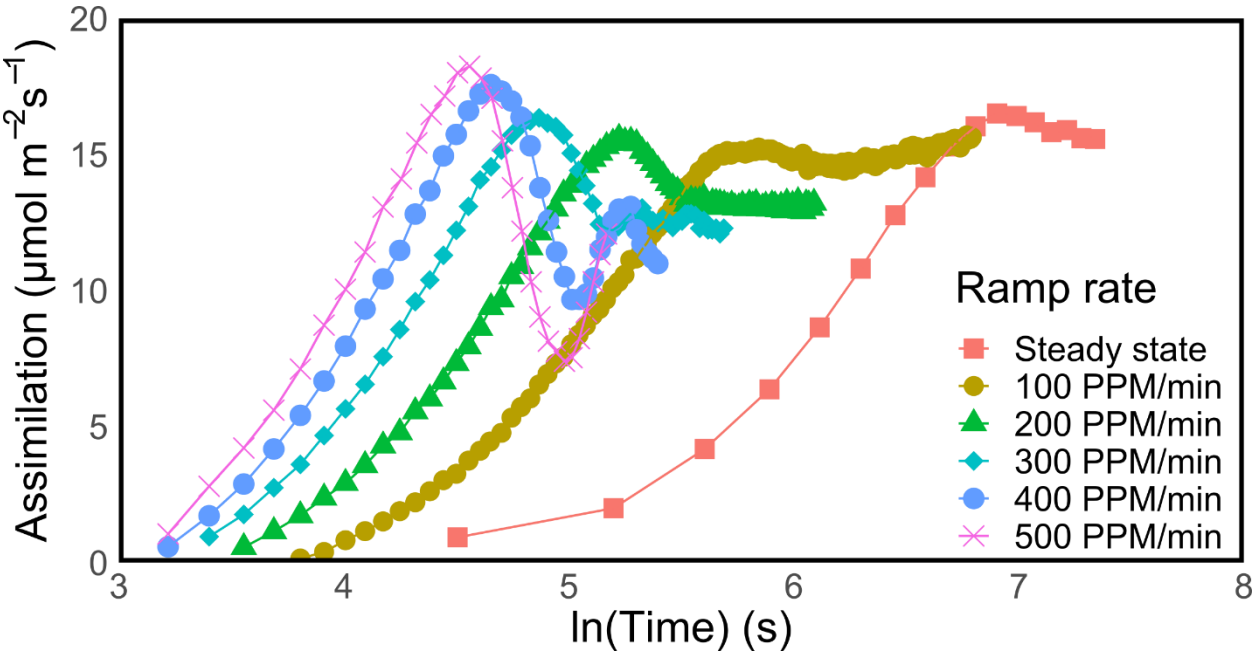

Figure 3.4 Overshooting and resulting oscillations shown in Figure 3.3 compared by time, rather than C_i. The peak of the oscillations increases with reduced time to reach the peak, caused by increased ramp rate.

Oscillations are intensified when TPU is enhanced through low temperature

Plants were acclimated until steady state at 20°C at 400 ppm CO_2, then held at 50 ppm CO_2 for one min before ramping from 50 to 1500 ppm CO_2 at a variable rate (Figure 3.5). The peak amplitudes compared to the steady state were higher relative to those found at room temperature. Additionally, the ramp rate required to achieve overshooting was lower, 200 ppm min^{-1} rather than 400. These two components combine to increase the oscillation amplitude through the connecting factor of TPU capacity, even though they affect TPU limitation in different ways.

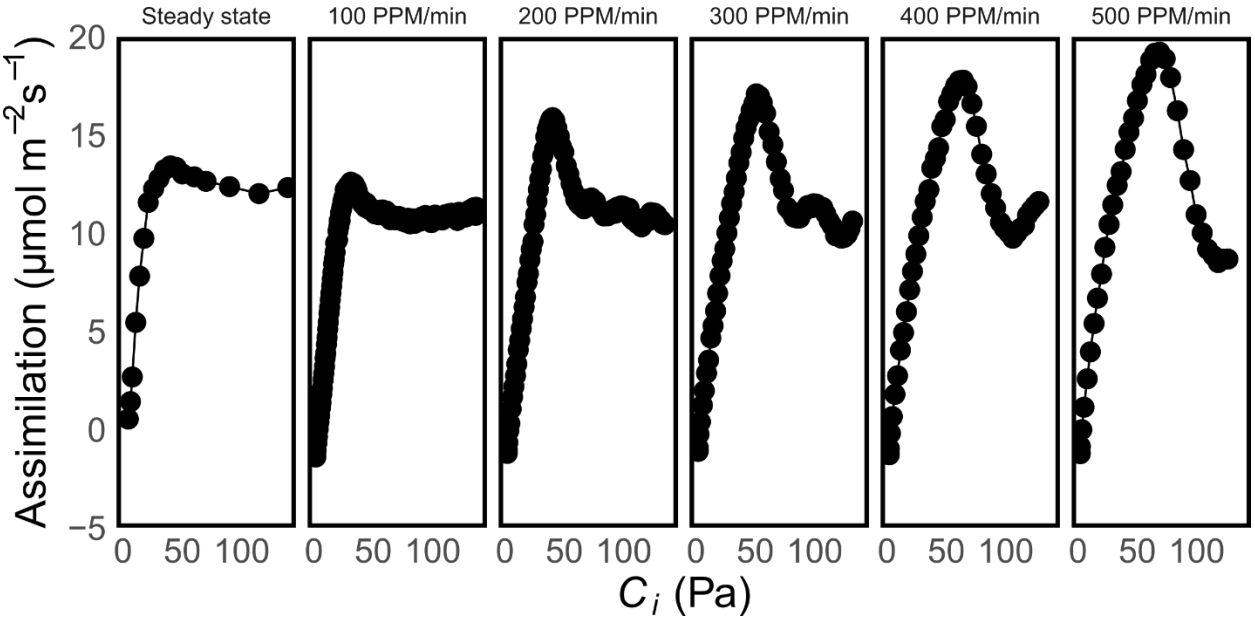

Figure 3.5 A set of DAT ramps at reduced temperature. Reference CO_2 is ramped from 50 to 1500 ppm at rates of 100 to 500 ppm/min, compared to an 18-point steady-state A/C_i, all at 20°C. The amplitude of the induced oscillations increases with ramp rate, and is also greater than the amplitude of oscillations at 25°C.

Overshooting dynamically exceeds both TPU and the electron transport limitation of photosynthesis

The oscillations caused by the CO_2 ramp were plotted with limitations calculated from curve fitting (Gregory *et al.*, 2021) for data measured at discreet CO_2 concentrations. Peak dynamic *A* often exceeded the steady-state TPU limitation during a ramp of CO_2 (Figure 3.6). At higher ramp rates, peak dynamic *A* also exceeded the RuBP regeneration limitation of

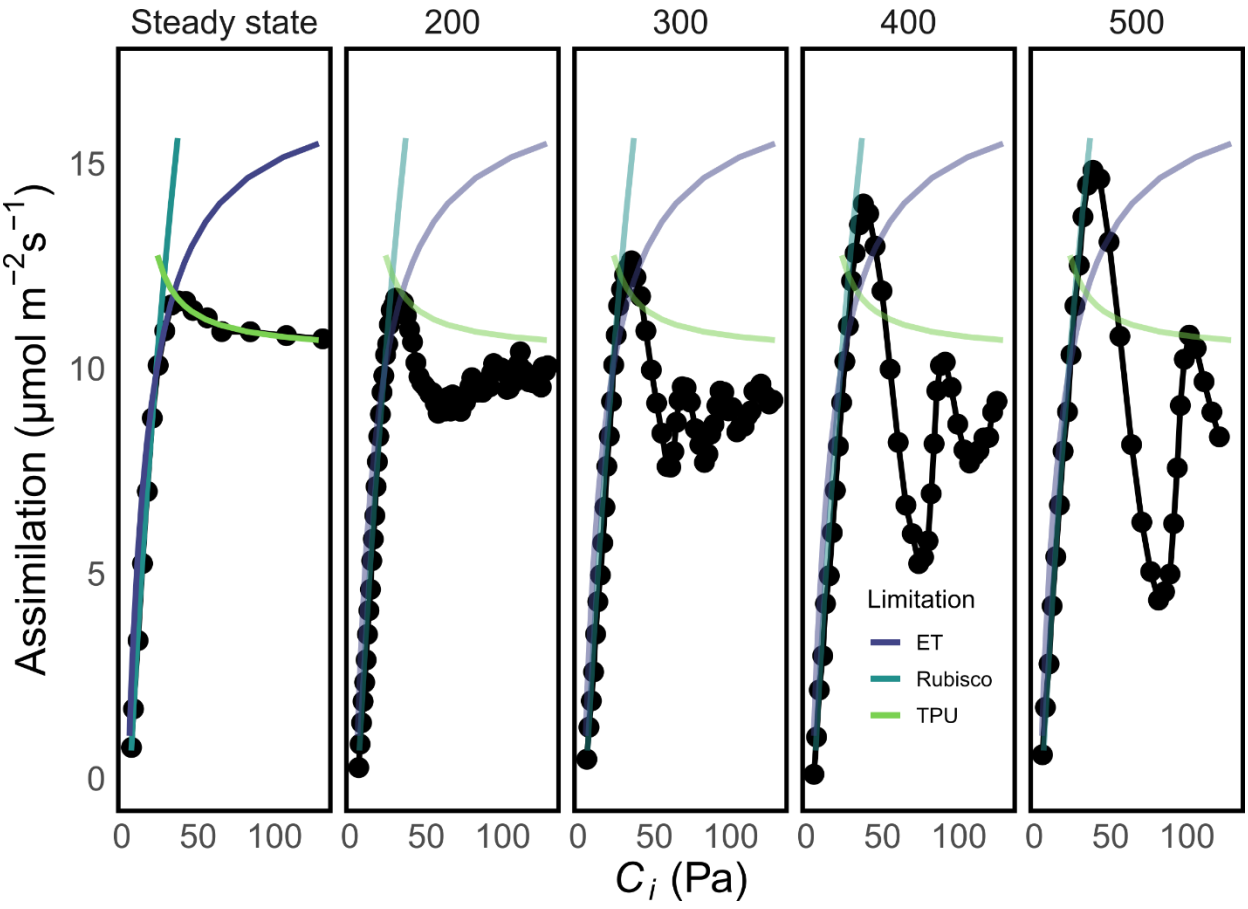

Figure 3.6 Comparison of oscillations versus fitting parameters from the steady-state A/C_i. Oscillations are induced by ramping from 50 ppm to 1500 ppm at rates varying from 200 ppm/min to 500 ppm/min. Oscillations can easily surpass TPU limitation, and at higher ramp rates can surpass the RuBP regeneration limitation but cannot surpass the rubisco limitation. At the highest ramp rates, the entire overshoot closely matches the rubisco limitation.

photosynthesis. However, at no point did the overshoots exceed the rubisco limitation of photosynthesis.

PSI reduction was involved in oscillations during CO_2 ramps

Plants were ramped from 50 to 1500 ppm CO_2 in a special chamber adapted to house an LED array for measuring electrochromic shift and PSI oxidation in combination with PSII fluorescence (Figure 3.7) based on components of the IdeaspeQ (Hall *et al.*, 2013). Assimilation and ϕ_{II} were correlated, as previously seen. However, PSI oxidation remained constant throughout the ramp until the first trough, at which point PSI became very reduced. This suggests that the availability of $NADP^+$ to accept electrons from PSI became limited.

Discussion

Historically, most of the photosynthetic oscillations research has been performed using sudden shifts in environmental conditions to induce oscillations. The use of ramps of varying speeds helps describe the phenomenology of oscillations to a greater degree, with some implications on the mechanisms of oscillations. The amplitude of oscillations resulting from ramps are greater and the oscillations damp more slowly than oscillations resulting from spikes (Table 3.2). Oscillations produced by spikes tend towards the steady state assimilation value. Oscillations produced by ramps, however, tend towards a different midline that diverges from the steady-state assimilation rate. We propose that this is due to the continuous change of the requirements for photosynthetic regulation, which is the damping force of these oscillations. The amplitude of the oscillations is also affected by the rate of the ramp. If the ramp is too

slow, overshooting can still occur but not oscillations. In this situation, a simple damped harmonic oscillator model cannot describe the behavior, as overshooting is not seen in an overdamped or critically damped model, and an underdamped model cannot account for the extended trough following.

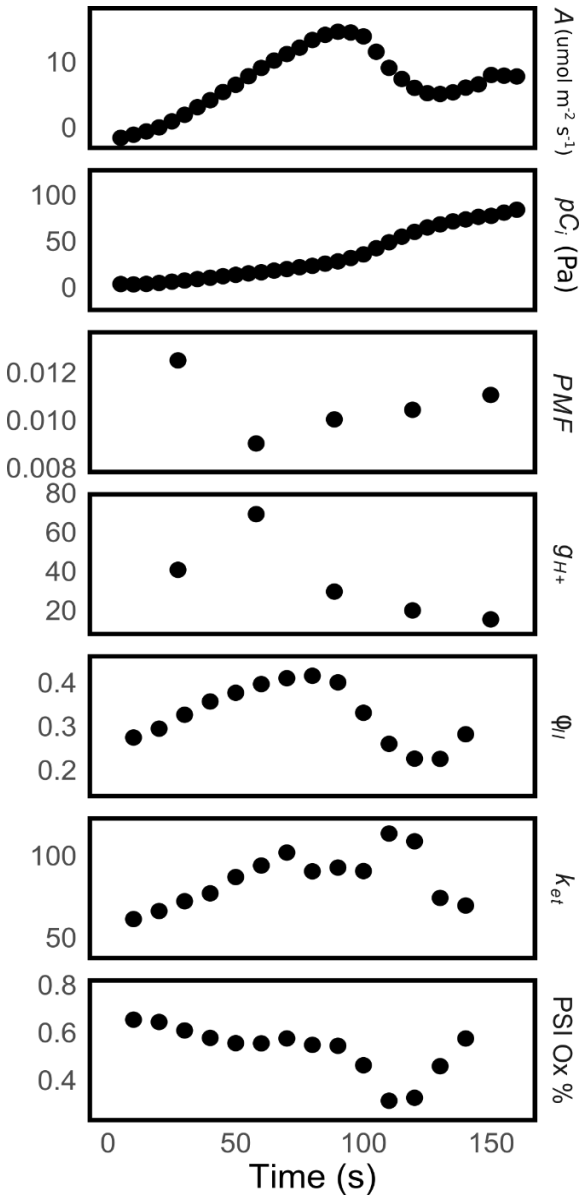

Figure 3.7 Combination of optical measurements with DAT. Oscillations are induced by ramping from 50 ppm to 1500 ppm at 400 ppm/min. φ_{II} and PSI oxidation state are calculated from saturation flashes. *PMF*, g_{H+}, and $\Delta A820_t$ are calculated from dark interval kinetics. g_{H+}, φ_{II} and PSI oxidation state correspond with assimilation, but *PMF* responds in the reverse.

The use of ramps also allows us to compare the oscillations to the photosynthetic limitations fit from steady-state behavior. The peak exceeds the RuBP regeneration limitation and the TPU limitation, both of which are functions of metabolite pools. For short periods of time metabolites such as RuBP can be used faster than they are produced, depleting the pool and adding instability to the system. However, the rubisco limitation is not a function of metabolite pools, it is believed to represent the kinetics of RuBP-saturated rubisco and be unaffected by changes in RuBP pool size (Farquhar, 1979; Sharkey, 2022). It is therefore

Replicate	Ramp Damping Ratio	Spike Damping Ratio
1	0.0683	0.1058
2	0.1418	0.2054
3	0.0793	0.1233
4	0.1274	0.1709

Table 3.2 A comparison of the harmonic oscillator damping constants from a set of four plants, with each being tested in both oscillations induced by CO_2 ramp and a spike in CO_2. The damping constants were estimated by logarithmic descent of peak height. The mean difference is not 0 at p=0.95 using a two-sided paired t-test (95% CI 0.0291 – 0.065).

unsurprising that oscillations did not exceed the rubisco-limited portion of the curve. Similar transient peaks in *A* above the steady-state rate of RuBP regeneration were induced by short periods of CO_2-free air (Ruuska *et al.*, 1998). Short dark periods can also allow photosynthesis in subsequent light periods to exceed its steady state rate for short periods (Stitt 1986). On this basis, we propose that the overshooting achieved during oscillations results from the transient reduction in pools of metabolites which would otherwise be consumed at a steady-rate, allowing photosynthesis to temporarily exceed the steady state rate. In this model, the depth of the trough would be related to the quantity of newly-produced metabolites from the peak that

must be accumulated to restore metabolic balance. Because oscillations are induced by following a period of no TPU limitation with induction of TPU limitation, it is possible that the plant has plentiful inorganic phosphate free during the start of the ramp, and then the excess is used to transiently surpass the TPU limitation of photosynthesis. Similarly, the plant should be able to dynamically exceed the RuBP regeneration limited portion of the curve if RuBP is initially in excess. The height of the peak would then be related to the size of the available metabolite pool.

Entering TPU limitation causes a change in the rate of triose phosphate production, while consumption is unchanged. This mismatch results in oscillations. Many metabolite pools both inside and outside of the chloroplast need to adjust upon entering TPU and these can provide capacitance and delays. One such metabolite is phosphate, which must be at a lowered concentration to maximize sucrose (Huber & Huber, 1996) and starch synthesis (Preiss, 1982), but must remain at a sufficient concentration to drive ATP synthesis. The transition from rubisco-limited to RuBP regeneration-limited conditions and vice versa involves much simpler adjustments in metabolism and so rarely produce oscillations. Elevated CO_2 alone is insufficient to induce oscillations. Increasing the temperature such that TPU limitation cannot be seen prevents oscillations. When ramped from high CO_2 to low CO_2 at ambient temperature, oscillations were not observed.

The amplitude of the oscillations is affected by several factors. The plants will not begin oscillating unless they enter TPU limitation suddenly. Ramps that are too slow allow time for complex adjustments in metabolism and so do not induce oscillations, and the amplitude of the oscillations varies with the speed at which the plants are induced into TPU limitation. This is

emphasized in Figure 3.4, where the size of the overshoot varies with the length of time required to reach the beginning of oscillations. Plants ramped through an *A/Ci* curve at low temperature are particularly susceptible and will oscillate with greater amplitude. The greatest amplitude is seen in the initial overshoot, and if the initial peak does not overshoot, there are no oscillations seen (for instance, the 100 ppm min^{-1} and 200 ppm min^{-1} ramps in (Figure 1). The overshoot amplitude is related to ramp speed by metabolite pools. When the ramp speed is fast, the rate of photosynthesis has been lower leading up to the beginning of oscillations, which would mean that the sum of metabolites consumed during the ramp is lower, while the potential to produce said metabolites should be approximately the same. When the plant reaches a C_i that would typically cause RuBP regeneration or TPU limitation, greater pool sizes would produce a higher peak.

If TPU limitation in the steady state is best described as a collection of regulatory components, these oscillations are the result of the time delay to activate those regulatory components. The strength of the perturbation is important to the phenomenology because it puts strain on photosynthetic regulation. The plant cannot handle photosynthetic rates exceeding the steady state TPU limitation for any extended period, and despite overshooting, the plant performs worse. Oscillations are damped over a period of a few minutes, enough time to activate *PMF*-dependent control through energy-dependent quenching and photosynthetic control at cytochrome *b6f* (Kramer & Crofts, 1993, 1996), as well as rubisco deactivation which can begin in the first minutes of elevated CO_2 (Sage *et al.*, 1988) or just one min of exposure to low O_2 to induce TPU (Sharkey *et al.*, 1986c). The oscillations are triggered when photosynthetic regulation is too slow to keep up with the changes in *A*, and then damped when given enough

time to activate regulatory controls on a timescale of minutes. This observation is supported by the reduced damping rate in oscillations induced via ramp. The constantly changing setpoint for regulation causes the plant to perform worse and recover more slowly.

The reduction of photosystem I during oscillatory troughs suggests a critical role of electron carriers in oscillations. Reduction of PSI without a corresponding increase in electron flow from the cytochrome *b6f* complex means that $NADP^+$ must be limiting. This situation could occur if there is insufficient ATP production to process PGA into downstream products, limiting the flux through the reduction step. This data supports the conclusions of Laisk *et al.* (1991), who also found reduction of P_{700} during oscillations and calculated that NADPH/$NADP^+$ ratios were antiparallel with oscillations in both photosynthesis and in ATP/ADP ratios. This data also provides a compelling rationale for the regulatory components surrounding TPU limitation. If PSI becomes reduced, it becomes a redox threat to the plant (Li *et al.*, 2009; Suorsa *et al.*, 2012), which may be a natural consequence of exceeding the steady-state TPU limitation.

The occurrence of oscillations suggests the existence of an "acute" TPU crisis that is rarely seen in the steady-state. Plants exceed the steady-state rate of photosynthesis temporarily, but they don't end up assimilating more carbon than they would have been able to, suggesting that the overall rate of photosynthate utilization does not change over the course of the transients. The troughs, then, are caused by a lack of ATP, caused by a combination of lacking inorganic phosphate and reduction of electron transport rate due to reduction of PSI electron acceptors. This conclusion is supported by the decline in ATPase conductivity to protons and the reduction of PSI. This acute restriction shows the photosynthetic rate as limited by a rapidly changing TPU limitation in response to phosphate

levels, as opposed to the steady-state, which shows only the steady-state rate determined by the regulatory features that limit photosynthesis in response to TPU limitation.

Our understanding of the oscillations is that they are caused by the phosphate pool interrupting ATPase throughput, and the delay period is the rate of processing the pools of Calvin-Benson cycle intermediates plus photosynthesis-related sugar phosphates in the cytosol. To recycle phosphate, carbon must leave the Calvin-Benson cycle and become dephosphorylated, which overwhelmingly proceeds from triose phosphates (exported for sucrose synthesis) and fructose 6-phosphate (converted to glucose 6-phosphate to supply starch synthesis). For both starch and sucrose synthesis there are pools of organic carbon (especially glucose 6-phosphate) that are disconnected from Calvin-Benson cycle intermediates but whose metabolism is essential for freeing phosphate. This, combined with the reduction of electron carriers that will prevent additional production of ATP, causes the delay seen in the troughs of the oscillations.

The presence of an acute TPU crisis explains some non-obvious facets of steady-state TPU limitation. Triose phosphates do not necessarily build up in steady-state TPU limitation, a counterintuitive fact considering it is the first output of a cycle that, according to the model, is going too fast. Instead, it is common that RuBP builds up, which is unexpected as TPU limitation implicitly limits the ATPase and RuBP requires ATP to be regenerated. The lack of ATP causes PGA to increase by as much as 77% and RuBP pools shrink immediately after the imposition of TPU but RuBP recovers as rubisco is deactivated (Sharkey *et al.*, 1986c) and presumably other regulatory mechanisms are engaged. It will take additional studies of the effect of transients in metabolite pools to examine these regulatory mechanisms.

Conclusions

TPU limitation shows flexibility during dynamic assimilation measurements, for precisely the same reason it is insensitive to O_2 and CO_2 changes: it is separated from rubisco by layers of metabolites. In the steady-state, inorganic phosphate pools are quite low (Sharkey & Vanderveer, 1989), but regulatory features balance the flux of inorganic phosphate into and out of the organic phosphate pool. Changing these fluxes dynamically imbalances photosynthesis and causes alternatively better and worse photosynthetic rate, and slower regulatory control is required to stabilize the photosynthetic rate again. This situation is a more intuitive understanding of TPU limitation – rather than being determined by a series of regulatory steps, the photosynthetic rate is determined by a crisis in metabolic pools.

At this point it may be useful to divide the phenomenon of TPU limitation into two separate categories. In the steady state, TPU-limited photosynthesis is described primarily by regulatory features such as rubisco deactivation and energy-dependent quenching. In the acute, however, the photosynthetic rate temporarily defies some assumptions of the three-limitation model of steady-state photosynthesis. Dynamic TPU limitation must be controlled by pool sizes, and it is reflected in electron transport dynamics.

CHAPTER IV

Conclusions on regulation of and adaptation to TPU limitation

Triose phosphate use (TPU) limitation is considered one of the three classical limits to the rate of photosynthesis in C_3 plants. It is a paradigm of photosynthesis where carbon assimilation is limited by the rate of dephosphorylation of organic phosphates for end products such as sucrose or starch. When photosynthesis is limited by TPU, plants engage regulatory mechanisms that reduce the amount of CO_2 being fixed by the plant, including reduction of rubisco activation state and reduced electron transport rate as a result of increased nonphotochemical quenching. These effects balance the flux of phosphate into and out of the phosphate pool. A number of questions surrounding TPU limitation have evolved over the roughly 40 years of study of TPU limitation. Why is it that TPU limitation is so easy to trigger in laboratory conditions, but very rare to find in ambient conditions in the field? Why is it that triose phosphates do not accumulate under TPU limitation? And why is it that TPU limitation exists in the first place, given the relatively low nitrogen investment it would take to prevent its occurrence at all? The research presented in this dissertation advances the field by analyzing TPU limitation not just as an outcome of elevated photosynthetic rate, but fundamentally as a stressor which provokes acclimation. The regulatory features associated with TPU limitation were analyzed as a time-course that protects the plant from immediate redox danger and eventually results in the abolition of TPU limitation in the steady-state. High-speed measurements of assimilation and electron transport not only contribute to the time-course of acclimation but help to divide TPU limitation into two related phenomena: first, a crisis in metabolism that includes serious perturbation in photosynthesis that lasts for up to a few

minutes; then, the slower response in which the crisis in metabolism has been resolved and the maximum photosynthetic rate has been limited by regulatory features.

Regulatory features associated with TPU limitation eventually cause plants to stop being TPU limited

The steady-state assimilation rate under a TPU limitation is determined by regulatory features which balance phosphate flux. TPU limited plants experience reduced rubisco activation state (Socias *et al.*, 1993; Viil *et al.*, 2004) (Figure 2.3). TPU-limited plants develop elevated transthylakoid proton-motive force (*PMF*) leading to increased nonphotochemical quenching and greater photosynthetic control at cytochrome *b6f* (Kramer & Crofts, 1993; Takizawa *et al.*, 2008). In the steady state, these regulations reduce the maximum rate of photosynthesis in balance with TPU capacity (Sharkey, 1985b). These features are important in diagnosing TPU limitation, and the characteristic decline in PSII efficiency with increasing CO_2 (Stitt, 1986; Sharkey *et al.*, 1988) is one of the most reliable indicators of TPU limitation (McClain & Sharkey, 2019).

We found that over a 30 h period of adaptation to TPU limitation caused by elevated CO_2, rubisco activation state remained low (Figure 2.3), and *NPQ* increased across the whole *A*/*Ci* curve (Figure 2.2). Furthermore, at the end of the 30 h period, the plant no longer exhibited symptoms of TPU limitation (Figure 2.2). It lacked the characteristic decline of φ_{II} and the matching increase in *NPQ* in response to increasing CO_2, and the photosynthetic rate did not remain flat against increasing CO_2. The overall increased *NPQ* and flat response of *NPQ* to CO_2 tells us that elevated photoinhibition (q_i) was responsible for the elevated NPQ rather than energy dependent quenching (q_e). These slow control mechanisms increased in their

importance over time and resulted in the total acclimation of the leaf to TPU limitation after just over a day. Notably, this acclimation was achieved by reducing the capacity for photosynthesis through rubisco and electron transport controls. The nitrogen cost of increasing TPU capacity would be very low, while rubisco and electron transport enzymes contain 47% of the average leaf's nitrogen content (Evans & Clarke, 2019). This method of acclimation in elevated CO_2 therefore reduces the nitrogen efficiency of the leaf.

There is a lifetime for TPU limitation

Acclimation has now been observed in plants subjected to both low temperatures and elevated CO_2. Plants held at low temperatures are frequently subjected to TPU limitation due to the temperature sensitivity of sucrose-phosphate synthase (Sharkey & Bernacchi, 2012; Yang *et al.*, 2016). Plants subjected to TPU limitation by low temperature are known to increase their TPU capacity by expressing greater quantities of sucrose synthesis enzymes in as little as 5 h (Guy *et al.*, 1992; Holaday *et al.*, 1992; Strand *et al.*, 1999) so that they are no longer TPU limited. Even though the source of the acclimation is different for the low temperature case than for the elevated CO_2 case, it does imply that acclimation to TPU limitation will occur regardless. The route through which acclimation is achieved under low temperature increases the total amount of photosynthate that can be fixed, unlike in the elevated CO_2 case. Possibly it is that under low temperature the plant is growing slowly due to lack of photosynthate, but under elevated CO_2 the plant is already growing as fast as it can and will not be able to grow faster with greater photosynthesis, causing this divergence in acclimation. This connection is a source of continued interest (Paul & Pellny, 2003; Fabre *et al.*, 2019; Dingkuhn *et al.*, 2020) but

it is very hard to draw any direct connection between sink strength and leaf-level photosynthesis.

The acclimation to TPU limitation justifies the removal of TPU limitation from global models

The qualitative understanding that TPU limitation symptoms are rare in the field under ambient conditions has been used recently as justification to remove the consideration of TPU from global models of photosynthesis (Lombardozzi *et al.*, 2018; Rogers *et al.*, 2020). Our new understanding of the acclimation of the leaf to TPU limiting conditions provides a concrete rationale for this removal. If a plant would be TPU limited under field conditions, it will eventually stop being TPU limited over a period of days to weeks. This conclusion has some evolutionary importance as well. The *Nicotiana benthamiana* used extensively in this dissertation becomes TPU-limited at saturating light (1000 µmol m^{-2} s^{-1}) and slightly elevated CO_2 levels ($C_i \approx 400$). This level of CO_2 has occurred in the past and seems likely to be achieved in the future (Rae *et al.*, 2021). The ability to cope with changing CO_2 across geologic timescales is an important aspect of TPU acclimation.

TPU limitation causes dangerous accumulation of electrons in the very short term

A step change in CO_2 concentration induces TPU limitation, and sharply entering TPU limitation causes transient effects on photosynthesis (Figure 2.4). Initially, the plant gains additional electron acceptors and PSI becomes oxidized. However, after 40 s, the plant enters TPU limitation, as evidenced by the decreased proton conductivity across the thylakoid (g_{H+}), and PSI becomes reduced rather than oxidized. This reduction is the result of an acceptor-side limitation and causes backup of electrons all the way to PSII electron acceptors (oxidation state of Q_a measured as q_L). Reduction of Q_a causes excess energy to be diverted to NPQ and is the

first response to TPU limitation that safely dissipates excess light energy. It is important to handle this excess light energy because the reduction of PSI quickly becomes a redox threat to the plant (Li *et al.*, 2009). Over the next 80 seconds, slower control mechanisms, such as rubisco deactivation and NPQ (measured as NPQ_t) begin, diverting energy and allowing Q_a to become more oxidized again.

These short-term effects on electron transport are mirrored by transients in assimilation rate. Entering TPU limitation suddenly introduces oscillations in assimilation (Figure 3.1 – Figure 3.4). These oscillations have long been associated with TPU limitation (Ogawa, 1982; Sivak & Walker, 1986, 1987), but the cause of the oscillations had never been conclusively established. Our measurements of PSI oxidation state during transients following imposition of TPU limitation suggest acceptor side limitation of PSI as a primary cause of oscillations (Figure 2.4; Figure 3.6). These measurements support the theory of Laisk *et al.* (1991), who calculated that TPU limitation caused antiparallel variation in the supply of ATP and NADPH. The mismatch of time constants for NADPH, ATP, and carbon metabolism lead to oscillations in the photosynthetic rate.

The transient effects of TPU limitation support the division of TPU limitation into two phenomena

TPU limitation, when suddenly introduced, causes effects that are either not present in, or are intensified when compared to, the steady state. Though assimilation can achieve transient overshoots due to available phosphate pools, it soon experiences a reduction in rate during which it performs much worse, while the extra carbon is cycled around and exported (Figure 3.3). TPU limitation includes reduction in available phosphate (Sharkey & Vanderveer,

1989) and reduced g_{H+}, but when TPU limitation is introduced, chloroplasts transiently experience even lower g_{H+} (Figure 2.4). During this time, the orthophosphate availability must be even lower than what is typical of steady-state TPU limitation.

The existence of transients in TPU limitation is due to the relatively slow response of regulatory factors that would control photosynthesis and how they must react to the crisis in phosphate supply. This is supported by the worse overall assimilation achieved by plants when subjected to CO_2 ramps compared to CO_2 spikes (Figure 3.1), as ramps constantly change the "set point" of regulation. This increases the period during which the plant cannot reach the appropriate level of control. We therefore propose the existence of a critical "acute" TPU limitation, where phosphate availability is more strained, and instead of assimilation rate being determined by regulatory factors, it is determined directly by metabolite pools.

APPENDICES

APPENDIX I

Building a better equation for electron transport estimated from chlorophyll fluorescence: Accounting for non-photosynthetic light absorption

Chlorophyll fluorescence measurements of electron transport rate are an important companion of gas exchange analysis of photosynthesis. Detailed models allow prediction of gas exchange behavior based on fluorescence measurements, critical for converting low-throughput photosynthetic measurements to greater scales (Damm *et al.*, 2010). Recently, a problem with using fluorescence-estimated electron transport rates in red versus blue light was discussed (Evans *et al.*, 2017). The explanation was that high absorptance of blue light leads to saturation of photosystems near the light-exposed surface, but the red measuring beam may sample deeper in the leaf (Vogelmann, 1993; Vogelmann & Han, 2000). In this case, fluorescence will report the quantum yield of photosystem II (φ_{II}) averaged from different photosystems than those important for the carbon-based quantum yield. The photosystems lower in the mesophyll will absorb less light, but will have a higher φ_{II} than tissues nearer the light-exposed surface (Lichtenberg *et al.*, 2017), and so electron transport will be overestimated. The overestimation caused by this sampling error will be higher for wavelengths of light which are more strongly absorbed, so highest under blue actinic light and lowest under green actinic light (Evans, 2009). Based on this effect, some investigators are now choosing to use the minimum amount of blue needed to open stomata to minimize the overestimation of electron transport from blue light during gas exchange measurements.

However, another effect that can cause overestimation of electron transport rates under blue actinic light is absorption of blue light by non-photosynthetic pigments. This effect is easily accounted for, reducing the justification for minimizing the use of blue light, allowing routine use of light quality that more closely resembles natural conditions.

Linear electron flow estimated from chlorophyll fluorescence (J_F) is calculated as

$$J_F = \Phi_{II} \sum_{\lambda=400}^{700} \alpha(\lambda) \cdot \beta \cdot I(\lambda) \qquad \text{Eq. A1.1}$$

where α is the absorptance of the leaf, a function of wavelength; β is the proportion of total incoming radiation absorbed by PSII; and I is the photosynthetic photon flux density (PPFD), a function of wavelength. The absorptance of the leaf can be measured with an integrating sphere (Mõttus *et al.*, 2017), though it is usually just estimated. The current default estimate for absorptances in LI-COR instruments is 0.87 for blue light and 0.84 for red light. β is possible to measure through a destructive process (Strand & Kramer, 2014), or estimated via a Laisk plot (Laisk & Loreto, 1996), but is typically assumed to be 0.5. β would be changeable over the course of an experiment due to state transitions (Ruban & Johnson, 2009), introducing some uncertainty in electron transport rate estimates. φ_{II} is measured from chlorophyll fluorescence analysis (Genty *et al.*, 1989). There are some assumptions made when measuring φ_{II}, notably that φ_{II} is homogenous throughout the leaf and that $F_M^{`}$, the maximum fluorescence in the light, is being measured accurately, which is not always the case. A multiphase flash protocol can improve the measurement of $F_M^{`}$ (Loriaux *et al.*, 2013; Avenson & Saathoff, 2018). Equation A1.1 can be put into words as: linear electron flow is the amount of light (I) absorbed by the leaf (α) that is partitioned to photosystem II (β) that leads to transport of an energetically excited electron to downstream quinol carriers (φ_{II}). When stated this way, it becomes clear that it is assumed every absorbed photon will lead to electron transport downstream. We specifically believe this assumption is incorrect.

If there is absorption of light by non-photosynthetic pigments, equation 1 is no longer correct. There are a number of pigments that absorb blue light but that do not contribute to

photosynthetic electron flow, especially carotenoids. The role of carotenoids in leaves has been debated for decades. Some experiments on reaction centers *in-vitro* show energy transfer efficiency from carotenoids of up to 100% (Siefermann-Harms & Ninneann, 1982; Croce *et al.*, 2001), while other studies show reduced transfer efficiency of 90% (Connelly *et al.*, 1997) or 80% (Holt *et al.*, 2003) or less (Emerson & Lewis, 1942). Laisk et al. (2014) estimated that approximately 30% of the light can be absorbed by carotenoids unable to transfer energy to the photosystems. Non-photosynthetic albino leaves can absorb more than 20% of blue light (Hogewoning *et al.*, 2012). Together, these effects produce a disparity between blue photons absorbed and the blue photons that result in electron transport. In this instance, even if φ_{II} is being measured correctly, calculations of linear electron transport will be incorrect; the error will be wavelength dependent.

The assumption of constant β is an additional source of error in equation 1. The pigments associated with photosystems I and II are not identical, and each may absorb certain wavelengths preferentially (Evans & Anderson, 1987). In this case β would be a function of wavelength, and the two photosystems would have different levels of excitation (Hogewoning *et al.*, 2012) resulting in inefficient loss of exciton energy to quenching (Evans, 1987; Pfannschmidt, 2005). The wavelength sensitivity of β may lead to an underestimation of J_F as discussed in Loreto *et al.* (2009); this must be considered even though this effect is in the opposite direction of the typical overestimation of J_F in blue light. There may also be some mid-experiment changes in α due to blue light-induced chloroplast movements (Wada *et al.*, 2003). This effect can be estimated from leaf reflectance changes (Woolley, 1971), but probably cannot be estimated using an integrating sphere which uses pre-scattered light.

An action spectrum uses quantum yield calculations to measure the efficiency of transfer to, or use of absorbed light energy at reaction centers (McCree, 1970). For a correction involving only red and blue light it is possible to measure the quantum yield for the two colors and reduce the calculated electron transport yield for blue light according to the relative efficiency of blue light

$$Relative\ Blue\ Efficiency = \frac{Quantum\ yield\ (blue\ light)}{Quantum\ yield\ (red\ light)} \quad \text{Eq. A1. 2}$$

Equation A1.2 is generalizable to any color or wavelength. This term will include the wavelength sensitivity of β, but cannot measure β.

It is possible to estimate the rate of electron transport from the rate of carbon assimilation (J_C) (Harley *et al.*, 1992) and calibrate J_F (Yin *et al.*, 2009). The calibration factor would include α, β, a correction for non-linear electron transport, and the action spectrum correction. This empirical approach can be useful for many purposes. However, the empirical approach makes significant assumptions about the destination of electrons, such as ignoring the use of reducing power in nitrate assimilation. We propose that J_F should be corrected with independent measurements to the greatest possible extent before considering a clustered calibration, especially in cases where deviation between J_F and J_C is part of the signal (e.g., using fluorescence to estimate the rate of nitrogen reduction or day respiration).

We tested the quantum yield-based correction of electron transport rate measurement using *Nicotiana benthamiana* grown under different conditions to cause a variation in leaf absorptivity. Some plants were grown for seven weeks under low intensity fluorescent lamps (approximately 130 µmol m^{-2} s^{-1}) to increase the absorptance of the leaves while other plants

were grown in a greenhouse, resulting in relatively low absorptance leaves. Leaf absorptance was measured with a pair of integrating spheres spectroscopically. Absorptance of blue and red light was calculated as the average absorptance over the wavelengths at half peak intensity of the actinic lights. For this experiment the red light absorptance was measured over 622-637 nm and the blue light absorptance was measured over 471-494 nm. J_C versus absorbed light was measured from 20 to 60 µmol m^{-2} s^{-1} PPFD (Figure A1.1a). Using low light levels increases the linearity of assimilation response to PPFD, and decreases mis-estimation of the CO_2 concentration at rubisco if mesophyll conductance is inaccurate. The relative efficiency for blue versus red light was calculated as the ratio of the slope extrapolated to 100% blue or 100% red (Figure A1.1b). Extrapolation is necessary due to occasional non-linearity at 100% red light. There is a difference ($P<0.05$) in the relative efficiency for blue light for the two treatments (Table A1.1).

Treatment	Blue Absorptance	Red Absorptance	Relative Blue Efficiency
Low light	0.970 ± 0.003	0.917 ± 0.017	0.734 ± 0.006
Greenhouse	0.944 ± 0.002	0.872 ± 0.010	0.693 ± 0.013

Table A1.1 Variation in absorptances and relative quantum yield in *Nicotiana benthamiana* grown two different ways. Plants grown with reduced light (approximately 130 µmol m^{-2} s^{-1}) have greater absorptance of both blue and red light, as well as greater relative blue efficiency (Eq. 2) when compared to greenhouse-grown plants. N=5 for greenhouse-grown plants and N=4 for plants grown under reduced light. Values are mean ± SE.

Variation in both absorptance and efficiency for blue light will affect the actual electron transport rate. Therefore, for precise electron transport measurements, it is advisable to verify each parameter on a plant-by-plant basis.

To test the effectiveness of relative efficiency for correcting overestimation of electron transport rate in blue light, light response curves up to 1000 µmol $m^{-2}s^{-1}$ were measured under

five ratios of red to blue light on a single plant. Electron transport rate was measured by fluorescence. The electron transport rate was corrected to measured absorptance values of 0.873 for red and 0.951 for blue. The efficiency of blue light relative to red light was measured separately to be 0.69. The uncorrected data shows nonlinearity between J_C and J_F across different ratios of red and blue light (Figure A1.2a). To correct this data, the calculation for linear electron flow was modified by multiplying the calculated amount of absorbed blue light by 0.69, the difference in quantum yield that we found. The corrected dataset shows excellent linearity compared to the uncorrected dataset, although J_f overpredicts electron transport rates at high rates of photosynthesis (light intensity about 650 µmol $m^{-2}s^{-1}$ and above) (Figure A1.2b). This may be when sampling errors described by a multilayer model (Evans *et al.*, 2017) begin to affect measurement accuracy. There may also be a change in the composition of nonphotosynthetic pigments at elevated light (for example, the xanthophyll cycle), which would lead to an intensity dependent change in γ. Other issues that could be explored for the high light deviation include chloroplast movement and state transitions.

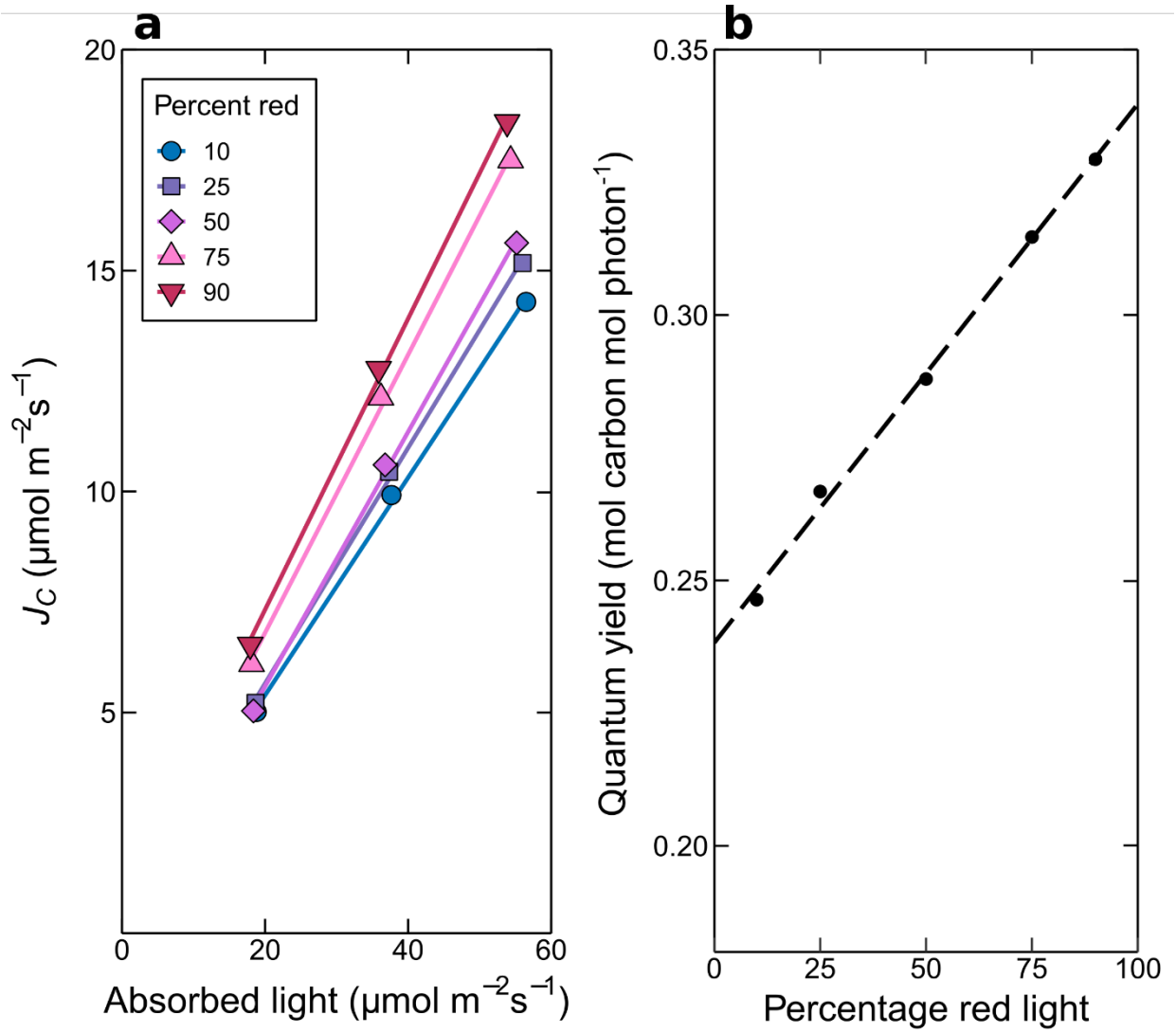

Figure A1.1 Measurement of quantum yield for blue and red light of a leaf of *Nicotiana benthamiana*. **a**: Light response curves from intensity = 20 to 60 µmol m^{-2} s^{-1} at five different color specifications from 10% red to 90% red (balance blue) have different quantum yields. Electron flux based on CO_2 measurements (J_C) calculated according to Harley *et al.* (1992) with plants held at 25°C under an atmosphere containing 2% oxygen (1.98 kPa) and 750 ppm CO_2 (74 Pa). *Γ** was set to 0.36, calculated from *Γ** measured in tobacco (Bernacchi *et al.*, 2002). Respiration in the light was set to 1.1 µmol m^{-2} s^{-1} as extrapolated from the light response curve at low light. **b**: Quantum yield (slope from **a**) plotted against the proportion of red light reveals a linear relationship (R^2 = 0.997) and can be extrapolated to 0% and 100% red light to determine relative blue efficiency.

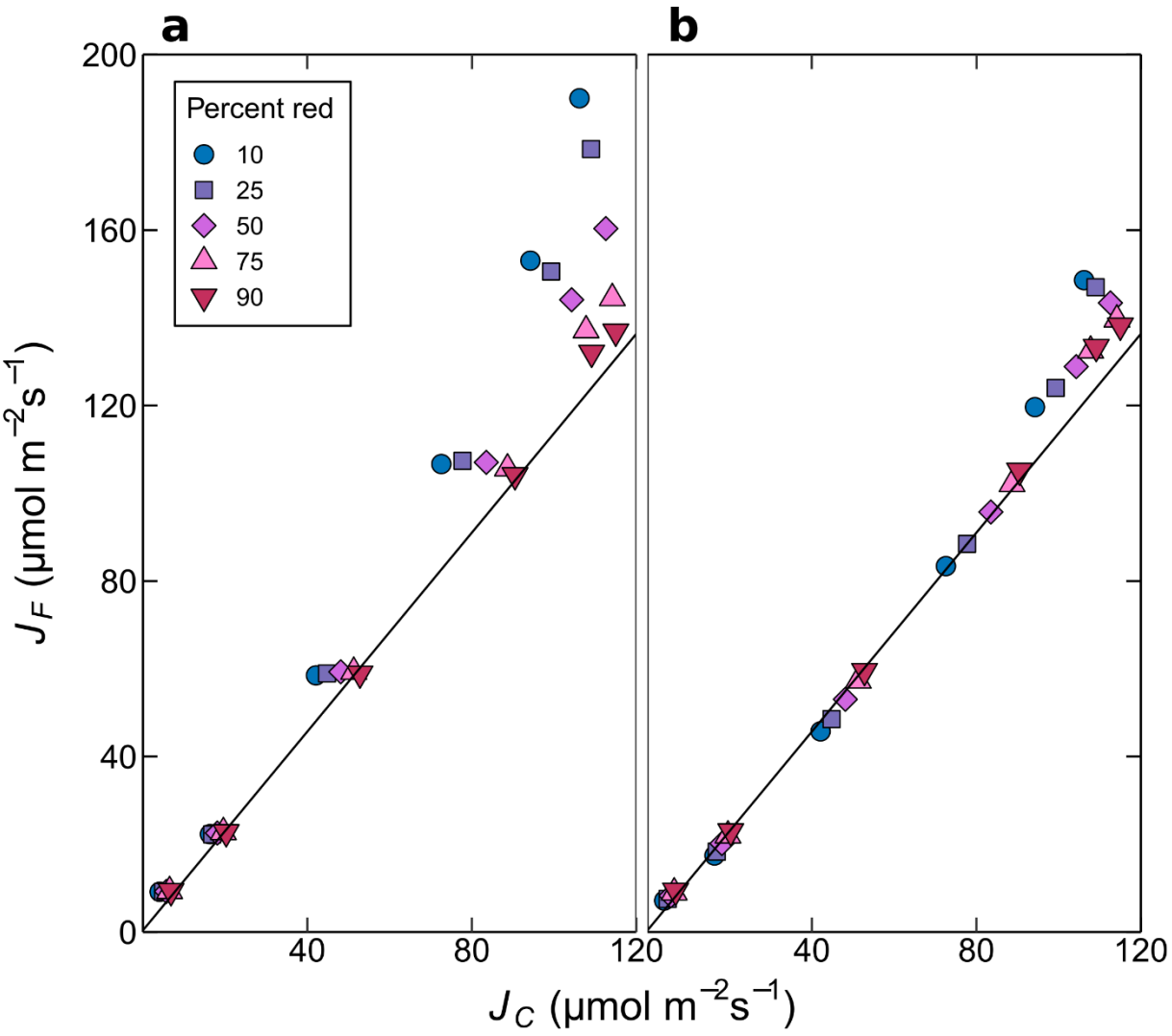

Figure A1.2 Actual fluorescence-derived electron transport data from a light-response curve before (**a**) and after (**b**) correcting for the relative efficiency of blue light for a leaf of *Nicotiana benthamiana*. **a**: Data is corrected for absorptance of the leaf alone and is uncorrected for relative efficiency of blue versus red light. Electron flux estimated from fluorescence (J_F) shows poor linearity with electron flux based on CO_2 measurements (J_C). **b**: Data from **a** is corrected per equation 3, with γ = 0.69 for blue light. After correction, J_F shows considerably better linearity with J_C. At the highest light levels (650 and 1000 µmol m^{-2} s^{-1}) J_F begins to deviate from linearity with J_C.

The relative efficiency of provided light is very important to actual electron transport rates *in planta*, but rarely make it into standard calculations of electron transport. To include it, we recommend modifying Equation A1.1 to

$$LEF = \Phi_{II} \cdot \sum_{\lambda=0}^{\infty} \alpha(\lambda) \cdot \beta \cdot I(\lambda) \cdot \gamma(\lambda) \qquad \text{Eq. A1.3}$$

where γ is relative efficiency, a function of wavelength. Absorptance and quantum yield for extreme wavelengths will be small and we can expand the limits on the sum. The parameter γ was originally proposed by Loreto et al. (2009) as a qualitative correction between electron transport estimated from measurements of the rate of carbon assimilation versus electron transport measured by fluorescence under varying amounts of blue light. Relative efficiency, calculated from quantum yield, is a quantitative measurement that achieves the qualitative goal of increasing linearity between J_C and J_F. However, this formulation assumes that there are some wavelengths of light (red) that are used 100% for photosynthetic electron flow. This is likely incorrect, but we assume the error is minor relative to other uncertainties in this analysis.

The fluorescence sampling error may be an issue for correctly measuring leaf electron transport at saturating photon flux density. However, the nonphotosynthetic absorption of blue light is a bigger effect than the sampling error at the light levels measured and is easily corrected. We strongly recommend that that a third term be added to Equation A1.1 as recommended by Loreto *et al.* (2009).

The incorporation of absorption efficiency into the calculation improves the accuracy of measurements of LEF, especially at sub-saturating intensities and higher proportions of blue light. Blue actinic light is essential to maintain large stomatal aperture (Iino

et al., 1985), which is important for gas exchange measurements. While 10% blue light may be sufficient for the first opening of the day with unstressed plants, when new conditions are encountered it will be advantageous to have amounts of blue light similar to the natural condition in case there are variations in stomatal responses determined by blue light availability. Sunlight spectra were measured from 380 nm-780 nm with a LI-180 spectrometer. Our measurements of sunlight show 2.02 times as many red photons as blue, depending on how these colors are defined. Sunlight contains about 1.25 times as many photons in the wavelengths emitted by the LI6800-01 blue LEDs relative to the red LEDs (Table A1.2).

Classification	Wavelengths	Percentage of Sunlight
LI 6800 Blue	471-494	5.84
LI 6800 Red	622-637	4.65
Full Spectrum Blue	450-490	9.59
Full Spectrum Red	635-700	19.3
All Visible	400-700	76.6

Table A1.2 Spectrum from 380 nm to 780 nm of sunlight taken under bright sun at noon at 42°43'N 84°28'W (East Lansing, Michigan, USA). LI 6800 Red and LI 6800 Blue refer to the wavelengths at half of peak intensity for LI 6800-01 red and blue LEDs.

These would represent percentages of 33% or 56% blue, respectively. We recommend the routine use of 50% blue light to improve the similarity between natural sunlight and LED illumination in this case. The reduced value of 33% blue light will also probably produce reasonable results. The current practice of using just 10% blue light is not justified, especially when stomatal function is under study. Using more realistic values of red versus blue light for gas exchange improves the chance that the data obtained from artificially lit gas exchange chambers will accurately reflect physiological responses under natural conditions. We recommend a quantum yield-derived correction be applied to calculations of electron transport on a plant-by-plant basis. We also recommend that when only red or blue light is available, a

50/50 mix of photon fluxes should be used to increase the likelihood of physiologically relevant light responses, especially stomatal responses.

APPENDIX II

The triose phosphate utilization limitation of photosynthetic rate: out of global models but important for leaf models

Foreword: Designing a tool for fitting A/C_i curves

The programmatic fitting of Assimilation (A)/internal CO_2 concentration (C_i) curves presents several unique challenges compared to other nonlinear fitting models. One of the biggest challenges is that A/C_i curve model is a step function – it comprises three individual models, each of which fits a contiguous section of the collected data points. The first is based on Michaelis-Menten kinetics and is fit around the parameter maximum velocity of carboxylation V_{cmax}; the second is based on the regeneration rate of RuBP and revolves around the electron transport rate J; and the third is the utilization rate of triose phosphates, TPU. The other biggest challenge is that collected data is in the form of A/C_i; however, the true concentration of CO_2 at the site of carboxylation (C_c) is what governs assimilation. The measurement of C_c in intact leaves is not compatible with the collection methods used for these data sets, so conductivity to diffusion of CO_2 from the internal airspace of the leaf to the site of carboxylation (mesophyll conductance, g_m) is one of the fit parameters of the A/C_i curve. This means that one of the fitting variables affects the x-axis variable. While neither of these challenges are critically damaging to the fitting algorithm itself (here we used the Levenberg-Marquardt least-squares algorithm) both are prohibitive to statistical analysis of the A/C_i curve fitting problem.

In all nonlinear curve fitting algorithms, it is impossible to guarantee the selection of the global minimum sum-of-squares (SSR). Instead, algorithms will select the proximal critical point. This presents several problems with the step-function nature of the A/C_i model. The first is that, since data points are not continuous, if the initial step size of the fitting algorithm is not sufficiently large, it is possible that the algorithm won't be able to adequately shift the break

point for the three steps to sample possible configurations of which points are fit by which curve (that is, there may be a local minima in which points are assessed according to the wrong curve which prevents discovery of a lower SSR). The second is that, in a data set in which no data points should be fit according to any one of the steps, the algorithm will always be able to improve the SSR by erroneously incorporating the missing curve. The algorithm would be able to target whichever point has the greatest individual residual and fit it perfectly – a clear example of over-fitting.

Three efforts were made to ameliorate these issues. The first is the addition of a real-time graphical interface provided via the Shiny, plotly, and ggplotly packages. The ability to assess immediately whether the curve qualitatively fits properly is one of the major advantages over other fitting packages such as plantecophys (Duursma, 2015). The user is also able to manually adjust the starting conditions of the fitting algorithm to help coerce the algorithm to find a more accurate fit. The plot also makes it obvious if any single point at the edge of the plot is being over-fit. As an additional effort to counter the overfitting issue, we added the ability to outright disable analysis of the most frequently over-fit limitation, the TPU limitation. TPU limitation only occurs when the plant is photosynthesizing quickly and is the most likely of the three limitations to be unseen in a typical A/C_i curve (Kumarathunge *et al.*, 2019; Rogers *et al.*, 2021). TPU limitation can be modeled as simply as a straight line (Sharkey, 1985b) which makes overfitting very accessible for the algorithm. The last effort made to improve off-target fitting is a set of heuristics designed to provide the A/Ci fitting algorithm a favorable starting guess based on the fundamental biology. The initial guess for *TPU* is 3 times the highest measured assimilation rate, one for each carbon in a triose phosphate and the simplest model for TPU

limitation (Sharkey, 1985a). For *J*, it is 5 times the highest assimilation rate, which is 20% higher than the necessary 4 electrons per carbon to account for photooxidation. V_{cmax} tends to be just a bit lower than J, so it is set to 75% of *J*. Finally, R_L is set to 10% of maximum assimilation, and g_m is set to 3 – these are intermediate values which after some testing tended to lead to acceptable fits across a variety of samples. These initial guesses ensure that the starting condition of the nonlinear fit is both on the same scale as the collected data and approximately the same shape. These simple heuristics also help prevent researcher bias from entering the fit. Because there are often so many local minima possible in the seven-parameter fitting model (Busch & Sage, 2017) the selection of starting conditions will affect the results of the nonlinear fit. No matter what, the starting condition selection will cause some level of bias. A machine-based heuristic at least guarantees consistent bias based on the general shape of the A/C_i curve, and helps researchers prevent their own bias from entering the data analysis.

Discussion

Xiao *et al.* **Error! Bookmark not defined.**(2021) present a method for estimating the variability of estimated parameters of the Farquhar, von Caemmerer, Berry (FvCB) model of photosynthesis (Farquhar *et al.*, 1980). This model has been very effective at predicting photosynthetic responses to CO_2, light, and temperature but estimating the parameters of the model can be difficult, with the fitted parameters having various degrees of uncertainty as demonstrated by Xiao *et al*. The original model assumed one of two conditions: (1) rubisco is saturated with ribulose 1,5-bisphosphate (RuBP) and so responds to CO_2 with Michalis-Menten kinetics (rubisco-limited) or (2) rubisco uses RuBP as fast as it is made (RuBP regeneration-limited). In condition (2), rubisco activity is determined by the rate of RuBP regeneration,

typically as a result of being light-limited. But even though photosynthetic CO_2 assimilation (*A*) is light limited, it responds to increasing CO_2 because of suppression of photorespiration. Carboxylation plus oxygenation stays constant under RuBP regeneration limited conditions so if oxygenation goes down as CO_2 increases, carboxylation will go up. The model was expanded to include a third condition, where RuBP regeneration is limited by how fast phosphorylated intermediates, primarily triose phosphates, are converted to end products, thereby releasing phosphate (Sharkey, 1985b). This is usually called triose phosphate utilization (*TPU*) limitation.

The FvCB model is most often parameterized by measuring CO_2 assimilation as a function of CO_2 inside the air spaces of the leaf (C_i), called an A/C_i curve. While rubisco-limited, assimilation shows a strong response to CO_2 while RuBP-regeneration-limited points show less response but still increase with increasing CO_2. TPU-limited points are characterized by no response to CO_2 and sometimes an inhibition under increasing CO_2 (Laporte *et al.*, 2001). The condition is further diagnosed by a decline in photosynthetic electron transport caused by an increase in CO_2 or decrease in O_2 (measured by chlorophyll fluorescence analysis). The TPU limitation is rarely seen at physiological CO_2 partial pressure and temperature but is very frequently seen when CO_2 is marginally higher than what the plant experienced during growth, especially if the temperature during the measurement is lower than the growth temperature (Sage & Sharkey, 1987). Increasing the capacity for sucrose synthesis, reduces the temperature at which *TPU* is observed (Laporte *et al.*, 2001). *TPU* limitations are also associated with oscillations in photosynthetic rate (Sharkey *et al.*, 1986c), complicating measurements of *TPU*-limited photosynthesis rates.

The parameters that can be estimated by the fitting models are the maximum rate of rubisco carboxylation (V_{cmax}) and the rate of electron transport (J) (since the analysis can be done at limiting light, this need not be J_{max}). Also estimated are respiration in the light (R_L) (previously called day respiration, R_d) and mesophyll conductance (g_m). If *TPU* is considered, it too is estimated. We have used equations proposed by Busch et al. (2018) to include carbon flow out of photorespiration as glycine (α_G) or serine (α_S) which can affect estimates of *TPU* and *J*.

Some groups have concluded that TPU limitations are likely to be small and thus constitute an unnecessary complication for modeling photosynthesis at global scales (Kumarathunge *et al.*, 2019; Rogers *et al.*, 2021). Moreover, there is evidence that when plants experience *TPU* for a sustained period, both rubisco capacity and electron transport capacity are reduced until *TPU* is no longer evident. Xiao *et al.* (2021) recently described Bayesian methods for estimating parameters of the FvCB model and the uncertainties in those estimates but without including *TPU* in their fitting. We have reanalyzed the data of Xiao *et al.* (2021) to test the effect of inclusion of *TPU* on estimates of other parameters.

We began by re-analyzing the experimental data provided by Xiao *et al.* (2021). Four A/C_i curves measured with rice were provided. In three out of four cases, reverse sensitivity to CO_2 of A was observed and in all four cases, photochemical yield of photosystem II (Φ_{II}) (measured by chlorophyll fluorescence analysis) declined at high CO_2 (Figure A2.1). In repetition 2, Φ_{II} increased at low CO_2 as rubisco activity increased then abruptly began to decline with increasing CO_2 indicating a transition to *TPU* limitation with no points showing clear RuBP regeneration limitation (constant Φ_{II} with changing CO_2).

These behaviors indicate that *TPU* was occurring in all four repetitions. The authors specified in their methods section that they had to wait much longer for stability at the high CO_2 concentrations and the data at high CO_2 was noisy, also an indicator of *TPU*. Because TPU limitation is evident in the data, it must be included in the A/C_i fitting model. We tested the effect of adding *TPU* to the analysis.

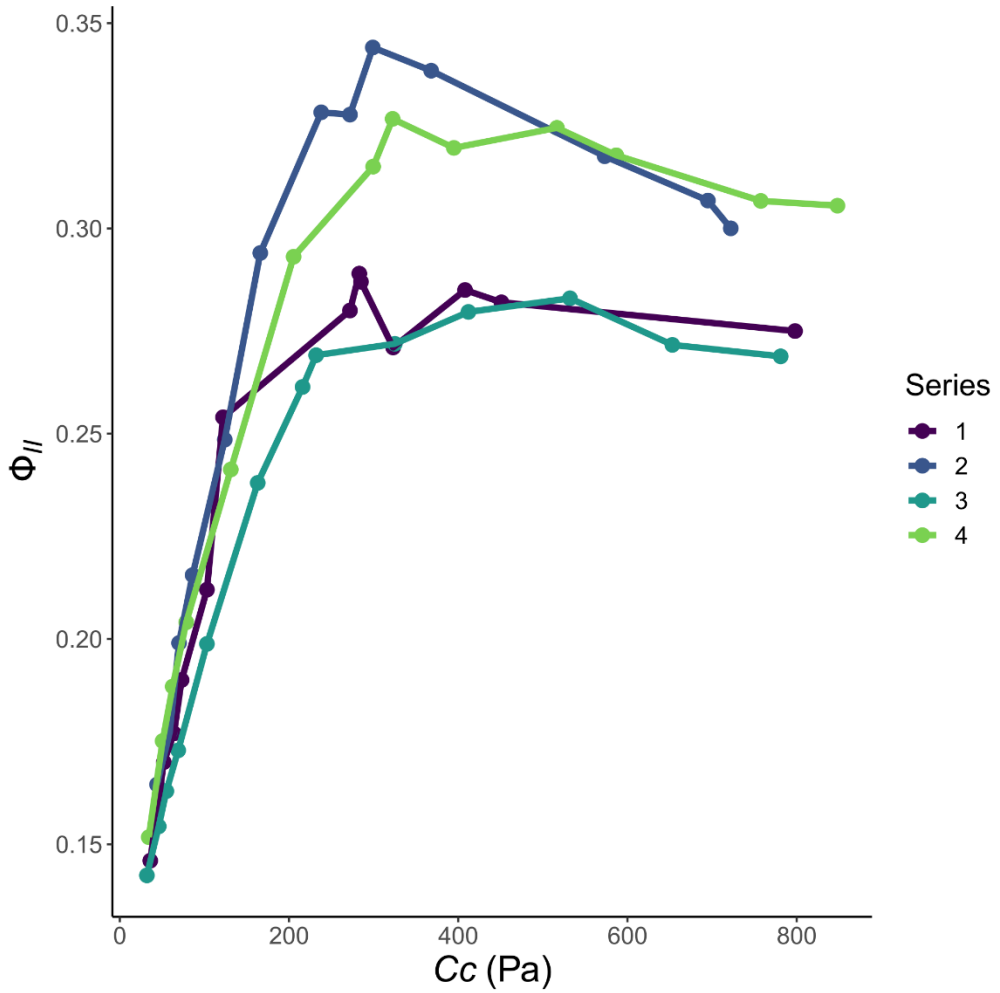

Figure A2.1 Φ_{II} values reported for the four replications of Xiao et al. (2021). Values were determined by chlorophyll fluorescence analysis. Curves 2 and 4 show an abrupt reversal from rubisco-limited (Φ_{II} increasing with increasing CO_2) to *TPU*-limited (Φ_{II} decreasing with increasing CO_2) behavior with no definitive RuBP regeneration limitation (Φ_{II} independent of changes in CO_2).

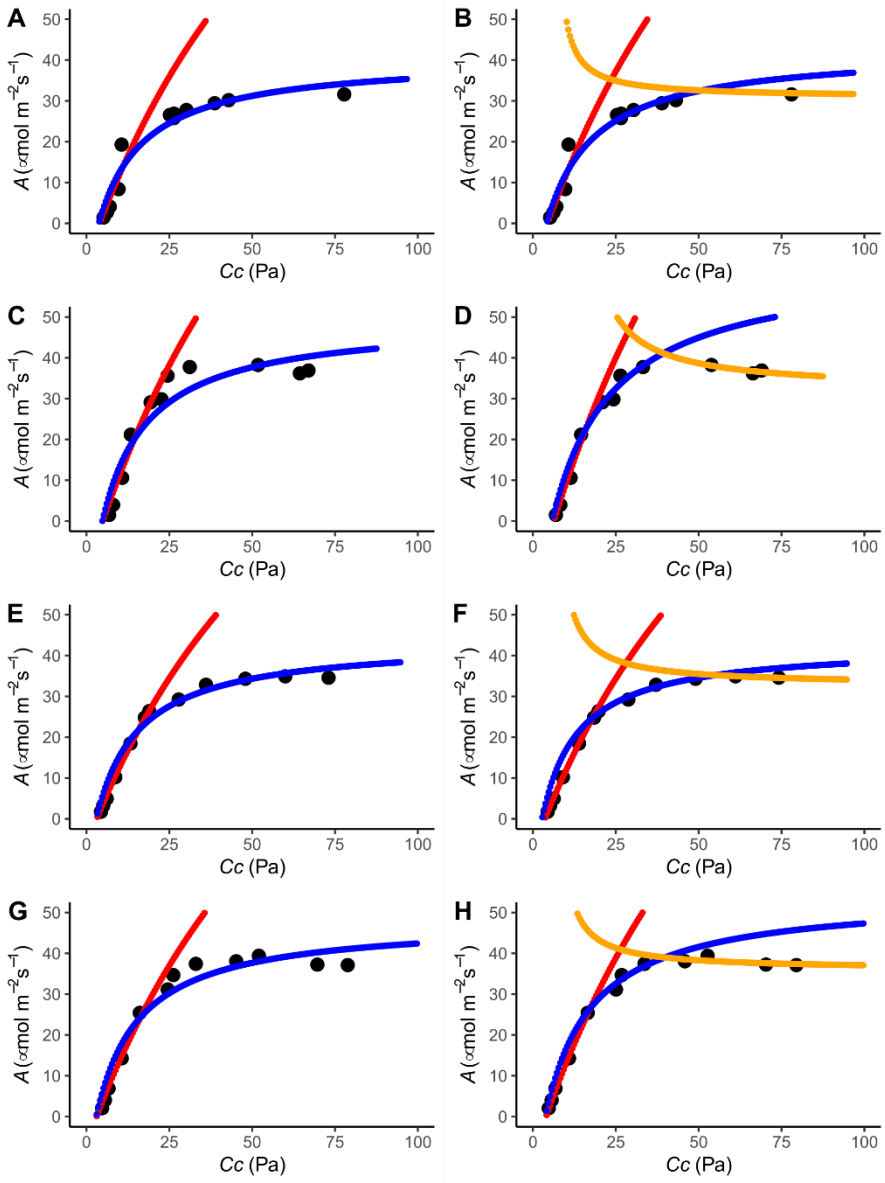

Figure A2.2 Fits to rice data (replications 1-4 of Xiao et al. 2021) without *TPU* (A,C,E,G) or with *TPU* (B,D,F,H). Red is the fitted shape for rubisco-limited condition, blue is for the RuBP regeneration-limited condition and gold is for the *TPU*-limited condition.

We converted the most recent version (2.9) of the fitting spreadsheet that has been provided by Plant Cell and Environment (Sharkey, 2016) to an R script with a user-friendly interface (Shiny app), see https://github.com/poales/msuRACiFit.

The script iteratively fits data sets to biochemical models using rubisco-limited, RuBP-regeneration-limited, or *TPU*-limited assumptions, then calculates which process is likely to be

rate-limiting for each data point, thus eliminating the need to assign specific limiting process to each of the data points.

We then fitted the data supplied by Xiao et al. (2021), first without *TPU* and then with *TPU* (Figure A2.2). For all four curves supplied, including *TPU* in the fitting improved the fit to the data at high CO_2 and this was reflected in a reduction in the sum of the squared residuals (SSR), by 90% in three out of four repetitions (Table A2.1). The reduction in SSRs was much greater than could be accounted for by the increase in degrees of freedom introduced by fitting additional parameters (i.e., *TPU*).

		Rep 1		Rep 2		Rep 3		Rep 4	
	Units	woTPU	wTPU	woTPU	wTPU	woTPU	wTPU	woTPU	wTPU
V_{cmax}	µmol m^{-2} s^{-1}	183	194	203	232	167	174	179	197
J	µmol m^{-2} s^{-1}	170	178	201	273	177	185	194	222
TPU	µmol m^{-2} s^{-1}	-	10.9	-	12.3	-	12.1	-	12.4
g_m	µmol m^{-2} s^{-1} Pa^{-1}	11.4	12.4	6.2	9.5	5.9	7.3	5.5	6.0
R_L	µmol m^{-2} s^{-1}	1.91	1.82	0.72	4.60	0.60	3.55	0.41	1.24
a_G	unitless	0.33	0.22	0.00	0.01	0.40	0.59	0.38	0.26
a_S	unitless	0.00	0.00	0.00	0.36	0.00	0.00	0.00	0.00
SSR	(µmol m^{-2} s^{-1})^2	73.3	53.3	174.4	16.9	19.0	1.2	73.8	7.0

Table A2.1 Comparisons of parameter values and sum of squared residuals (SSR). Rice data Xiao et al. (2021) showing the differences that occur when the triose phosphate utilization (TPU) limitation is considered and when it is not (fittings of the data in Figure 1 A-H). *J* will always be underestimated when *TPU* limited points are treated as being *J*-limited.

When data points are treated as *J*-limited but are actually limited by another process such as *TPU*, *J* is likely to be underestimated. The estimate of *J* was higher when *TPU* was included in the analysis (Table A2.1) but if none of the points are definitely *J*-limited (e.g., repetition 2) then the estimate of *J* is an estimate of the minimum *J*, not a true estimate of *J*.

Because *J*-limited measurements hold the most information concerning g_m, g_m can be difficult to measure when A/C_i curves are measured at saturating light. Using high but not saturating light can de-emphasize *TPU* limitation and increase the amount of *J*-limited data, which can improve estimates of g_m (Sharkey, 2019) (see box 1 of that paper). We also note that the method of splitting the measurement of the A/C_i, going from ambient down, returning to ambient and going up sometimes introduces noise that is more apparent in the chlorophyll fluorescence data than *A* (see for example repetition 4, Figure A2.1 light green data, Figure A2.2 panels G and H). This noise in the data comes at the part of the curve that provides most information about g_m and so it is best to avoid the split method of measuring A/C_i curves.

We conclude that 1. It is important to include *TPU* when fitting A/C_i curves when there is evidence that *TPU* is occurring; 2. Additional data may be needed depending on how the fittings are to be used, for example it may be necessary to measure curves at saturating and also sub saturating light to get robust measures of all parameters. Because there are many parameters being fitted, some of which are complimentary, there is a danger of over fitting. When possible, parameters should be determined by independent measures. For example, g_m and R_L can be estimated independently and then fixed during fitting.

It must be accepted that some parameters can change within minutes and this biological source of variance should be considered. Very rapid, monotonic A/C_i curves are likely to be very helpful in assessing the physiology of photosynthesis just as a high-speed shutter on a camera helps bring things into focus, especially when the subject is dynamic. The latest technology released by LI-COR allows A/C_i curves to be measured in under five minutes (https://www.licor.com/env/support/LI-6800/videos/dynamic-assimilation-technique.html).

Reporting the parameters of the FvCB model can be helpful for global modeling, for detecting effects of the environment on photosynthesis, and changes in specific components of photosynthetic capacity. Because *TPU* is normally a temporary condition, it likely will not improve global models of photosynthesis (Kumarathunge *et al.*, 2019; Rogers *et al.*, 2021). However, for laboratory studies or studies of initial effects of environmental changes on photosynthetic capacity, *TPU* is an important parameter to include in fitting routines and significant uncertainties can arise when it is not included in analysis of A/C_i curves.

For large datasets fitting batches of curves using programs like R can be very helpful. We supply a R package used in this work together with a Shiny app for ease of fitting. What is presented expands on part of an earlier R Package (Duursma, 2015). The Shiny app allows users to test specific hypotheses and can be a convenient way to explore how changing conditions such as temperature and light affect predicted rates of photosynthesis. Please see https://github.com/poales/msuRACiFit for how to access and use the R script and Shiny app used for this work.

BIBLIOGRAPHY

BIBLIOGRAPHY

Abadie C, Bathellier C, Tcherkez G. **2018**. Carbon allocation to major metabolites in illuminated leaves is not just proportional to photosynthesis when gaseous conditions (CO_2 and O_2) vary. *New Phytologist* **218**: 94–106.

Abadie C, Tcherkez G. **2018**. In vivo phosphoenolpyruvate carboxylase activity is controlled by CO_2 and O_2 mole fraction and represents a major flux at high photorespiration rates. *New Phytologist*.

Allen LH, Kimball BA, Bunce JA, Yoshimoto M, Harazono Y, Baker JT, Boote KJ, White JW. **2020**. Fluctuations of CO2 in Free-Air CO2 Enrichment (FACE) depress plant photosynthesis, growth, and yield. *Agricultural and Forest Meteorology* **284**: 107899.

Andrews TJ, Kane HJ. **1991**. Pyruvate is a by-product of catalysis by ribulosebisphosphate carboxylase/oxygenase. *Journal of Biological Chemistry* **266**: 9447–9452.

Arp WJ. **1991**. Effects of souce-sink relations on photosynthetic acclimation to elevated CO_2. *Plant Cell & Environment* **14**: 869–875.

Arrivault S, Guenther M, Ivakov A, Feil R, Vosloh D, Van Dongen JT, Sulpice R, Stitt M. **2009**. Use of reverse-phase liquid chromatography, linked to tandem mass spectrometry, to profile the Calvin cycle and other metabolic intermediates in Arabidopsis rosettes at different carbon dioxide concentrations. *Plant Journal* **59**: 824–839.

Avenson TJ, Saathoff AJ. **2018**. Sub-saturating multiphase flash irradiances to estimate maximum fluorescence yield. In: Covshoff S, ed. Photosynthesis: Methods and Protocols. New York, NY: Springer New York, 105–120.

Badger MR, Sharkey TD, von Caemmerer S. **1984**. The relationship between steady-state gas exchange of bean leaves and the levels of carbon-reduction-cycle intermediates. *Planta* **160**: 305–313.

Baker NR. **2008**. Chlorophyll Fluorescence: A Probe of Photosynthesis In Vivo. *Annual Review of Plant Biology* **59**: 89–113.

Bao X, Focke M, Pollard M, Ohlrogge J. **2000**. Understanding *in vivo* carbon precursor supply for fatty acid synthesis in leaf tissue. *Plant Journal* **22**: 39–50.

Bellasio C, Beerling DJ, Griffiths H. **2016**. An Excel tool for deriving key photosynthetic parameters from combined gas exchange and chlorophyll fluorescence: theory and practice. *Plant Cell & Environment* **39**: 1180–1197.

Bernacchi CJ, Portis AR, Nakano H, von Caemmerer S, Long SP. **2002**. Temperature response of

mesophyll conductance. Implications for the determination of rubisco enzyme kinetics and for limitations to photosynthesis in vivo. *Plant Physiology* **130**: 1992–1998.

Brooks A. **1986**. Effects of phosphorus nutrition on ribulose-1,5-bisphosphate carboxylase activation, photosynthetic quantum yield and amounts of some Calvin-cycle metabolites in spinach leaves. *Australian Journal of Plant Physiology* **13**: 221–237.

Brunkard JO. **2020**. Exaptive Evolution of Target of Rapamycin Signaling in Multicellular Eukaryotes. *Developmental Cell* **54**: 142–155.

Busch FA, Sage RF. **2017**. The sensitivity of photosynthesis to O_2 and CO_2 concentration identifies strong Rubisco control above the thermal optimum. *New Phytologist* **213**: 1036–1051.

Busch FA, Sage RF, Farquhar GD. **2018**. Plants increase CO_2 uptake by assimilating nitrogen via the photorespiratory pathway. *Nature Plants* **4**: 46–54.

von Caemmerer S. **2000**. *Biochemical Models of Leaf Photosynthesis*. Collingwood, Victoria, Australia: CSIRO Publishing.

von Caemmerer S, Farquhar GD. **1981**. Some relationships between the biochemistry of photosynthesis and the gas exchange of leaves. *Planta* **153**: 376–387.

von Caemmerer S, Farquhar GD. **1984**. Effects of partial defoliation, changes of irradiance during growth, short-term water stress and growth at enhanced p(CO_2) on the photosynthetic capacity of leaves of *Phaseolus vulgaris* L. *Planta* **160**: 320–329.

Canvin DT. **1978**. Photorespiration and the effect of oxygen on photosynthesis. In: Siegelman HW, Hind G, eds. Photosynthetic Carbon Assimilation. Boston, MA: Springer US, 61–76.

Cen Y, Sage RF. **2005**. The regulation of Rubisco activity in response to variation in temperature and atmospheric CO_2 partial pressure in sweet potato. *Plant Physiology* **139**: 979–990.

Chia DW, Yoder TJ, Reiter WD, Gibson SI. **2000**. Fumaric acid: An overlooked form of fixed carbon in *Arabidopsis* and other plant species. *Planta* **211**: 743–751.

Christof K, Ulrich S. **1994**. An improved method, using saturating light pulses, for the determination of photosystem I quantum yield via P700<super>+</super>-absorbance changes at 830 nm. *Planta* **192**: 261–268.

Collatz G, Ribas-Carbo M, Berry J. **1992**. Coupled photosynthesis-stomatal conductance model for leaves of C_4 plants. *Australian Journal of Plant Physiology* **19**: 519.

Connelly JP, Müller MG, Bassi R, Croce R, Holzwarth AR. **1997**. Femtosecond transient absorption study of carotenoid to chlorophyll energy transfer in the light-harvesting complex II of photosystem II. *Biochemistry* **36**: 281–287.

Cornic G, Ghashghaie J, Genty B, Briantais J-M. **1992**. Leaf photosynthesis is resistant to a mild drought stress. *Photosynthetica* **27**: 295–309.

Cornic G, Louason G. **1980**. The effects of O_2 on net photosynthesis at low temperature (5°C). *Plant, Cell & Environment* **3**: 149–157.

Croce R, Müller MG, Bassi R, Holzwarth AR. **2001**. Carotenoid-to-chlorophyll energy transfer in recombinant major light-harvesting complex (LHCII) of higher plants I. Femtosecond transient absorption measurements. *Biophysical Journal* **80**: 901–915.

Dahal K, Martyn GD, Vanlerberghe GC. **2015**. Improved photosynthetic performance during severe drought in *Nicotiana tabacum* overexpressing a nonenergy conserving respiratory electron sink. *New Phytologist* **208**: 382–395.

Dahal K, Wang J, Martyn GD, Rahimy F, Vanlerberghe GC. **2014**. Mitochondrial alternative oxidase maintains respiration and preserves photosynthetic capacity during moderate drought in *Nicotiana tabacum*. *Plant Physiology* **166**: 1560–1574.

Damm A, Elber J, Erler A, Gioli B, Hamdi K, Hutjes R, Kosvancova M, Meroni M, Miglietta F, Moersch A, *et al.* 2010. Remote sensing of sun-induced fluorescence to improve modeling of diurnal courses of gross primary production (GPP). *Global Change Biology* **16**: 171–186.

Dietz K-J. **1985**. A possible rate-limiting function of chloroplast hexosemonophosphate isomerase in starch synthesis of leaves. *Biochimica et Biophysica Acta* **839**: 240–248.

Dingkuhn M, Luquet D, Fabre D, Muller B, Yin X, Paul MJ. **2020**. The case for improving crop carbon sink strength or plasticity for a CO2-rich future. *Current Opinion in Plant Biology* **56**: 259–272.

Dissanayaka DMSB, Plaxton WC, Lambers H, Siebers M, Marambe B, Wasaki J. **2018**. Molecular mechanisms underpinning phosphorus-use efficiency in rice. *Plant Cell and Environment* **41**: 1483–1496.

Dubois J-JB, Fiscus EL, Booker FL, Flowers MD, Reid CD. **2007**. Optimizing the statistical estimation of the parameters of the Farquhar – von Caemmerer – Berry model of photosynthesis. *New Phytologist* **176**: 402–414.

Duursma RA. **2015**. Plantecophys - An R package for analysing and modelling leaf gas exchange data. *PLoS ONE* **10**: 1–13.

Ellsworth DS, Crous KY, Lambers H, Cooke J. **2015**. Phosphorus recycling in photorespiration maintains high photosynthetic capacity in woody species. *Plant, Cell & Environment* **38**: 1142–1156.

Emerson R, Lewis CM. **1942**. The photosynthetic efficiency of phycocyanin in chroococcus, and

the problem of carotenoid participation in photosynthesis. *The Journal of General Physiology* **25**: 579–595.

Escobar-Gutiérrez AJ, Gaudillère JP. **1997**. Carbon partitioning in source leaves of peach, a sorbitol-synthesizing species, is modified by photosynthetic rate. *Physiologia Plantarum* **100**: 353–360.

Evans J. **1987**. The dependence of quantum yield on wavelength and growth irradiance. *Australian Journal of Plant Physiology* **14**: 69–79.

Evans JR. **2009**. Potential errors in electron transport rates calculated from chlorophyll fluorescence as revealed by a multilayer leaf model. *Plant and Cell Physiology* **50**: 698–706.

Evans JR, Anderson JM. **1987**. Absolute absorption and relative fluorescence excitation spectra of the five major chlorophyll-protein complexes from spinach thylakoid membranes. *Biochimica et Biophysica Acta - Bioenergetics* **892**: 75–82.

Evans JR, Clarke VC. **2019**. The nitrogen cost of photosynthesis. *Journal of Experimental Botany* **70**: 7–15.

Evans JR, Morgan PB, von Caemmerer S. **2017**. Light quality affects chloroplast electron transport rates estimated from chl fluorescence measurements. *Plant & Cell Physiology* **58**: 1652–1660.

Fabre D, Yin X, Dingkuhn M, Clément-Vidal A, Roques S, Rouan L, Soutiras A, Luquet D, Lawson T. **2019**. Is triose phosphate utilization involved in the feedback inhibition of photosynthesis in rice under conditions of sink limitation. *Journal of Experimental Botany* **70**: 5773–5785.

Farquhar GD. **1979**. Models describing the kinetics of ribulose biphosphate carboxylase-oxygenase. *Archives of Biochemistry and Biophysics* **193**: 456–468.

Farquhar GD, von Caemmerer S. **1982**. Modelling of photosynthetic response to environmental conditions. In: Lange OL, Nobel PS, Osmond CB, Ziegler H, eds. Physiological Plant Ecology II. Springer-Verlag Berlin Heidelberg New York, 549–582.

Farquhar GD, von Caemmerer S, Berry JA. **1980**. A biochemical model of photosynthetic CO2 assimilation in leaves of C3 species. *Planta* **149**: 78–90.

Foyer C, Spencer C. **1986**. The relationship between phosphate status and photosynthesis in leaves: effects on intracellular orthophosphate distribution, photosynthesis and assimilate partitioning. *Planta* **167**: 369–375.

Furbank RT, Foyer CH, Walker DA. **1987**. Regulation of photosynthesis in isolated spinach chloroplasts during orthophosphate limitation. *Biochimica et Biophysica Acta* **894**: 552–

561.

Gauthier PPG, Bligny R, Gout E, Mahé A, Nogués S, Hodges M, Tcherkez GGB. **2010**. *In folio* isotopic tracing demonstrates that nitrogen assimilation into glutamate is mostly independent from current CO_2 assimilation in illuminated leaves of *Brassica napus*. *New Phytologist* **185**: 988–999.

Genty B, Briantais JM, Baker NR. **1989**. The relationship between the quantum yield of photosynthetic electron transport and quenching of chlorophyll fluorescence. *Biochimica et Biophysica Acta - General Subjects* **990**: 87–92.

Gregory LM, McClain AM, Kramer DM, Pardo JD, Smith KE, Tessmer OL, Walker BJ, Ziccardi LG, Sharkey TD. **2021**. The triose phosphate utilization limitation of photosynthetic rate: Out of global models but important for leaf models. *Plant Cell and Environment*: 3223–3226.

Grotjohann I, Gräber P. **2002**. The H+-ATPase from chloroplasts: effect of different reconstitution procedures on ATP synthesis activity and on phosphate dependence of ATP synthesis. *Biochimica et Biophysica Acta* **1556**: 208–216.

Gu L, Pallardy SG, Tu K, Law BE, Wullschleger SD. **2010**. Reliable estimation of biochemical parameters from C3 leaf photosynthesis-intercellular carbon dioxide response curves. *Plant, Cell and Environment* **33**: 1852–1874.

Guy CL, Huber JL, Huber SC. **1992**. Sucrose phosphate synthase and sucrose accumulation at low temperature. *Plant Physiology* **100**: 502–508.

Hall CC, Cruz JA, Zegarac R, DeMars D, Carpenter J, Kanazawa A, Kramer DM. **2013**. Photosynthetic Measurements with the Idea Spec: an Integrated Diode Emitter Array Spectrophotometer/Fluorometer. In: Photosynthesis Research for Food, Fuel and the Future. Springer Berlin Heidelberg, 184–188.

Harley PC, Loreto F, Marco G Di, Sharkey TD. **1992**. Theoretical considerations when estimating the mesophyll conductance to CO_2 flux by analysis of the response of photosynthesis to CO_2. *Plant Physiology* **98**: 1429–1436.

Harley PC, Sharkey TD. **1991**. An improved model of C_3 photosynthesis at high CO_2: reversed O_2 sensitivity explained by lack of glycerate reentry into the chloroplast. *Photosynthesis Research* **27**: 169–178.

Harris GC, Cheesbrough JK, Walker DA. **1983**. Effects of mannose on photosynthetic gas exchange in spinach. *Plant Physiol.* **71**: 108–111.

Heldt HW, Chon CJ, Maronde D, Herold A, Stankovic ZS, Walker DA, Kraminer A, Kirk MR, Heber U. **1977**. Role of orthophosphate and other factors in the regulation of starch formation in leaves and isolated chloroplasts. *Plant Physiology* **59**: 1146–1155.

Herold A. **1980**. Regulation of photosynthesis by sink activity - the missing link. *New Phytologist* **86**: 131–144.

Herold A, Lewis DH. **1977**. Mannose and green plants: occurrence, physiology and metabolism, and use as a tool to study the role of orthophosphate. *New Phytologist* **79**: 1–40.

Hoagland DR, Arnon DI. **1938**. The water culture method for growing plants without soil. In: UC Agric. Exp. Sta. Circular 347. Berkley, 1–39.

Hogewoning SW, Wientjes E, Douwstra P, Trouwborst G, van Ieperen W, Croce R, Harbinson J. **2012**. Photosynthetic quantum yield dynamics: from photosystems to leaves. *The Plant Cell* **24**: 1921–1935.

Holaday AS, Martindale W, Alred R, Brooks AL, Leegood RC. **1992**. Changes in Activities of Enzymes of Carbon Metabolism in Leaves during Exposure of Plants to Low Temperature. *Plant Physiology* **98**: 1105–1114.

Holt NE, Kennis JTM, Dall'Osto L, Bassi R, Fleming GR. **2003**. Carotenoid to chlorophyll energy transfer in light harvesting complex II from Arabidopsis thaliana probed by femtosecond fluorescence upconversion. *Chemical Physics Letters* **379**: 305–313.

Huber SC. **1981**. Interspecific variation in activity and regulation of leaf sucrose phosphate synthetase. *Zeitschrift für Pflanzenphysiologie* **102**: 443–450.

Huber SC, Huber JL. **1996**. Role and regulation of sucrose-phosphate synthase in higher plants. *Annual Review of Plant Physiology and Plant Molecular Biology* **47**: 431–444.

Hurry V, Strand Å, Furbank R, Stitt M. **2000**. The role of inorganic phosphate in the development of freezing tolerance and the acclimation of hotosynthetic carbon metabolism to low growth temperature is revealed by studies of *pho* mutants of *Arabidopsis thaliana*. *The Plant Journal* **24**: 383–396.

Iino M, Ogawa T, Zeiger E. **1985**. Kinetic properties of the blue-light response of stomata. *Proceedings of the National Academy of Sciences* **82**: 8019–8023.

Ireland CR, Telfer A, Covello PS, Baker NR, Barber J. **1988**. Studies on the limitations to photosynthesis in leaves of the atrazine-resistant mutant of *Senecio vulgaris* L. *Planta* **173**: 459–467.

Jolliffe PA, Tregunna EB. **1973**. Environmental regulation of the oxygen effect on apparent photosynthesis in wheat. *Canadian Journal of Botany* **51**: 841–853.

Kanazawa A, Kramer DM. **2002**. *In vivo* modulation of nonphotochemical exciton quenching (NPQ) by regulation of the chloroplast ATP synthase. *Proceedings of the National Academy of Sciences of the United States of America* **99**: 12789–12794.

Kanazawa A, Ostendorf E, Kohzuma K, Hoh D, Strand DD, Sato-Cruz M, Savage L, Cruz JA, Fisher N, Froehlich JE, *et al.* 2017. Chloroplast ATP synthase modulation of the thylakoid proton motive force: implications for photosystem I and photosystem II photoprotection. *Frontiers in Plant Science* **8**: 1–12.

Keys AJ, Major L, Parry MAJ. **1995**. Is there another player in the game of Rubisco regulation? *Journal of Experimental Botany* **46**: 1245–1251.

Kiirats O, Cruz JA, Edwards GE, Kramer DM. **2009**. Feedback limitation of photosynthesis at high CO_2 acts by modulating the activity of the chloroplast ATP synthase. *Functional Plant Biology* **36**: 893–901.

King RW, Wardlaw IF, Evans LT. **1967**. Effect of assimilate utilization on photosynthetic rate in wheat. *Planta* **77**: 261–276.

Kocks P, Ross J. **1995**. Kinetic model for (damped) oscillations of transthylakoid pH in plants. *Journal of Physical Chemistry* **99**: 16490–16497.

Körner C. **2015**. Paradigm shift in plant growth control. *Current Opinion in Plant Biology* **25**: 107–114.

Kötting O, Pusch K, Tiessen A, Geigenberger P, Steup M, Ritte G. **2004**. Identification of a novel enzyme required for starch metabolism in arabidopsis leaves. The phosphoglucan, water dikinase. *Plant Physiology* **137**: 1–11.

Kramer DM, Crofts AR. **1993**. The concerted reduction of the high- and low-potential chains of the *bf* complex by plastoquinol. *BBA - Bioenergetics* **1183**: 72–84.

Kramer DM, Crofts AR. **1996**. Control and measurement of photosynthetic electron transport *in vivo*. In: Baker NR, Govindjee, eds. Photosynthesis and the Environment. Dordrecht: Kluwer Academic, 25–66.

Kramer DM, Johnson G, Kiirats O, Edwards GE. **2004**. New fluorescence parameters for the determination of QA redox state and excitation energy fluxes. *Photosynthesis Research* **79**: 209–218.

Kumarathunge DP, Medlyn BE, Drake JE, Rogers A, Tjoelker MG. **2019**. No evidence for triose phosphate limitation of light-saturated leaf photosynthesis under current atmospheric CO2 concentration. *Plant Cell and Environment* **42**: 3241–3252.

Labate CA, Leegood RC. **1988**. Limitation of photosynthesis by changes in temperature: factors affecting the response of carbon-dioxide assimilation to temperature in barley leaves. *Planta* **173**: 519–527.

Laisk A, Eichelmann H. **1989**. Towards understanding oscillations: a mathematical model of the biochemistry of photosynthesis. *Philosophical Transactions of the Royal Society B* **323**:

369–384.

Laisk A, Eichelmann H, Oja V, Eatherall A, Walker DA. **1989**. A mathematical model of the carbon metabolism in photosynthesis. Difficulties in explaining oscillations by fructose 2,6-bisphosphate regulation. *Proceedings of the Royal Society B* **237**: 389–415.

Laisk A, Loreto F. **1996**. Determining photosynthetic parameters from leaf CO_2 exchange and chlorophyll fluorescence. *Plant Physiology*: 903–912.

Laisk A, Oja V, Eichelmann H, Dall'Osto L. **2014**. Action spectra of photosystems II and I and quantum yield of photosynthesis in leaves in state 1. *Biochimica et Biophysica Acta - Bioenergetics* **1837**: 315–325.

Laisk A, Siebke K, Gerst U, Eichelmann H, Oja V, Heber U. **1991**. Oscillations in photosynthesis are initiated and supported by imbalances in the supply of ATP and NADPH to the Calvin cycle. *Planta* **185**: 554–562.

Laisk A, Walker DA. **1986**. Control of phosphate turnover as a rate-limiting factor and possible cause of oscillations in photosynthesis: a mathematical model. *Proceedings of the Royal Society B* **227**: 281–302.

Lantz AT, Solomon C, Gog L, McClain AM, Weraduwage SM, Cruz JA, Sharkey TD. **2019**. Isoprene suppression by CO2 is not due to triose phosphate utilization (TPU) limitation. *Frontiers in Forests and Global Change* **2**: 1–13.

Laporte MM, Galagan JA, Prasch AL, Vanderveer PJ, Hanson DT, Shewmaker CK, Sharkey TD. **2001**. Promoter strength and tissue specificity effects on growth of tomato plants transformed with maize sucrose-phosphate synthase. *Planta* **212**: 817–822.

Lastdrager J, Hanson J, Smeekens S. **2014**. Sugar signals and the control of plant growth and development. *Journal of Experimental Botany* **65**: 799–807.

Leegood RC, Edwards GE. **1996**. Carbon metabolism and photorespiration: temperature dependence in relation to other environmental factors. In: Baker NR, ed. Photosynthesis and the Environment. Springer Dordrecht, 191–221.

Leegood RC, Furbank RT. **1986**. Stimulation of photosynthesis by 2% oxygen at low temperatures is restored by phosphate. *Planta* **168**: 84–93.

Leegood RC, Walker DA. **1983**. The role of transmembrane solute flux in regulation of CO_2 fixation in chloroplasts. *Biochemical Society Transactions* **11**: 74–76.

Li XP, Müller-Moulé P, Gilmore AM, Niyogi KK. **2002**. PsbS-dependent enhancement of feedback de-excitation protects photosystem II from photoinhibition. *Proceedings of the National Academy of Sciences of the United States of America* **99**: 15222–15227.

Li Z, Wakao S, Fischer BB, Niyogi KK. **2009**. Sensing and responding to excess light. *Annual Review of Plant Biology* **60**: 239–260.

Li J, Weraduwage SM, Preiser AL, Tietz S, Weise SE, Strand DD, Froehlich JE, Kramer DM, Hu J, Sharkey TD. **2019**. A cytosolic bypass and g6p shunt in plants lacking peroxisomal hydroxypyruvate reductase1[open]. *Plant Physiology* **180**: 783–792.

Lichtenberg M, Trampe ECL, Vogelmann TC, Kühl M. **2017**. Light sheet microscopy imaging of light absorption and photosynthesis distribution in plant tissue. *Plant Physiology* **175**: 721–733.

Loescher WH, Everard JD, Leegood RC, Sharkey TD, Von Caemmerer S. **2000**. Regulation of sugar alcohol biosynthesis. In: Leegood RC, Sharkey TD, von Caemmerer S, eds. Photosynthesis: Physiology and Metabolism. Advances in Photosynthesis. Dordrecht: Kluwer Academic, 275–299.

Lombardozzi DL, Smith NG, Cheng SJ, Dukes JS, Sharkey TD, Rogers A, Fisher R, Bonan GB. **2018**. Triose phosphate limitation in photosynthesis models reduces leaf photosynthesis and global terrestrial carbon storage. *Environmental Research Letters* **13**: 074025.

Loreto F, Tsonev T, Centritto M. **2009**. The impact of blue light on leaf mesophyll conductance. *Journal of Experimental Botany* **60**: 2283–2290.

Loriaux SD, Avenson TJ, Welles JM, Mcdermitt DK, Eckles RD, Riensche B, Genty B. **2013**. Closing in on maximum yield of chlorophyll fluorescence using a single multiphase flash of sub-saturating intensity. *Plant, Cell and Environment* **36**: 1755–1770.

Ludwig LJ, Canvin DT. **1971**. The rate of photorespiration during photosynthesis and the relationship of the substrate of light respiration to the products of photosynthesis in sunflower leaves. *Plant Phyisology* **48**: 712–719.

Ma F, Jazmin LJ, Young JD, Allen DK. **2014**. Isotopically nonstationary 13C flux analysis of changes in Arabidopsis thaliana leaf metabolism due to high light acclimation. *Proceedings of the National Academy of Sciences of the United States of America* **111**: 16967–16972.

McClain AM, Sharkey TD. **2019**. Triose phosphate utilization and beyond: from photosynthesis to end product synthesis. *Journal of Experimental Botany* **70**: 1756–1766.

McCree KJ. **1970**. The action spectrum, absorptance and quantum yield of photosynthesis in crop plants. *Agricultural Meteorology* **9**: 191–216.

McPherson AE, Jane J. **1999**. Comparison of waxy potato with other root and tuber starches. *Carbohydrate Polymers* **40**: 57–70.

McVetty PBE, Canvin DT. **1981**. Inhibition of photosynthesis by low oxygen concentrations.

Canadian Journal of Botany **59**: 721–725.

Mengin V, Pyl ET, Moraes TA, Sulpice R, Krohn N, Encke B, Stitt M. **2017**. Photosynthate partitioning to starch in arabidopsis thaliana is insensitive to light intensity but sensitive to photoperiod due to a restriction on growth in the light in short photoperiods. *Plant Cell and Environment* **40**: 2608–2627.

Mo Q, Li Z, Sayer EJ, Lambers H, Li Y, Zou B, Tang J, Heskel M, Ding Y, Wang F. **2018**. Foliar phosphorus fractions reveal how tropical plants maintain photosynthetic rates despite low soil phosphorus availability. *Functional Ecology*.

Mõttus M, Hovi A, Rautiainen M. **2017**. Theoretical algorithm and application of a double-integrating sphere system for measuring leaf transmittance and reflectance spectra. *Applied Optics* **56**: 563.

Moualeu-Ngangue DP, Chen T-W, Stützel H. **2017**. A new method to estimate photosynthetic parameters through net assimilation rate–intercellular space CO_2 concentration ($A–C_i$) curve and chlorophyll fluorescence measurements. *New Phytologist* **213**: 1543–1554.

Ogawa T. **1982**. Simple oscillations in photosynthesis of higher plants. *BBA - Bioenergetics* **681**: 103–109.

Ohad I, Kyle DJ, Arntzen CJ. **1984**. Membrane protein damage and repair: removal and replacement of inactivated 32-kilodalton polypeptides in chloroplast membranes. *The Journal of cell biology* **99**: 481–485.

Owens TG. **1996**. Processing of excitation energy by antenna pigments. In: Govindjee, Baker NR, eds. Photosynthesis and the Environment. Dordrecht: Kluwer Academic, 1–23.

Pammenter NW, Loreto F, Sharkey TD. **1993**. End product feedback effects on photosynthetic electron transport. *Photosynthesis Research* **35**: 5–14.

Parry MAJ, Andralojc PJ, Parmar S, Keys AJ, Habash D, Paul MJ, Alred R, Quick WP, Servaites JC. **1997**. Regulation of Rubisco by inhibitors in the light. *Plant, Cell and Environment* **20**: 528–534.

Paul MJ, Andralojc PJ, Banks FM, Parry MAJ, Knight JS, Gray JC, Keys AJ. **1996**. Altered Rubisco activity and amounts of a daytime tight-binding inhibitor in transgenic tobacco expressing limiting amounts of phosphoribulokinase. *Journal of Experimental Botany* **47**: 1963–1966.

Paul MJ, Foyer CH. **2001**. Sink regulation of photosynthesis. *Journal of Experimental Botany* **52**: 1383–1400.

Paul MJ, Pellny TK. **2003**. Carbon metabolite feedback regulation of leaf photosynthesis and development. *Journal of Experimental Botany* **54**: 539–547.

Peet MM, Huber SC, Patterson DT. **1986**. Acclimation to high CO2 in monoecious cucumbers II. Carbon exchange rates, enzyme activities, and starch and nutrient concentrations. *Plant Physiology* **80**: 63–67.

Peixoto B, Moraes TA, Mengin V, Margalha L, Vicente R, Feil R, Hohne M, Sousa AGG, Lilue J, Stitt M, *et al.* 2021. Impact of the SnRK1 protein kinase on sucrose homeostasis and the transcriptome during the diel cycle. *Plant Physiology* **187**: 1357–1373.

Peterson RB, Sivak MN, Walker DA. **1988**. Carbon dioxide-induced oscillations in fluorescence and photosynthesis: role of thylakoid membrane energization in regulation of photosystem II activity. *Plant Physiology* **88**: 1125–1130.

Pfannschmidt T. **2005**. Acclimation to varying light qualities: toward the functional relationship of state transitions and adjustment of photosystem stoichiometry. *Journal of Phycology* **41**: 723–725.

Powles SB. **1984**. Photoinhibition of Photosynthesis Induced by Visible Light. *Annual Review of Plant Physiology* **35**: 15–44.

Pracharoenwattana I, Zhou W, Keech O, Francisco PB, Udomchalothorn T, Tschoep H, Stitt M, Gibon Y, Smith SM. **2010**. Arabidopsis has a cytosolic fumarase required for the massive allocation of photosynthate into fumaric acid and for rapid plant growth on high nitrogen. *Plant Journal* **62**: 785–795.

Preiss J. **1982**. Regulation of the biosynthesis and degradation of starch. *Annual Review of Plant Physiology and Plant Molecular Biology* **33**: 431–454.

Rae JWB, Zhang YG, Liu X, Foster GL, Stoll HM, Whiteford RDM. **2021**. Atmospheric CO_2 over the past 66 million years from marine archives. *Annual Review of Earth and Planetary Sciences* **49**: 609–641.

Ramonell KM, Kuang A, Porterfield DM, Crispi ML, Xiao Y, Mcclure G, Musgrave ME. **2001**. Influence of atmospheric oxygen on leaf structure and starch deposition in *Arabidopsis thaliana*. *Plant, Cell & Environment* **24**: 419–428.

Rasulov B, Bichele I, Laisk A, Niinemets Ü. **2014**. Competition between isoprene emission and pigment synthesis during leaf development in aspen. *Plant, Cell & Environment* **37**: 724–741.

Rebeille F, Bligny R, Martin JB, Douce R. **1983**. Relationship between the cytoplasm and the vacuole phosphate pool in *Acer pseudoplatanus* cells. *Archives of Biochemistry and Biophysics* **225**: 143–148.

Riesmeier JW, Flügge UI, Schulz B, Heineke D, Heldt HW, Willmitzer L, Frommer WB. **1993**. Antisense repression of the chloroplast triose phosphate translocator affects carbon partitioning in transgenic potato plants. *Proceedings of the National Academy of*

Sciences of the United States of America **90**: 6160–6164.

Ritte G, Lloyd JR, Eckermann N, Rottmann A, Kossmann J, Steup M. **2002**. The starch-related R1 protein is an α-glucan, water dikinase. *Proceedings of the National Academy of Sciences of the United States of America* **99**: 7166–7171.

Rochaix JD. **2011**. Regulation of photosynthetic electron transport. *Biochimica et Biophysica Acta - Bioenergetics* **1807**: 375–383.

Rogers A, Kumarathunge DP, Lombardozzi DL, Medlyn BE, Serbin SP, Walker AP. **2020**. Triose phosphate utilization limitation: an unnecessary complexity in terrestrial biosphere model representation of photosynthesis. *New Phytologist*.

Rogers A, Kumarathunge DP, Lombardozzi DL, Medlyn BE, Serbin SP, Walker AP. **2021**. Triose phosphate utilization limitation: an unnecessary complexity in terrestrial biosphere model representation of photosynthesis. *New Phytologist* **230**: 17–22.

Ruban A V, Johnson MP. **2009**. Dynamics of higher plant photosystem cross-section associated with state transitions. *Photosynthesis Research* **99**: 173–183.

Ruuska S, Andrews TJ, Badger MR, Hudson GS, Laisk A, Price DG, von Caemmerer S. **1998**. The interplay between limiting processes in C_3 photosynthesis studied by rapid-response gas exchange using transgenic tobacco impaired in photosynthesis. *Australian Journal of Plant Physiology* **25**: 859–870.

Saathoff AJ, Welles J. **2021**. Gas exchange measurements in the unsteady state. *Plant Cell and Environment* **44**: 3509–3523.

Sage RF, Kubien DS. **2007**. The temperature response of C_3 and C_4 photosynthesis. *Plant, Cell & Environment* **30**: 1086–1106.

Sage RF, Sharkey TD. **1987**. The effect of temperature on the occurrence of O_2 and CO_2 insensitive photosynthesis in field grown plants. *Plant Physiology* **84**: 658–664.

Sage RF, Sharkey TD, Pearcy RW. **1990**. The effect of leaf nitrogen and temperature on the CO_2 response of photosynthesis in the C_3 dicot *Chenopodium album* L . *Australian Journal of Plant Physiology* **17**: 135–148.

Sage RF, Sharkey TD, Seemann JR. **1988**. The in-vivo response of the ribulose-1,5-bisphosphate carboxylase activation state and the pool sizes of photosynthetic metabolites to elevated CO_2 in *Phaseolus vulgaris* L. *Planta* **174**: 407–416.

Sage RF, Sharkey TD, Seemann JR. **1989**. Acclimation of photosynthesis to elevated CO_2 in five C_3 species. *Plant Physiology* **89**: 590–596.

Salvucci ME, Crafts-Brandner SJ. **2004**. Mechanism for deactivation of Rubisco under moderate

heat stress. *Physiologia Plantarum* **122**: 513–519.

Sanjaya, Durrett TP, Weise SE, Benning C. **2011**. Increasing the energy density of vegetative tissues by diverting carbon from starch to oil biosynthesis in transgenic Arabidopsis. *Plant Biotechnology Journal* **9**: 874–883.

Sasek TW, Delucia EH, Strain BR. **1985**. Reversibility of photosynthetic inhibition in cotton after long-term exposure to elevated CO_2 concentrations. *Plant Physiology* **78**: 619–622.

Schrader SM, Wise RR, Wacholtz WF, Ort DR, Sharkey TD. **2004**. Thylakoid membrane responses to moderately high leaf temperature in Pima cotton. *Plant, Cell and Environment* **27**: 725–735.

Selman-Reimer S, Merchant S, Selman BR. **1981**. Isolation, purification, and characterization of coupling factor 1 from *Chlamydomonas reinhardi*. *Biochemistry* **20**: 5476–5482.

Sharkey TD. **1985a**. O_2 - insensitive photosynthesis in C_3 plants. *Plant Physiology* **78**: 71–75.

Sharkey TD. **1985b**. Photosynthesis in intact leaves of C_3 plants. *The Botanical Review* **5**: 53–105.

Sharkey TD. **2016**. What gas exchange data can tell us about photosynthesis. *Plant Cell & Environment* **39**: 1161–1163.

Sharkey TD. **2019**. Is triose phosphate utilization important for understanding photosynthesis. *Journal of Experimental Botany* **70**: 5521–5525.

Sharkey TD. **2022**. Maximising the efficiency of RuBP (ribulose biphosphate) regeneration to optimise photosynthesis in crops. In: Sharwood R, ed. Understanding and improving crop photosynthesis. Burleigh Dodds Science Publishing Limited.

Sharkey TD, Bernacchi CJ. **2012**. Photosynthetic responses to high temperature. In: Flexas J, Loreto F, Medrano H, eds. Terrestrial Photosynthesis in a Changing Environment: A Molecular, Physiological, and Ecological Approach. Cambridge: Cambridge University Press, 294–302.

Sharkey TD, Berry JA, Raschke K. **1985**. Starch and sucrose synthesis in *Phaseolus vulgaris* as affected by light, CO_2, and abscisic acid. *Plant Physiology* **77**: 617–620.

Sharkey TD, Berry JA, Sage RF. **1988**. Regulation of photosynthetic electron-transport in *Phaseolus vulgaris* L., as determined by room-temperature chlorophyll a fluorescence. *Planta* **176**: 415–424.

Sharkey TD, Imai K, Farquhar GD, Cowan IR. **1982**. A direct confirmation of the standard method of estimating intercellular partial-pressure of CO_2. *Plant Physiology* **69**: 657–659.

Sharkey TD, Seemann JR, Berry JA. **1986a**. Regulation of ribulose-1,5-bisphosphate carboxylase activity in response to changing partial pressure of O_2 and light in *Phaseolus vulgaris*. *Plant Physiology* **81**: 788–791.

Sharkey TD, Seemann JR, Berry JA. **1986b**. Regulation of ribulose-1,5-bisphosphate carboxylase activity in response to changing partial pressure of O2 and light in Phaseolus vulgaris. : 788–791.

Sharkey TD, Stitt M, Heineke D, Gerhardt R, Raschke K, Heldt HW. **1986c**. Limitation of photosynthesis by carbon metabolism II. O_2-insensitive CO_2 uptake results from limitation of triose phosphate utilization. *Plant Physiology* **81**: 1123–1129.

Sharkey TD, Vanderveer PJ. **1989**. Stromal phosphate concentration is low during feedback limited photosynthesis. *Plant Physiology* **91**: 679–684.

Sharkey TD, Vassey TL. **1989**. Low oxygen inhibition of photosynthesis is caused by inhibition of starch synthesis. *Plant Physiology* **90**: 385–7.

Shi L, Wu Y, Sheen J. **2018**. TOR signaling in plants: conservation and innovation. *Development (Cambridge, England)* **145**: 1–13.

Siefermann-Harms D, Ninneann H. **1982**. Pigment organization in the light harvesting chlorophyll a/b complex of lettuce chloroplasts. Evidence obtained from proton attack from exitation energy transfer. *Photochem. Photobiol.* **35**: 719–731.

Sivak MN, Walker DA. **1986**. Photosynthesis *in vivo* can be limited by phosphate supply. *New Phytologist* **102**: 499–512.

Sivak MN, Walker DA. **1987**. Oscillations and other symptoms of limitation of in vivo photosynthesis by inadequate phosphate supply to the chloroplast. *Plant Physiology and Biochemistry* **25**: 635–648.

Smeekens S, Ma J, Hanson J, Rolland F. **2010**. Sugar signals and molecular networks controlling plant growth. *Current Opinion in Plant Biology* **13**: 273–278.

Socias FX, Medrano H, Sharkey TD. **1993**. Feedback limitation of photosynthesis of *Phaseolus vulgaris* L. grown in elevated CO_2. *Plant, Cell & Environment* **16**: 81–86.

Sonoike K. **1996**. Photoinhibition of photosystem I: Its physiological significance in the chilling sensitivity of plants. *Plant and Cell Physiology* **37**: 239–247.

Sonoike K. **2011**. Photoinhibition of photosystem I. *Physiologia Plantarum* **142**: 56–64.

South PF, Walker BJ, Cavanagh AP, Rolland V, Badger M, Ort DR. **2017**. Bile acid sodium symporter BASS6 can transport glycolate and is involved in photorespiratory metabolism in *Arabidopsis thaliana*. *The Plant Cell* **29**: 808–823.

Stinziano JR, McDermitt DK, Lynch DJ, Saathoff AJ, Morgan PB, Hanson DT. **2019**. The rapid A/Ci response: a guide to best practices. *New Phytologist* **221**: 625–627.

Stinziano JR, Morgan PB, Lynch DJ, Saathoff AJ, McDermitt DK, Hanson DT. **2017**. The rapid A–Ci response: photosynthesis in the phenomic era. *Plant Cell and Environment* **40**: 1256–1262.

Stitt M. **1986**. Limitation of photosynthesis by carbon metabolism I. Evidence for excess electron transport capacity in leaves carrying out photosynthesis in saturating light and CO_2. *Plant Phyisology* **81**: 1115–1122.

Stitt M, Grosse H. **1988**. Interactions between sucrose synthesis and CO_2 fixation IV. Temperature-dependent adjustment of the relation between sucrose synthesis and CO_2 fixation. *Journal of Plant Physiology* **133**: 392–400.

Stitt M, Heldt HW. **1981**. Simultaneous synthesis and degradation of starch in spinach chloroplasts in the light. *Biochimica et Biophysica Acta* **638**: 1–11.

Stitt M, Kürzel B, Heldt HW. **1984**. Control of photosynthetic sucrose synthesis by fructose 2,6-bisphosphate II. Partitioning between sucrose and starch. *Plant Physiology* **75**: 554–560.

Stitt M, Wirtz W, Heldt HW. **1980**. Metabolite levels during induction in the chloroplast and extrachloroplast compartments of spinach protoplasts. *Biochimica et Biophysica Acta - Bioenergetics* **593**: 85–102.

Stitt M, Wirtz W, Heldt HW. **1983**. Regulation of sucrose synthesis by cytoplasmic fructosebisphosphatase and sucrose phosphate synthase during photosynthesis in varying light and carbon dioxide. *Plant Physiology* **72**: 767–774.

Strand Å, Hurry V, Henkes S, Huner N, Gustafsson P, Gardeström P, Stitt M. **1999**. Acclimation of Arabidopsis leaves developing at low temperatures. Increasing cytoplasmic volume accompanies increased activities of enzymes in the Calvin cycle and in the sucrose-biosynthesis pathway. *Plant physiology* **119**: 1387–98.

Strand DD, Kramer DM. **2014**. Towards a more precise measure of electron transfer rates through photosystem II. https://d.lib.msu.edu/etd/2925/.

Sulpice R, Flis A, Ivakov AA, Apelt F, Krohn N, Encke B, Abel C, Feil R, Lunn JE, Stitt M. **2014**. *Arabidopsis* coordinates the diurnal regulation of carbon allocation and growth across a wide range of photoperiods. *Molecular Plant* **7**: 137–155.

Sulpice R, Pyl ET, Ishihara H, Trenkamp S, Steinfath M, Witucka-Wall H, Gibon Y, Usadel B, Poree F, Piques MC, *et al.* 2009. Starch as a major integrator in the regulation of plant growth. *Proceedings of the National Academy of Sciences of the United States of America* **106**: 10348–10353.

Suorsa M, Järvi S, Grieco M, Nurmi M, Pietrzykowska M, Rantala M, Kangasjärvi S, Paakkarinen V, Tikkanen M, Jansson S, *et al.* 2012. PROTON GRADIENT REGULATION5 is essential for proper acclimation of Arabidopsis photosystem I to naturally and artificially fluctuating light conditions. *Plant Cell* **24**: 2934–2948.

Szecowka M, Heise R, Tohge T, Nunes-Nesi A, Vosloh D, Huege J, Feil R, Lunn J, Nikoloski Z, Stitt M, *et al.* 2013. Metabolic fluxes in an illuminated *Arabidopsis* rosette. *The Plant Cell* **25**: 694–714.

Takizawa K, Cruz JA, Kanazawa A, Kramer DM. **2007**. The thylakoid proton motive force *in vivo*. Quantitative, non-invasive probes, energetics, and regulatory consequences of light-induced *pmf*. *Biochimica et Biophysica Acta - Bioenergetics* **1767**: 1233–1244.

Takizawa K, Kanazawa A, Kramer DM. **2008**. Depletion of stromal Pi induces high 'energy-dependent' antenna exciton quenching (qE) by decreasing proton conductivity at CFO-CF1 ATP synthase. *Plant, Cell & Environment* **31**: 235–243.

Tietz S, Hall CC, Cruz JA, Kramer DM. **2017**. NPQ(T): a chlorophyll fluorescence parameter for rapid estimation and imaging of non-photochemical quenching of excitons in photosystem-II-associated antenna complexes. *Plant Cell & Environment* **40**.

Vass I, Styring S, Hundal T, Koivuniemi A, Aro EM, Andersson B. **1992**. Reversible and irreversible intermediates during photoinhibition of photosystem II: Stable reduced QA species promote chlorophyll triplet formation. *Proceedings of the National Academy of Sciences of the United States of America* **89**: 1408–1412.

Vassey TL, Sharkey TD. **1989**. Mild water stress of *Phaseolus vulgaris* plants leads to reduced starch synthesis and extractable sucrose phosphate synthase activity. *Plant Physiology* **89**: 1066–70.

Viil J, Ivanova H, Pärnik T, Pärsim E. **2004**. Regulation of ribulose-1,5-bisphosphate carboxylase/oxygenase *in vivo*: control by high CO_2 concentration. *Photosynthetica* **42**: 283–290.

Viil J, Laisk A, Oja V, Pärnik T. **1977**. Enhancement of photosynthesis caused by oxygen under saturating irradiance and high CO_2 concentrations. *Photosynthetica* **11**: 251–259.

Vogelmann TC. **1993**. Plant tissue optics. *Annu. Rev. Plant Physiol. Plant Mol. Biol.* **44**: 231–51.

Vogelmann TC, Han T. **2000**. Measurement of gradients of absorbed light in spinach leaves from chlorophyll fluorescence profiles. *Plant, Cell and Environment* **23**: 1303–1311.

Wada M, Kagawa T, Sato Y. **2003**. Chloroplast Movement. *Annual Review of Plant Biology* **54**: 455–468.

Walker DA, Sivak MN, Prinsley RT, Cheesbrough JK. **1983**. Simultaneous measurement of

oscillations in oxygen evolution and chlorophyll a fluorescence in leaf pieces. *Plant Physiology* **73**: 542–9.

Warburg VO. **1919**. Über die Geschwindigkeit der photocliemischen Kohlen- saürezersetzung in lebenden Zellen. *Biochemische Zeitschrift* **100**: 230–270.

Woodrow IE, Ellis JR, Jellings A, Foyer CH. **1984**. Compartmentation and fluxes of inorganic-phosphate in photosynthetic cells. *Planta* **161**: 525–530.

Woolley JT. **1971**. Reflectance and transmittance of light by leaves. *Plant Physiology* **47**: 656–662.

Wullschleger SD. **1993**. Biochemical limitations to carbon assimilation in C_3 plants—a retrospective analysis of the A/C_i curves from 109 species. *Journal of Experimental Botany* **44**: 907–920.

Xiao Y, Sloan J, Hepworth C, Osborne CP, Fleming AJ, Chen X, Zhu X. **2021**. Estimating uncertainty: A Bayesian approach to modelling photosynthesis in C3 leaves . *Plant, Cell & Environment*: 0–2.

Yang JT, Preiser AL, Li Z, Weise SE, Sharkey TD. **2016**. Triose phosphate use limitation of photosynthesis: short-term and long-term effects. *Planta* **243**: 687–698.

Yin X, Struik PC, Romero P, Harbinson J, Evrs JB, van der Putten PEL, Vos J. **2009**. Using combined measurements of gas exchange and chlorophyll fluorescence to estimate parameters of a biochemical C3 photosynthesis model: a critical appraisal and a new integrated approach applied to leaves in a wheat (Triticum aestivum). *Plant, Cell & Environment* **32**: 448–464.

Zell MB, Fahnenstich H, Maier A, Saigo M, Voznesenskaya E V., Edwards GE, Andreo C, Schleifenbaum F, Zell C, Drincovich MF, *et al.* 2010. Analysis of Arabidopsis with highly reduced levels of malate and fumarate sheds light on the role of these organic acids as storage carbon molecules. *Plant Physiology* **152**: 1251–1262.